UNIVERSIDADE FEDERAL RURAL DE PERNAMBUCO

GABRIEL HENRIQUE MAXIMO CLARINDO SILVA

ORGANIC MATTER AND MINERALOGY OF SOILS ALONG CONTAMINATED MANGROVE FORESTS: A CASE STUDY OF BOTAFOGO RIVER ESTUARY- PE, BRAZIL

RECIFE

2024

Gabriel Henrique Maximo Clarindo Silva
Agronomist

Organic matter and mineralogy of soils along contaminated mangrove forests: a case study of Botafogo River estuary- PE, Brazil

Tese apresentada ao Programa de Pós-Graduação em Ciência do Solo, da Universidade Federal Rural de Pernambuco, como parte dos requisitos para obtenção do título de Doutor em Ciência do Solo.

Orientadora: Prof. Dra. Caroline Miranda Biondi

Coorientadoras:
Dra. Paula Renata Muniz Araújo
Profa. Dra. Giselle Gomes Monteiro Fracetto

RECIFE

2024

Dados Internacionais de Catalogação na Publicação
Universidade Federal Rural de Pernambuco
Sistema Integrado de Bibliotecas
Gerada automaticamente, mediante os dados fornecidos
pelo(a) autor(a)

S586o Silva, Gabriel Henrique Maximo Clarindo Silva
Organic matter and mineralogy of soils along contaminated mangrove forests: a case of study of Botafogo river estuary- PE, Brazil / Gabriel Henrique Maximo Clarindo Silva Silva. - 2024.
93 f. : il.

Orientadora: Caroline Miranda Biondi. Coorientadora: Paula Renata Muniz Araujo. Inclui referências.

Tese (Doutorado) - Universidade Federal Rural de Pernambuco, Programa de Pós-Graduação em Ciência do Solo, Recife, 2024.

1. Contaminação. 2. Variabilidade vegetal. 3. Sulfetos. 4. Atividades antrópicas. I. Biondi, Caroline Miranda, orient. II. Araujo, Paula Renata Muniz, coorient. III. Título

CDD 631.4

GABRIEL HENRIQUE MAXIMO CLARINDO SILVA

Organic matter and mineralogy of soils along contaminated mangrove forests: a case study of Botafogo River estuary- PE, Brazil

Tese apresentada ao Programa de Pós-Graduação em Ciência do Solo, da Universidade Federal Rural de Pernambuco, como parte dos requisitos para obtenção do título de Doutor em Ciência do Solo.

Aprovada em 26 de março de 2024

Prof. Dra. Caroline Miranda Biondi

Orientadora

Universidade Federal Rural de Pernambuco

BANCA EXAMINADORA

Prof. Dr. Francis Henrique Tenório Firmino

Universidade Federal de Viçosa

Dra. Jane Kelly Silva Araújo

Universidade Federal Rural de Pernambuco

Prof. Dr. Renato Marques

Universidade Federal do Paraná

Prof. Dr. Valdomiro Severino de Souza Júnior

Universidade Federal Rural de Pernambuco

ACKNOWLEDGEMENT

À Deus, que para mim corresponde a natureza, pela coleção de maravilhas que têm me proporcionado e que nunca falhou em me ouvir quando pedia a energia e sabedoria para completar minhas atividades, bem como a proteção da minha família que infelizmente vivem distante de mim.

À minha amada, Clarissa, por toda parceria durante todos esses anos. Certamente a vida passou a ganhar sentido ao seu lado. Você me ensinou a ser um cidadão, filho, amigo e noivo. Saiba que apenas estamos iniciando nossa jornada da vida. Te amo.

Aos meus pais e irmão, guerreiros maiores dificilmente encontrarei novamente. Meus pais, nunca esquecerei a árdua batalha em nos educar, amar, proteger, assegurar, apoiar e nos manter. Meu querido irmão, agradeço todas as suas orações. Vocês são minha inspiração e exemplos dos mais belos sentimentos existentes. Amo vocês!

Aos meus sogros, Cicera e Adalberto, pelo acolhimento, ensinamentos e suporte que foram essenciais para enfrentar os desafios da vida.

À minha querida orientadora, que durante estes seis anos de orientação demonstrou ser uma dupla profissional, me guiando como professora e me auxiliando na pesquisa como colega de trabalhos científicos. Sou grato a sua amizade, respeito e contribuições que me fizeram crescer.

À Paula Renata. Você se tornou um exemplo para nosso programa de pós-graduação. Sua educação, atenção e inteligência foram cruciais na elaboração deste trabalho. Ganhei uma parceira e amiga neste doutorado.

Aos amigos Amanda, Fabiano, Crissogno, Joel e Luiz. Os momentos de conversa suavizavam as dificuldades.

Aos queridos professores Maria Betânia e Fernando Freire, por todos os conselhos, parcerias e por acreditarem em meu potencial.

Ao Prof. Dr. Clistenes Williams e à Dra. Simone Lins, por todo suporte na estrutura laboratorial.

Ao Prof. Dr. Valdomiro Severino, Dra. Jane Kelly e Prof. Dr. Jean Cheyson, pelas análises realizadas no Laboratório de Mineralogia e contribuições nas discussões acerca da matéria orgânica e mineralogia.

Aos técnicos do CENAPESQ, Nathan e Mila pelo auxílio nas análises microscópicas.

Aos professores e colaboradores do Programa de Pós-graduação em Ciência do Solo por todos os conhecimentos.

Aos colegas do laboratório de Mineralogia e Quimica Ambiental, Artur e Djennifer, pelo suporte nas análises mineralógicas.

Ao professor Plinio Camargo, pelas análises realizadas no Laboratório de Isótopos Estáveis do Centro de Energia Nuclear - USP.

À minha "Californian Family": Profa. Dra. Samantha Ying, pela orientação na pesquisa e aos colegas Alexander MacDonald, Benjamin Maki, Miranda Vega, Shannel Thorpe e Cameron Daley, pelas contribuições durante meu periodo no Enviromental Science Department da Universidade da California - Riverside (UCR). Ainda na UCR fomos abraçados por Makbule Koksal, Candace Jorgensen, bem como os colegas do coffee hour: Martins, Leandro, Bruno, Pamella, Mariana, Marine, Mitchell e Emily.

Ainda durante o intercâmbio acabei ganhando uma segunda família, o USDA – Salinity Lab. Agradeço imensamente ao querido Prof. Dr. Jorge Ferreira por tão bem nos receber, além dos conselhos e parcerias científicas. Estendo meus agradecimentos aos queridos Todd, Nydia, Ananda, Elia, Duc, Devinder e Mark pelos momentos de descontração que atenuavam os efeitos da distância. Por fim, acabei ganhando um "coorientador" e amigo nas pesquisas de matéria orgânica, Dr. Mike Schmidt, obrigado pelos ensinamentos em quimica orgânica.

À FACEPE e à CAPES, pelas concessões das bolsas imprescindíveis para a execução do trabalho.

“Dreams without goals are just dreams and ultimately, they fuel disappointment. On the road, to achieving your dreams, you must apply discipline, but more importantly, consistency. because without commitment you'll never start, but without consistency, you'll never finish.”

Denzel Washington

Matéria orgânica e mineralogia de solos ao longo de manguezais contaminados: um estudo de caso do estuário do Rio Botafogo - PE, Brasil

RESUMO GERAL

O estuário do rio Botafogo, localizado no litoral norte de Pernambuco, é considerado uma das mais importantes faixas de mangues da região Nordeste do Brasil. A sua bacia hidrográfica contribui para o abastecimento de água potável para toda região metropolitana da capital do estado. Entretanto, há décadas que os impactos antrópicos vêm causando danos significativos aos manguezais deste estuário. Após a instalação da indústria soda-cloro na região nos anos 60, a liberação de contaminantes altamente tóxicos, como o mercúrio (Hg), no rio Botafogo contribuiu para o acúmulo deste metal nas florestas de manguezais. O trabalho objetivou identificar e relacionar os atributos químicos e a mineralogia do solo com a diversidade vegetal e a posição no estuário, com enfoque na atuação da matéria orgânica (MO) e minerais na dinâmica de Hg. Para isto, foram coletadas amostras de solo ao longo de diferentes domínios vegetais: *Laguncularia racemosa*, coexistência, *Rhizophora mangle* do estuário do rio Botafogo. A partir disto, os atributos químicos e físicos do solo e os teores totais dos metais pesados foram determinados. Em seguida, a matéria orgânica do solo foi caracterizada, sendo avaliada a origem, estabilidade e composição bioquímica. Também foi realizada a caracterização mineralógica do solo e especiação de S. Os resultados apontam a contaminação de Hg nas três florestas, com concentrações seguindo um gradiente crescente em direção a fonte poluidora. A MO mostrou diferenças em origem, estabilidade e grupos funcionais, principalmente em relação a floresta de *R. mangle,* localizada próximo à foz do rio. A caracterização da MO revelou também maior proporção de C oxidado na floresta de *L. racemosa*, os quais podem atuar na retenção de Hg. A assembleia de silicatos dos solos não variou e destacou as presenças de caulinita, quartzo, muscovita, ilita e esmectita. Pirita e carbonatos foram identificados, porém a presença de carbonatos ficou restrita às áreas próximas à foz do rio. O Hg se encontrou associado à pirita, e os dados de especiação de S revelaram possível contribuição também de S orgânico, como tiol. A qualidade da MO, mineralogia do solo e especiação de S possibilitaram o avanço nas discussões de caracterização de manguezais contaminados com ênfase na interação com Hg, destacando o papel de filtro geoquímico dos sulfetos minerais e orgânicos na retenção deste metal. Logo, ressaltamos o cuidado em evitar alterações nas condições biogeoquímicas do solo, principalmente pelas atividades antrópicas, caso contrário esses solos não apresentarão mais papel de filtro, e sim de fonte de contaminantes para os demais ambientes em volta.

Palavras-chave: Contaminação. Variabilidade vegetal. Sulfetos. Atividades antrópicas.

Organic matter and mineralogy of soils along contaminated mangrove forests: A case study of Botafogo River estuary- PE, Brazil

GENERAL ABSTRACT

The Botafogo River estuary, located on the north coast of Pernambuco, is considered one of the most important strips of mangroves in the Northeast region of Brazil. Its river basin contributes to the supply of drinking water for the entire metropolitan region of the state capital. However, anthropogenic impacts have been causing significant damage to the mangroves in this estuary for decades. After the installation of a chlor-alkali plant in the region in the 1960s, the release of highly toxic contaminants, such as mercury (Hg), into the Botafogo River contributed to the accumulation of this metal in mangrove forests. The work aimed to identify and relate the chemical attributes and mineralogy of the soil with plant diversity and position in the estuary, focusing on the role of organic matter (OM) and minerals in Hg dynamics. For this, soil samples were collected throughout different plant domains: *Laguncularia racemosa*, coexistence, *Rhizophora mangle* from the Botafogo river estuary. Then, the chemical and physical attributes of the soil and the total content of heavy metals were determined. Organic matter in the soil was analyzed by the evaluation of its origin, stability, and biochemical composition. Mineralogical characterization of the soil and S speciation were also carried out. The results indicate Hg contamination in the three forests, with concentrations following an increasing gradient towards the polluting source. The MO showed differences in origin, stability, and functional groups, mainly in relation to the *R. mangle* forest, located close to the river mouth. The characterization of MO also revealed a higher proportion of oxidized C at the *L. racemosa* forest, which can act on Hg retention. The silicate assemblage of the soils did not vary and highlighted the presence of kaolinite, quartz, muscovite, illite and smectite. Pyrite and carbonates were identified, but the presence of carbonates was restricted to areas close to the river mouth. Hg was found associated with pyrite, and S specification data revealed a possible contribution also from organic S, as a thiol. The quality of OM, soil mineralogy and specification of S made it possible to advance the discussion on the characterization of contaminated mangroves with an emphasis on the interaction with Hg, highlighting the role of geochemical filter of mineral and organic sulfides in the retention of this metal. Therefore, we emphasize the care to avoid changes in the biogeochemical conditions of the soil, mainly due to human activities, otherwise these soils will no longer play a role as a filter, but rather as a source of contaminants for other surrounding environments.

Keywords: Contamination. Plant variability. Sulfides. Anthropogenic activities.

FIGURE LIST

TABLE LIST

SUMMARY

GENERAL INTRODUCTION

The mangrove is the tropical ecosystem with the largest stock of carbon (C) per area on the planet. The numbers indicate an accumulation of 10.7 ± 9.4 Mg C ha^{-1} $year^{-1}$. Organic matter (OM) confers different ecological functions, such as acting in the biogeochemical cycles of the elements and providing shelter and food for different organisms. The OM also acts as a "natural filter" where C compounds can be associated with different contaminants, coming from industrial and domestic waste, discarded daily in the water bodies that follow towards the estuaries. Interactions with these contaminants, can make them unavailable to the local biota, as well as reduce their mobility to other compartments, such the oceans.

In this protective role, the OM stored in the mangroves soils can react with relevant inorganic contaminants, such mercury (Hg). Hg has a long persistence and toxicity in these environments and can pose serious risks to the entire ecosystem. However, studies focused on the presence of Hg in mangroves are limited to polluting sources and the assessment of environmental impacts. Information about the relations between this metal and OM is still unclear, as well as the influence on the distribution of Hg in the different geochemical compartments. In this context, only the levels of OM and metal in the soil are insufficient, requiring further investigation into the chemical composition and transformations of organic compounds, as well as the main forms of Hg found in this environment. Added to the information from the local biological matrices, it is also possible to carry out a risk assessment.

On the north coast of Pernambuco, the mangrove areas located on the edge of the Botafogo River estuary provide important conditions for the development of the riverside population. However, in recent decades, these areas have suffered intense anthropic impact, mainly due to the release of waste from industries, shrimp farming, and agricultural activities.

The Botafogo River estuary has the highest levels of Hg of the brazilian coast. Based on this, further investigations are needed, highlighting the role of organic matter in the retention of contaminants in these soils.

1.1. Hypothesis

- The plant species: *Rhizophora mangle, Laguncularia racemosa* and *Avicennia shaueriana* are the main sources that most contribute to the OM chemical composition variation in these soils;
- The soil organic matter under *R. mangle* forest summed with a higher anaerobic condition present greater stability, aromaticity, and therefore less reactivity. It can exert low influence on Hg retention compared to other forests.
- The mineral retention of Hg is governed by sulfide, such pyrite, and the silicate assemblage does not influence Hg fate.
- Coexistence of species can reduce the releasement of low oxidation state S groups and it represent a decrease in S components, responsible for Hg retention.
- Besides the known factors, such as particle distribution size and distance from the sea, the Hg concentration and its retention along the mangrove forests have different mineral and organic responsible.

1.2. Objectives

1.2.1. Main objective

Identify the sources of soil organic matter (SOM) and its chemical variations in the Botafogo River mangroves. In addition to evaluating the distribution, retention and dynamics of Hg, and its relationship with different organic compounds and soil mineralogical composition.

1.2.2. Specific objectives

- Identify the chemical nature of the SOM (origin, molecular composition, stability and dynamic) in these soils through spectroscopic and thermodegradative techniques;
- Identify how the chemical soil attributes affect the SOM quality;
- Observe relations between the organic groups of SOM and Hg;
- Identify the mineral assemblage of sand and clay fraction, and reduced minerals of the soil to relate them with the Hg dynamic.

2. LITERATURE REVIEW

2.1. The manguezal ecosystem

The mangrove ecosystem is composed of evergreen forests, formed of salinity-tolerant shrubs and trees, which grow along protected coasts, shallow water lagoons, estuaries, rivers, or deltas, distributed in 124 countries in tropical and subtropical regions of the planet (FAO, 2020). This ecosystem represents an interface between the marine and terrestrial zones, which presents peculiar characteristics that fulfill important environmental and socioeconomic functions.

The mangrove acts as multifunctional ecosystem, providing different services and products for all food chain (Figure 1). These forests protect important biodiversity, supports marine and terrestrial fauna organisms, and play a role in protecting the coast. Due to its characteristics, the mangroves provide important spawning, nursery, and feeding habitats for organisms such as the following ones: crustaceans (Ex: *Ucides cordatus, Farfantepenaeus subtilis, Callinectes danae*) fishes (Ex: *Abudefduf saxatilis, Anisotremus surinamensis, Eucinostomus melanopterus, Lutjanus alexandrei*) and migratory birds (Ex: *Buteogallus aequinoctialis, Eudocimus ruber, Bubulcus ibis, Egretta thula*), being considered an important source of food and income for the local population (CARMINATTO et al., 2020; HERRERA; COSTA, 2022; MESSIAS et al., 2019; MOTA et al., 2023; ROSELLI; BARBIERI, 2022; ZAMPROGNO et al., 2023).

Figure 1 - Ecosystem services provided by mangrove forests.

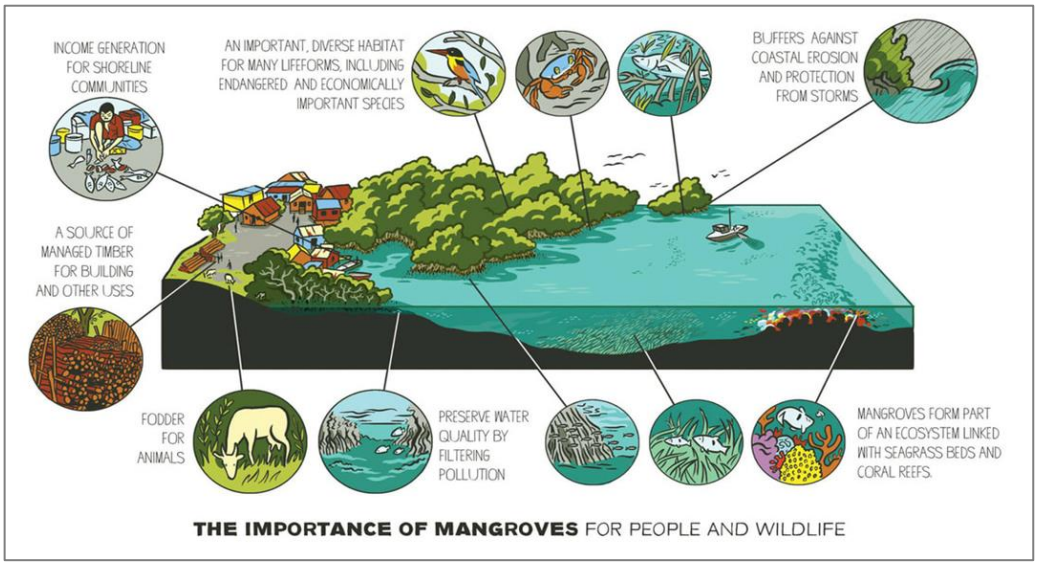

Source: news.scriberia (2023)

The mangrove flora maintains a select group of species (KUENZER et al., 2011). Unlike the higher number of species (~10.000) located in non-saline interphase zones, in the mangrove, globally, it is possible to observe a maximum of 80 of these species. This is due to the sum of adverse conditions (high salinity, anaerobiosis, strong ultraviolet light) generated by the variation of the tides, which, from an ecological evolutionary point of view, are needed and responsible for maintaining these halophytes species in the mangroves. However, these species created adaptation control, morphological structures such as rhizophores (*Rhizophora mangle*), a type of aerial stem that helps support plants in these soils. In some species (*Avicennia germinans, Laguncularia racemosa*) it is possible to identify pneumatophores, roots projecting out of the soil, which have the function of gas exchange (SRIKANTH; LUM; CHEN, 2016; XU et al., 2017). In addition, these environments play an important role in protecting the coast, attenuating the action of climatic events such as storms and tsunamis, thus protecting the coastal population (KELLEWAY et al., 2017).

The mangrove soils are formed under conditions of hydromorphism, conditioned by the action of the tides (GOMES et al., 2016). Periodic floods favor anaerobic conditions, reducing the decomposition of OM. Considering the efficient carbon sequestration, mangrove soils are considered the richest areas in carbon on the planet (ATWOOD et al., 2017; HATJE et al., 2021; SASMITO et al., 2020). The mineral phase of these soils, Holocene sediments, presents a wide granulometric variation that varies from very sandy to very clayey soils. These sediments can be fluvial, lagoon, marine-fluvial and marine (FERREIRA et al., 2007a).

According to FAO data (2020), mangroves occupy an area of 14.786.000 ha in the world, 40% of this total is present in only four countries: Indonesia (2.809.340 ha); Brazil (1.303.740 ha); Nigeria (1.035.020 ha) and Mexico (887.160 ha).

Brazil maintains the second largest mangrove area, being responsible for 9.3% of world's mangroves (ROVAI et al., 2022). Brazilian mangrove extension starts in the Amapá state (North) and goes to the state of Santa Catarina (South), following different coastal morphology and climate gradients. After the Amazon rainforest, the brazilian mangroves are the greatest forests in soil carbon storage, having the ability to store 2.7 to 4.7 times more carbon than any other ecosystem or biome. This represents a significant role in the carbon sequestration and consequently, in mitigating climate change (ROVAI et al., 2022).

The Northeast region comprises 49,7% of the mangrove forests of Brazil (ICMBIO, 2018). Due to its topographic characteristics, such as geographical position and low altitude, the mangroves growth in this part of the country is positively affected (PELAGE et al., 2021).

These conditions are marked in the East Coast of the region, where the mangrove forests of Pernambuco are located.

Pernambuco has 15 estuaries distributed along 187 km of coastline and 34 riverside communities depending on fishing and collecting mollusks and crustaceans' activities, which are economically relevant for about 13,000 fishermen who practice artisanal fishing (PELAGE et al., 2019).

2.2. Quality, dynamic and stability of organic matter of mangrove soils

Mangrove forests are considered the largest C accumulators per area on the planet (ATWOOD et al., 2017). It is estimated that this ecosystem can accumulate around 10.7 ± 9.4 Mg C ha^{-1} $year^{-1}$ through primary production, which is considered three to five times higher than any other humid forests (ALONGI, 2014). The mangrove has an effective ability to preserve the OM, produced in its forests or coming from sediments, mainly through the anoxic condition generated by tidal floods, which limits aerobic respiration (KIDA; FUJITAKE, 2020).

In the last few years, the OM derived from mangrove soils received even more attention due to the recognition of being one of the greatest C sinks on the planet. The C presents in OM stored in environments such as mangroves, salt marshes, and seagrass meadows reached such ecological importance that since 2009 it's been called "blue carbon" (BERTRAM et al., 2021). Consequently, actions of conservation and restoration of such blue carbon ecosystems (BCEs) have been a key contribution of coastal activities to mitigate environmental disasters, such as climate change and contamination.

Since mangroves are highly productive ecosystems that produce and trap disproportionately large masses of organic material, this SOM is a source not only of C but also of other elements, such as N, P and S (DAVIES et al., 2017; LEWIS et al., 2021; NÓBREGA et al., 2022).

The OM found in mangrove soils and sediments has autochthonous or allochthonous origin. Autochthonous, in situ production, corresponds to OM generated from the tree's tissues (roots, stem and leaves), microbial biomass, benthic algae, and phytoplankton. All these materials, mainly the roots, and leaves, contribute to the litter formed in the superficial layers of these soils. Allochthonous materials, derived from the oceans and land areas (urban and rural), appear in the mangroves through sediments, which are loaded with OM and contribute to the sequestration of C in these forests. The input of allochthonous OM, in terms of quantity and quality, is quite variable, considering it is totally dependent on its sources, mainly in relation

to anthropic sources (KIDA; FUJITAKE, 2020; KUSUMANINGTYAS et al., 2019; LIU et al., 2017; MARCHAND, 2017; NÓBREGA et al., 2022). Most of the OM in mangrove soils are produced in situ, being the autochthonous materials considered predominant (ALONGI et al., 1998). The greater input comes from the expressive production of subsurface fine roots, being able to achieve two to five times more OM than the leaves, the second contributor (LIU; XIONGI; LIAO, 2017).

Therefore, the autochthonous production is considered one important factor of OM entry and storage in these soils. Considering a vegetable variation in mangrove physiography, quantitative parameters related to the SOM, such as total organic carbon (TOC), C stock, plant biomass, and qualitative parameters: organic groups composition, isotopic C, and thermal stability, can change (ALONGI, 2014).

Regarding this context, the domain of the specie of tree on the mangrove forest is decisive in the quantity deposited, molecular composition and stability of SOM, which for a long time was attributed exclusively to abiotic factors such as tidal amplitude, particle size distribution and flooding period (LACERDA; ITTEKKOT; PATCHINEELAM, 1995).

The evaluation of OM composition, dynamics, and origin can be performed using spectroscopic, thermodegradative, and isotopic techniques (GIOVANELA et al., 2004; KUSUMANINGTYAS et al., 2019; SANTOS-ANDRADE et al., 2021). Fourier transform infrared spectroscopy (FTIR) and differential scanning calorimeter and thermogravimetry (DSC-TG) enable the identification of functional organic groups and the thermal stability of OM, respectively, considered relevant determinants of soil carbon stabilization and soil functions (LEI et al., 2023). A great example is the recalcitrance level of functional groups, aliphatic-C compounds, such amino acids, are more labile and easily degraded than aromatic-C, such as: lignin and tannin (LACERDA; ITTEKKOT; PATCHINEELAM, 1995). Furthermore, other groups such as aliphatic, phenolic, hydroxylic, carboxyl, and polysaccharide can be identified (PÄRNPUU et al., 2022). FTIR procedure permits the identification of organic groups due to molecule excitation that creates vibrational movement capable to be absorbed in wavelength between 4000 to 400 cm^{-1}.

DSC-TG consists in continuous and simultaneous measurement of weight loss (TG) and energy change (DSC) during heating (BARROS; SALGADO; FEIJÓO, 2007). The weight loss is manly divided in three phases: 1) residual water loss (<100ºC); 2) exothermic decomposition of aliphatic and carboxyl groups (≈300ºC), and 3) exothermic decomposition of refractory aromatic groups (≥450ºC) (LOPEZ-CAPEL et al., 2005). This procedure can act as a tool to confirm FTIR identification, since all organic groups have their own “thermal signature”.

Organic matter origin, on other hand, is described using isotopic procedures. Most common is quantify the natural abundance of $\delta^{13}C$ and $\delta^{15}N$. It assumes that SOM reflects the plant material from which it was derived (SASMITO et al., 2020). $\delta^{13}C$ is one of the three C isotope ($\delta^{12}C$, $\delta^{13}C$, and $\delta^{14}C$) identified in nature. $\delta^{13}C$ is a component of plants mechanisms and its signature reveals the photosynthetic process used, such as: C3, C4 and metabolism acid crassulacean (MAC). The $\delta^{15}N$ is also a relevant constituent of OM. The natural abundance of $\delta^{13}C$ and $\delta^{15}N$ is expressed in deviations (δ) per thousand (‰) from an international standard, with the carbon standard being Pee dee Belemnite (PDB), and the N standard being atmospheric air. Previous studies have reported the $\delta^{13}C$ and $\delta^{15}N$ abundance values of C_3 and C_4 mangrove plants, as well C from marine sources such as seagrass and algae (SASMITO et al., 2020). Subsequently, a comparison using these techniques can be performed with other soil mangrove forests covered by different species domain, as well as with the physiographic zones of the mangrove.

The soil's chemical characteristics are also responsible for the OM variation, specially the dynamic and stabilization of it. The main parameters that drive most of the reactions are pH, redox potential (Eh), and salinity (KIDA; FUJITAKE, 2020). Soil pH controls coprecipitation reactions of deprotonated acidic functional groups of OM with metals such as Fe and Al present in the aqueous-phase, being considered as one important mechanism of OM maintenance for the long-term C preservation in both soils and sediments (LALONDE et al., 2012; WAGAI; MAYER, 2007). Eh potential describes the redox processes of biogeochemical cycles due to the selection of electron acceptors by aerobic and anaerobic microorganisms during the OM decomposition (FERREIRA et al., 2007b). Salinity plays a protector role to mangrove OM by the formation of OM–clay complexes. The aggregation promoted by some sorptive interactions, such Van der Waals forces reduces the degradation processes of OM by the exposition to oxygenation and photodegradation in open coastal waters (KIDA; FUJITAKE, 2020).

2.3. Soil mineralogy of contaminated mangrove soils

In mangrove forests, the soil profile is formed by a mixture of allochthonous clastic sediments and organic materials. Mangrove areas are buffer zones between the coast and the ocean, where sediments are introduced by river discharge and the action of tidal currents, having terrestrial and marine origin (FURUKAWA; WOLANSKI, 1996). These allochthonous mineral sediments accumulate rapidly in mudbanks, which provide habitats for opportunistic organisms (WOODROFFE et al., 2016).

The mineral assemblage present in mangrove sediments and soils is highly variable (SOUZA-JÚNIOR et al., 2008). Silicates are an important mineral group in these soils, especially montmorillonite, kaolinite, illite, chlorite and interstratified clay minerals (ANDRADE et al., 2018). Also, due to the high concentration and oxi-redox conditions involving Mn, Fe and S, minerals such as: pyrite, jarosite, manganese sulfides, and gibbsite are also identified in mangrove soils (OTERO et al., 2009). Furthermore, due to water salinity contribution, minerals such halite is also present (BEHLING; DA COSTA, 2004).

The anoxic conditions of mangrove swamps promote a certain instability for crystalline Fe oxyhydroxides, as goethite, and in contact with reduced SO_4^{2-} can be readily reduced by the microbial activity and transformed into Fe sulfides, such as mackinawite, greigite, pyrite, and other metallic sulfides in short periods (FERREIRA et al., 2022; SOUZA-JÚNIOR et al., 2008).

The brazilian mangroves are multimineralic, represented mostly by kaolinite, smectite, illite and their mixed-layer phases, in addition to iron oxides, pyrite and other sulfides, gibbsite, quartz and less commonly minor amounts of primary minerals like feldspar and amphibole (ANDRADE et al., 2018; SOUZA-JÚNIOR et al., 2008; VILHENA; COSTA; BERRÊDO, 2010).

In Northeast of Brazil, the mangrove forests show mineralogical composition related to tertiary sediments of the “Barreiras formation”, a geological structure, characterized by white to yellow claystones (or mudstones), siltstones, sandstones, and conglomeratic sediments. These soils are mostly highly weathered, kaolinite-dominated and with minor amounts of Fe oxyhydroxides (BEHLING; DA COSTA, 2004).

Mangrove soils act as biogeochemistry filter in face of contaminants and this role can be provide not only by the OM compounds, but some minerals, especially reduced ones can act as sinks for trace metals (e.g., Cu, Zn, Ni, Cr). Co-precipitation reactions with minerals such pyrite, remove temporally some heavy metals out of the soil solution, being considering a trace metal-binding phase (MACHADO et al., 2014). However, the oxidation of these minerals can increase soil acidity and undo this binding process, releasing these contaminants in soil. These oxidation reactions occur, naturally, in response to spatial variability in tidal flooding, or due to anthropogenic actions, such soil drainage (MACHADO et al., 2014).

Studying the pyritization of trace metals in anoxic sediments, Huerta-diaz and Morse (1992) found a high incorporation of Hg, As, and Mo, and moderate for Co, Mn, Cu, and Ni. Furthermore, some elements, such Cu, are considered chalcophile, having more affinity with the sulfide phases than oxygen, thus forming highly insoluble compounds (ARAÚJO et al., 2022). The authors defend the importance to avoid any soil physical disturbance because it can

potentially oxidize the pyrite phase placing the heavy metals into solution, and consequently turn them more bioavailable.

Fe and Mn oxyhydroxides and carbonates also retain heavy metals dissolved in pore-waters of mangrove soils. Despite the low stability in anaerobic systems, some studies identified the contribution of Fe and Mn oxyhydroxides in heavy metals precipitation: As (THANH-NHO et al., 2019); Pb, Cu and Zn (VAN THINH et al., 2018); Cr (ARAÚJO et al., 2022); Mn (OTERO et al., 2009); Ni (NOËL et al., 2015); and Cd (JINGCHUN et al., 2008). Similar results were identified by these studies for carbonate-heavy metals association, especially for: Pb, Cu and Zn (ARAÚJO et al., 2022; VAN THINH et al., 2018); Mn (THANH-NHO et al., 2019).

2.4. Hg contamination and its retention in mangrove soils

The sediment deposition along coastal ecosystem is one of the main characteristics of these areas. In association with the sediments, heavy metals are transported for long distances and deposited in flooded areas such the mangrove forests (ARAÚJO et al., 2022). Therefore, sediments act as an important sink for anthropogenic pollution (e.g. industry, mining, urban discharges, atmospheric deposition, etc) (FENG et al., 2019).

Hg is one of the main inorganic contaminants in mangrove forests (ARAÚJO et al., 2019). It is considered one of the most worrying heavy metal due to its high toxicity, environmental persistence, and bioaccumulation (BECKERS; RINKLEBE, 2017). Furthermore, Hg bioaccumulation occurs by the consumption of high toxic forms, such methylmercury (MeHg), the most abundant Hg organic form. Based on this, Hg can cause serious risks to the ecosystems (fauna and flora) and the local population (ARAÚJO et al., 2021; SHI et al., 2020).

MeHg is an organic phase and is considered a hazardous contaminant to human health. Its neurotoxin effects were highly discussed after the Minamata disaster, in Minamata Bay in Japan between 1932 and 1968 (AASETH et al., 2020). Local Japanese population that lived around the bay of Minamata city suffered from MeHg poisoning after ingestion of seafood contaminated. The effluent was composed mainly by Hg and it was released by a local petrochemical and plastics maker. The final damages were 900 people died and thousands of others suffered from nervous system disorders, causing blindness, seizures, and a host of sensory disorders (MCCURRY, 2006).

Despite being found in low concentration in earth's upper crust (~0.05 ppm), Hg concentration can be increased by human activities. In coastal areas, the main anthropogenic actions responsible for the release of Hg are the following: gold mining (BECKERS;

RINKLEBE, 2017; LINO et al., 2019) and deposition of waste from the chemical and metallurgical industries (ARAÚJO et al., 2019; LIU et al., 2019).

Among the industries in the chemical sector, chlor–alkali plants (CAP) are the major sources of Hg in the environment. Hg contamination by these industries comes from the saline solution (NaCl) electrolysis process, carried out during production, where Hg cells are used. In this process, Hg losses occur, small but constant, generating effluents and emissions that can cause serious environmental risks (BOLAÑOS-ÁLVAREZ et al., 2016). Currently, 14% of Brazilian production in the soda-chlorine sector employs the technology of Hg (FERNANDES; GUIMARÃES; GLÓRIA, 2009).

A chlor-alkali plant located in Northeast region of Brazil responsible to produce caustic soda caused a severe environmental impact for estuaries. In the 1980s, high levels of Hg were identified in sediments, water and tissues of fish and oysters in mangrove areas (MEYER, 1996; MEYER; HAGEN; MEDEIROS, 1998). According to this study, 35 tons of Hg were dumped in the Botafogo River between 1964 and 1986. Since then, these Hg levels in the Botafogo River estuary have been considered the highest on the entire Brazilian coast. Araújo et al. (2021), evaluating soils and sediments in these areas, identified values of the order of 14.4 mg kg^{-1}, 180 times higher than the local background value (~0.085 mg kg^{-1} Hg).

Hg biogeochemical dynamic is highly correlated with OM due to the affinity with organic compounds. Therefore, considering the high OM sequestration in mangrove sediments is believed to have a major impact on Hg cycling and Hg methylation (DUAN et al., 2021). Additionally, for Hg contaminated areas such Botafogo River mangroves, beyond the role to serve as a huge pool for C storage, these soils and sediments consequently act as a large sink for sequestering Hg from external sources (HARIS; ARIS; MOKHTAR, 2017).

Hg can remain strongly retained in mangrove soils reducing its bioavailability and bioaccumulation (NDUNGU; SCHAANNING; BRAATEN, 2016). The decomposition of OM generates a significant amount of reactive compounds and two of them are relevant in terms of formation of complex Hg-OM, reduced sulfur groups and oxidized C groups (RAVICHANDRAN, 2004; SKYLLBERG et al., 2006). Among the S reduced groups, three significantly participates on Hg complexation: thiols, sulfides, and disulfides. These components are present in dissolved organic matter (DOM), a fraction of OM composed by low molecular weight functional groups that are reactive in soil. In aquatic environments, oxidized C groups represents 20% of DOM composition and in oxidized zones, as surface layer, carbohydrates, carboxylic acids, amino acids, hydrocarbons also act retaining contaminants, such Hg (RAVICHANDRAN, 2004).

Therefore, two topics are correlated and should be highlighted about Hg adsorption in aquatic ecosystem, such mangroves. First, the adsorption of contaminants by OM varies with the vegetation type and second, the anthropogenic activities can negative affect it due to the impacts caused in SOM.

However, only few studies have evaluated the influence of the vegetation domain in OM quality with Hg retention in mangrove soils, and the attention related to the anthropogenic activities usually stops on loss of C studies (DUAN et al., 2021; MACHADO et al., 2016; PÉREZ et al., 2020). For example, *R. mangle* forests can release more refractory components on soil, such tannins, a class of polyphenols, compared to *Avicennia* and *Laguncularia* forests. Tannins are known to suppress microbial activity, responsible for produce reactive compounds that complex Hg (LACERDA et al., 1995). At this case, Hg could be more environmentally available considering the decrease of organic C releasement, responsible for its complexation. In addition, other species can release less aromatic C and produce more labile C, such carboxylic acid, but human activities can reduce the availability of them by the deforestation advancement and soil drainage, actions that accelerate its decomposition and loss to atmosphere (SANTOS-ANDRADE et al., 2021).

REFERENCES

AASETH, J.; WALLACE, D. R.; VEJRUP, K.; ALEXANDER, J. Methylmercury and developmental neurotoxicity: A global concern. **Current Opinion in Toxicology**, v. 19, p. 80–87, 2020. https://doi.org/10.1016/j.cotox.2020.01.005

ALONGI, D. M.; SASEKUMAR, A.; TIRENDI, F.; DIXON, P. The influence of stand age on benthic decomposition and recycling of organic matter in managed mangrove forests of Malaysia. **Journal of Experimental Marine Biology and Ecology**, v. 225, p. 197–218, 1998. https://doi.org/10.1016/S0022-0981(97)00223-2

ALONGI, D. M. Carbon Cycling and Storage in Mangrove Forests. **Annual Review of Marine Science**, v. 6, p. 195–219, 2014. https://doi.org/10.1146/annurev-marine-010213-135020

ANDRADE, G. R.; CUADROS, J.; PARTITI, C. S.; COHEN, R.; VIDAL-TORRADO, P. Sequential mineral transformation from kaolinite to Fe-illite in two Brazilian mangrove soils. **Geoderma**, v. 309, p. 84–99, 2018. https://doi.org/10.1016/j.geoderma.2017.08.042

ARAÚJO, P. R. M.; BIONDI, C. M.; DO NASCIMENTO, C. W. A.; DA SILVA, F. B. V.; ALVAREZ, A. Bioavailability and sequential extraction of mercury in soils and organisms of a mangrove contaminated by a chlor-alkali plant. **Ecotoxicology and Environmental Safety**, v. 183, p. 109469, 2019. https://doi.org/10.1016/j.ecoenv.2019.109469

ARAÚJO, P. R. M.; BIONDI, C. M.; DO NASCIMENTO, C. W. A.; DA SILVA, F. B. V.; DA SILVA, W. R.; DA SILVA, F. L.; DE MELO FERREIRA, D. K. Assessing the spatial distribution and ecologic and human health risks in mangrove soils polluted by Hg in northeastern Brazil. **Chemosphere**, v. 266, p. 129019, 2021. https://doi.org/10.1016/j.chemosphere.2020.129019

ARAÚJO, P. R. M.; BIONDI, C. M.; DO NASCIMENTO, C. W. A.; DA SILVA, F. B. V.; FERREIRA, T. O.; DE ALCÂNTARA, S. F. Geospatial modeling and ecological and human health risk assessments of heavy metals in contaminated mangrove soils. **Marine Pollution Bulletin**, v. 177, p. 113489, 2022. https://doi.org/10.1016/j.marpolbul.2022.113489

ATWOOD, T. B.; CONNOLLY, R. M.; ALMAHASHEER, H.; CARNELL, P. E.; DUARTE, C. M.; EWERS LEWIS, C. J.; LOVELOCK, C. E. Global patterns in mangrove soil carbon stocks and losses. **Nature Climate Change**, v. 7, p. 523–528, 2017. https://doi.org/10.1038/nclimate3326

BARROS, N.; SALGADO, J.; FEIJÓO, S. Calorimetry and soil. **Thermochimica Acta**, v. 458, p. 11–17, 2007. https://doi.org/10.1016/j.tca.2007.01.010

BECKERS, F.; RINKLEBE, J. Cycling of mercury in the environment: Sources, fate, and human health implications: A review. **Critical Reviews in Environmental Science and Technology**, v. 47, p. 693–794, 2017. https://doi.org/10.1080/10643389.2017.1326277

BEHLING, H.; DA COSTA, M. L. Mineralogy, geochemistry, and palynology of modern and late Tertiary mangrove deposits in the Barreiras Formation of Mosqueiro Island, northeastern Pará state, eastern Amazonia. **Journal of South American Earth Sciences**, v. 17, p. 285–295, 2004. https://doi.org/10.1016/j.jsames.2004.08.002

BERTRAM, C.; QUAAS, M.; REUSCH, T. B.; VAFEIDIS, A. T.; WOLFF, C.; RICKELS, W. The blue carbon wealth of nations. **Nature Climate Change**, v. 11, p. 704–709, 2021. https://doi.org/10.1038/s41558-021-01172-w

BOLAÑOS-ÁLVAREZ, Y.; ALONSO-HERNÁNDEZ, C. M.; MORABITO, R.; DÍAZ-ASENCIO, M.; PINTO, V.; GÓMEZ-BATISTA, M. Mercury contamination of riverine sediments in the vicinity of a mercury cell chlor-alkali plant in Sagua River, Cuba. **Chemosphere**, v. 152, p. 376–382, 2016. https://doi.org/10.1016/j.chemosphere.2016.03.02

CARMINATTO, A. A.; ROTUNDO, M. M.; BUTTURI-GOMES, D.; BARRELLA, W.; JUNIOR, M. P. Effects of habitat complexity and temporal variation in rocky reef fish communities in the Santos estuary (SP), Brazil. **Ecological Indicators**, v. 108, p. 105728, 2020. https://doi.org/10.1016/j.ecolind.2019.105728

DAVIES, T. K.; LOVELOCK, C. E.; PETTIT, N. E.; GRIERSON, P. F. Short-term microbial respiration in an arid zone mangrove soil is limited by availability of gallic acid, phosphorus and ammonium. **Soil Biology and Biochemistry**, v. 115, p. 73–81, 2017. https://doi.org/10.1016/j.soilbio.2017.08.010

DUAN, D.; LEI, P., LAN, W.; LI, T.; ZHANG, H.; ZHONG, H.; PAN, K. Litterfall-derived organic matter enhances mercury methylation in mangrove sediments of South China. **Science of the Total Environment**, v. 765, p. 142763, 2021. https://doi.org/10.1016/j.scitotenv.2020.142763

FOOD AND AGRICULTURE ORGANIZATION (FAO). **Global Forest Resources Assessment.** Rome, Italy, 2020. p. 38-39.

FENG, C.; PEDRERO, Z.; LIMA, L.; OLIVARES, S.; DE LA ROSA, D.; BERAIL, S.; AMOUROUX, D. Assessment of Hg contamination by a Chlor-Alkali Plant in riverine and coastal sites combining Hg speciation and isotopic signature (Sagua la Grande River, Cuba). **Journal of Hazardous Materials**, v. 371, p. 558–565, 2019. https://doi.org/10.1016/j.jhazmat.2019.02.092

FERNANDES, E.; GUIMARÃES, B. D. A.; GLÓRIA, A. M. D. S. **O setor de soda-cloro no Brasil e no mundo**. BNDES Setorial, Rio de Janeiro, n. 29, 2009. p. 279-320.

FERREIRA, T. O.; VIDAL-TORRADO, P.; OTERO, X. L.; MACÍAS, F. Are mangrove forest substrates sediments or soils? A case study in southeastern Brazil. **Catena**, v. 70, p. 79–91, 2007a. https://doi.org/10.1016/j.catena.2006.07.006

FERREIRA, T. O.; OTERO, X. L.; VIDAL-TORRADO, P.; MACÍAS, F. Redox processes in mangrove soils under *Rhizophora mangle* in relation to different environmental conditions. **Soil Science Society of America Journal**, v. 71, p. 484–491, 2007b. https://doi.org/10.2136/sssaj2006.0078

FERREIRA, T. O.; QUEIROZ, H. M.; NÓBREGA, G. N.; DE SOUZA JÚNIOR, V. S.; BARCELLOS, D.; FERREIRA, A. D.; OTERO, X. L. Litho-climatic characteristics and its control over mangrove soil geochemistry: A macro-scale approach. **Science of the Total Environment**, v. 811, p. 152152, 2022. https://doi.org/10.1016/j.scitotenv.2021.152152

FURUKAWA, K.; WOLANSKI, E. Sedimentation in mangrove forests. **Mangroves and salt marshes**, v. 1, p. 3–10, 1996. https://doi.org/10.1023/A:1025973426404

GIOVANELA, M.; PARLANTI, E.; EJ, S. S.; MMD, S. Elemental compositions, FT-IR spectra and thermal behavior of sedimentary fulvic and humic acids from aquatic and terrestrial environments. **Geochemical Journal**, v. 38, p. 255–264, 2004. https://doi.org/10.2343/geochemj.38.255

GOMES, F. H.; KER, J. C.; FERREIRA, T. O.; MOREAU, A. M. S. D. S.; MOREAU, M. S. Characterization and pedogenesis of mangrove soils from Ilhéus-BA, Brazil. **Revista Ciência Agronômica**, v. 47, p. 599–608, 2016. https://doi.org/10.5935/1806-6690.20160072

HARIS, H.; ARIS, A. Z.; MOKHTAR, M. BIN. Mercury and methylmercury distribution in the intertidal surface sediment of a heavily anthropogenically impacted saltwater-mangrove-sediment interplay zone. **Chemosphere**, v. 166, p. 323–333, 2017. https://doi.org/10.1016/j.chemosphere.2016.09.045

HATJE, V.; MASQUÉ, P.; PATIRE, V. F.; DÓREA, A.; BARROS, F. Blue carbon stocks, accumulation rates, and associated spatial variability in Brazilian mangroves. **Limnology and Oceanography**, v. 66, p. 321–334, 2021. https://doi.org/10.1002/lno.11607

HERRERA, D. R.; COSTA, R. C. DA. Distributional patterns of two sympatric blue crabs (Callinectes) and the implications for conservation management at the South-west Atlantic subtropical shelf. **Marine Biology Research**, v. 18, p. 466–476, 2022. https://doi.org/10.1080/17451000.2022.2147950

HUERTA-DIAZ, M. A.; MORSE, J. W. Pyritization of trace metals in anoxic marine sediments. **Geochimica et Cosmochimica Acta**, v. 56, p. 2681–2702, 1992. https://doi.org/10.1016/0016-7037(92)90353-K

ICMBIO. **Atlas dos Manguezais do Brasil**. Em: Brasília: Instituto Chico Mendes, 2018. p. 218.

JINGCHUN, L.; CHONGLING, Y.; RUIFENG, Z.; HAOLIANG, L.; GUANGQIU, Q. Speciation changes of cadmium in mangrove (*Kandelia candel* (L.)) rhizosphere sediments. **Bulletin of environmental contamination and toxicology**, v. 80, p. 231–236, 2008. https://doi.org/10.1007/s00128-007-9351-z

KELLEWAY, J. J.; CAVANAUGH, K.; ROGERS, K.; FELLER, I. C.; ENS, E.; DOUGHTY, C.; SAINTILAN, N. Review of the ecosystem service implications of mangrove encroachment into salt marshes. **Global Change Biology**, v. 23, p. 3967–3983, 2017. https://doi.org/10.1111/gcb.13727

KIDA, M.; FUJITAKE, N. Organic carbon stabilization mechanisms in mangrove soils: a review. **Forests**, v. 11, p. 981, 2020. https://doi.org/10.3390/f11090981

KUENZER, C.; BLUEMEL, A.; GEBHARDT, S.; QUOC, T. V.; DECH, S. Remote Sensing of Mangrove Ecosystems: A Review. **Remote Sensing**, v. 3, p. 878–928, 2011. https://doi.org/10.3390/rs3050878

KUSUMANINGTYAS, M. A.; HUTAHAEAN, A. A.; FISCHER, H. W.; PÉREZ-MAYO, M.; RANSBY, D.; JENNERJAHN, T. C. Variability in the organic carbon stocks, sources, and accumulation rates of Indonesian mangrove ecosystems. **Estuarine, Coastal and Shelf Science**, v. 218, p. 310–323, 2019. https://doi.org/10.1016/j.ecss.2018.12.007

LACERDA, L. D.; ITTEKKOT, V.; PATCHINEELAM, S. R. Biogeochemistry of Mangrove Soil Organic Matter: A Comparison Between *Rhizophora* and *Avicennia* Soils in South-eastern Brazil. **Elsevier**, v. 40, p. 713–720, 1995. https://doi.org/10.1006/ecss.1995.0048

LALONDE, K.; MUCCI, A.; OUELLET, A.; GÉLINAS, Y. Preservation of organic matter in sediments promoted by iron. **Nature**, v. 483, p. 198–200, 2012. https://doi.org/10.1038/nature10855

LEI, W.; PAN, Q.; TENG, P.; YU, J.; LI, N. How does soil organic matter stabilize with soil and environmental variables along a black soil belt in Northeast China? An explanation using FTIR spectroscopy data. **Catena**, v. 228, p. 107152, 2023. https://doi.org/10.1016/j.catena.2023.107152

LEWIS, D. B.; JIMENEZ, K. L.; ABD-ELRAHMAN, A.; ANDREU, M. G.; LANDRY, S. M.; NORTHROP, R. J.; RICHARDS, C. L. Carbon and nitrogen pools and mobile fractions in surface soils across a mangrove saltmarsh ecotone. **Science of the Total Environment**, v. 798, p. 149328, 2021. https://doi.org/10.1016/j.scitotenv.2021.149328

LINO, A. S.; KASPER, D.; GUIDA, Y. S.; THOMAZ, J. R.; MALM, O. Total and methyl mercury distribution in water, sediment, plankton and fish along the Tapajós River basin in the Brazilian Amazon. **Chemosphere**, v. 235, p. 690–700, 2019. https://doi.org/10.1016/j.chemosphere.2019.06.212

LIU, L.; WANG, J.; WANG, L.; HU, Y.; MA, X. Vertical distributions of mercury in marine sediment cores from central and southern part of Bohai Sea, China. **Ecotoxicology and Environmental Safety**, v. 170, p. 399–406, 2019. https://doi.org/10.1016/j.ecoenv.2018.12.003

LIU, X.; XIONG, Y.; LIAO, B. Relative contributions of leaf litter and fine roots to soil organic matter accumulation in mangrove forests. **Plant and Soil**, v. 421, p. 493–503, 2017. https://doi.org/10.1007/s11104-017-3477-5

LOPEZ-CAPEL, E.; SOHI, S. P.; GAUNT, J. L.; MANNING, D. A. Use of thermogravimetry–differential scanning calorimetry to characterize modelable soil organic matter fractions. **Soil Science Society of America Journal**, v. 69, p. 136–140, 2005. https://doi.org/10.2136/sssaj2005.0136a

MACHADO, W.; SANDERS, C. J.; SANTOS, I. R.; SANDERS, L. M.; SILVA-FILHO, E. V.; LUIZ-SILVA, W. Mercury dilution by autochthonous organic matter in a fertilized mangrove wetland. **Environmental Pollution**, v. 213, p. 30-35, 2016. https://doi.org/10.1016/j.envpol.2016.02.002

MACHADO, W.; BORRELLI, N. L.; FERREIRA, T. O.; MARQUES, A. G. B.; OSTERRIETH, M.; GUIZAN, C. Trace metal pyritization variability in response to mangrove soil aerobic and anaerobic oxidation processes. **Marine pollution bulletin**, v. 79, p. 365–370, 2014. https://doi.org/10.1016/j.marpolbul.2013.11.016

MARCHAND, C. Soil carbon stocks and burial rates along a mangrove forest chronosequence (French Guiana). **Forest Ecology and Management**, v. 384, p. 92–99, 2017. https://doi.org/10.1016/j.foreco.2016.10.030

MCCURRY, J. Japan remembers minamata. **The Lancet**, v. 367, p. 99–100, 2006. https://doi.org/10.1016/S0140-6736(06)67944-0

MESSIAS, M. A.; ALVES, T. I.; MELO, C. M.; LIMA, M.; RIVERA-REBELLA, C.; RODRIGUES, D. F.; MADI, R. R. Ethnoecology of Lutjanidae (snappers) in communities of artisanal fisheries in northeast Brazil. **Ocean & Coastal Management**, v. 181, p. 104866, 2019. https://doi.org/10.1016/j.ocecoaman.2019.104866

MEYER, U. On the fate of mercury in the northeastern Brazilian mangrove system, Canal de Santa Cruz, Pernambuco. **ZMT Contrib**, p. 105, 1996.

MEYER, U.; HAGEN, W.; MEDEIROS, C. Mercury in a northeastern Brazilian mangrove area, a case study: potential of the mangrove oyster *Crassostrea rhizophorae* as bioindicator for mercury. **Marine Biology**, v. 131, p. 113–121, 1998. https://doi.org/10.1007/s002270050302

MOTA, T. A.; PINHEIRO, M. A. A.; EVANGELISTA-BARRETO, N. S.; DA ROCHA, S. S. Density and extractive potential of "uçá"crab, *Ucides cordatus* (Linnaeus, 1763), in mangroves of the "Todos os Santos" Bay, Bahia, Brazil. **Fisheries Research**, v. 265, p. 106733, 2023. https://doi.org/10.1016/j.fishres.2023.106733

NDUNGU, K.; SCHAANNING, M.; BRAATEN, H. F. V. Effects of organic matter addition on methylmercury formation in capped and uncapped marine sediments. **Water Research**, v. 103, p. 401–407, 2016. https://doi.org/10.1016/j.watres.2016.07.055

NEW.SCRIBERIA. **Mangrove mission made visible**. Disponível em: <https://news.scriberia.com/mangrove-mission> Acesso em 19 de agosto 2023.

NÓBREGA, M. S.; SILVA, B. S.; TSCHOEKE, D. A.; APPOLINARIO, L. R.; CALEGARIO, G.; VENAS, T. M.; THOMPSON, F. L. Mangrove microbiome reveals importance of sulfur metabolism in tropical coastal waters. **Science of The Total Environment**, v. 813, p. 151889, 2022. https://doi.org/10.1016/j.scitotenv.2021.151889

NOËL, V.; MORIN, G.; JUILLOT, F.; MARCHAND, C.; BREST, J.; BARGAR, J. R.; BROWN JR, G. E. Ni cycling in mangrove sediments from New Caledonia. **Geochimica et Cosmochimica Acta**, v. 169, p. 82–98, 2015. https://doi.org/10.1016/j.gca.2015.07.024

OTERO, X. L.; FERREIRA, T. O.; HUERTA-DÍAZ, M. A.; PARTITI, C. S. D. M.; SOUZA JR, V.; VIDAL-TORRADO, P.; MACÍAS, F. Geochemistry of iron and manganese in soils and sediments of a mangrove system, Island of Pai Matos (Cananeia—SP, Brazil). **Geoderma**, v. 148, p. 318–335, 2009. https://doi.org/10.1016/j.geoderma.2008.10.016

PÄRNPUU, S.; ASTOVER, A.; TÕNUTARE, T.; PENU, P.; KAUER, K. Soil organic matter qualification with FTIR spectroscopy under different soil types in Estonia. **Geoderma Regional**, v. 28, p. e00483, 2022. https://doi.org/10.1016/j.geodrs.2022.e00483

PELAGE, L.; DOMALAIN, G.; LIRA, A. S.; TRAVASSOS, P.; FRÉDOU, T. Coastal land use in Northeast Brazil: mangrove coverage evolution over three decades. **Tropical Conservation Science**, v. 12, p. 1940082918822411, 2019. https://doi.org/10.1177/1940082918822411

PELAGE, L.; GONZALEZ, J. G.; LE LOC'H, F.; FERREIRA, V.; MUNARON, J. M.; LUCENA-FREDOU, F.; FREDOU, T. Importance of estuary morphology for ecological connectivity with their adjacent coast: A case study in Brazilian tropical estuaries. **Estuarine, Coastal and Shelf Science**, v. 251, p. 107184, 2021. https://doi.org/10.1016/j.ecss.2021.107184

PÉREZ, A.; MACHADO, W.; GUTIÉRREZ, D.; SALDARRIAGA, M. S.; SANDERS, C. J. Shrimp farming influence on carbon and nutrient accumulation within Peruvian mangroves sediments. **Estuarine, Coastal and Shelf Science**, v. 243, p. 106879, 2020. https://doi.org/10.1016/j.ecss.2020.106879

RAVICHANDRAN, M. Interactions between mercury and dissolved organic matter—a review. **Chemosphere**, v. 55, p. 319–331, 2004. https://doi.org/10.1016/j.chemosphere.2003.11.011

ROSELLI, L. Y.; BARBIERI, E. Seasonal variation of estuarine birds from Trapandé Bay, Cananéia, Brazil. **Ocean and Coastal Research**, v. 70, p. e22003, 2022. https://doi.org/10.1590/2675-2824070.21067lyr

ROVAI, A. S.; TWILLEY, R. R.; WORTHINGTON, T. A.; RIUL, P. Brazilian mangroves: blue carbon hotspots of national and global relevance to natural climate solutions. **Frontiers in Forests and Global Change**, v. 4, p. 217, 2022. https://doi.org/10.3389/ffgc.2021.787533

SANTOS-ANDRADE, M.; HATJE, V.; ARIAS-ORTIZ, A.; PATIRE, V. F.; DA SILVA, L. A. Human disturbance drives loss of soil organic matter and changes its stability and sources in mangroves. **Environmental Research**, v. 202, p. 111663, 2021. https://doi.org/10.1016/j.envres.2021.111663

SASMITO, S. D.; KUZYAKOV, Y.; LUBIS, A. A.; MURDIYARSO, D.; HUTLEY, L. B.; BACHRI, S.; BORCHARD, N. Organic carbon burial and sources in soils of coastal mudflat and mangrove ecosystems. **Catena**, v. 187, 1 abr. 2020. https://doi.org/10.1016/j.catena.2019.104414

SHI, C.; YU, L.; CHAI, M.; NIU, Z.; LI, R. The distribution and risk of mercury in Shenzhen mangroves, representative urban mangroves affected by human activities in China. **Marine Pollution Bulletin**, v. 151, p. 110866, 2020. https://doi.org/10.1016/j.marpolbul.2019.110866

SKYLLBERG, U.; BLOOM, P. R.; QIAN, J.; LIN, C. M.; BLEAM, W. F. Complexation of mercury (II) in soil organic matter: EXAFS evidence for linear two-coordination with reduced sulfur groups. **Environmental science & technology**, v. 40, p. 4174–4180, 2006. https://doi.org/10.1021/es0600577

SOUZA-JÚNIOR, V. S. D.; VIDAL-TORRADO, P.; GARCIA-GONZALÉZ, M. T.; OTERO, X. L.; MACÍAS, F. Soil mineralogy of mangrove forests from the state of São Paulo, southeastern Brazil. **Soil Science Society of America Journal**, v. 72, p. 848–857, 2008. https://doi.org/10.2136/sssaj2007.0197

SRIKANTH, S.; LUM, S. K. Y.; CHEN, Z. Mangrove root: adaptations and ecological importance. **Trees**, v. 30, p. 451–465, 2016. https://doi.org/10.1007/s00468-015-1233-0

THANH-NHO, N.; MARCHAND, C.; STRADY, E.; VINH, T. V.; NHU-TRANG, T. T. Metals geochemistry and ecological risk assessment in a tropical mangrove (Can Gio, Vietnam). **Chemosphere**, v. 219, p. 365–382, 2019. https://doi.org/10.1016/j.chemosphere.2018.11.163

VAN THINH, N.; OSANAI, Y.; ADACHI, T.; THAI, P. K.; NAKANO, N.; OZAKI, A.; KUROSAWA, K. Chemical speciation and bioavailability concentration of arsenic and heavy metals in sediment and soil cores in estuarine ecosystem, Vietnam. **Microchemical Journal**, v. 139, p. 268–277, 2018. https://doi.org/10.1016/j.microc.2018.03.005

VILHENA, M. D. P. S. P.; COSTA, M. L. DA; BERRÊDO, J. F. Continental and marine contributions to formation of mangrove sediments in an Eastern Amazonian mudplain: The case of the Marapanim Estuary. **Journal of South American Earth Sciences**, v. 29, p. 427–438, 2010. https://doi.org/10.1016/j.jsames.2009.07.005

WAGAI, R.; MAYER, L. M. Sorptive stabilization of organic matter in soils by hydrous iron oxides. **Geochimica et Cosmochimica Acta**, v. 71, p. 25–35, 2007. https://doi.org/10.1016/j.gca.2006.08.047

WOODROFFE, C. D.; ROGERS, K.; MCKEE, K. L.; LOVELOCK, C. E.; MENDELSSOHN, I. A.; SAINTILAN, N. Mangrove sedimentation and response to relative sea-level rise. **Annual review of marine science**, v. 8, p. 243–266, 2016. https://doi.org/10.1146/annurev-marine-122414-034025

XU, S.; HE, Z.; ZHANG, Z.; GUO, Z.; GUO, W.; LYU, H.; SHI, S. The origin, diversification and adaptation of a major mangrove clade (Rhizophoreae) revealed by whole-genome sequencing. **National Science Review**, v. 4, p. 721–734, 2017. https://doi.org/10.1093/nsr/nwx065

ZAMPROGNO, G. C.; TOGNELLA, M. M. P.; DA COSTA, M. B.; OTEGUI, M. B. P.; MENEZES, K. M. Spatio-temporal distribution of benthic fauna in mangrove areas in the Bay of Vitória estuary, Brazil. **Regional Studies in Marine Science**, v. 62, p. 102939, 2023. https://doi.org/10.1016/j.rsma.2023.102939

3. CARACTERIZAÇÃO QUÍMICA E FÍSICA DE SOLOS DE MANGUEZAL CONTAMINADO POR Hg

Resumo

O estuário do rio Botafogo, localizado no litoral norte de Pernambuco, é um dos mais importantes sistemas biológicos do Brasil. A bacia hidrográfica do Botafogo contribui para o abastecimento de água potável de toda região metropolitana do Recife, capital do estado. Entretanto, há décadas que atividades antrópicas, como: indústrias do setor químico, cultivo de cana-de-açúcar e carcinicultura, vêm provocando a liberação de contaminantes altamente tóxicos, como o mercúrio, no rio Botafogo. Os objetivos foram: 1) determinar os atributos químicos e físicos dos solos das diferentes florestas de mangue; 2) determinar os teores de metais pesados no solo; 3) estabelecer a relação entre os atributos do solo e a contaminação por Hg e 4) avaliar a contaminação de Hg comparando com valores ambientalmente disponíveis e background. As amostras de solo foram coletadas nas áreas de bosque e a coleta contemplou a variabilidade vegetal, ou seja, coletadas em solos de diferentes florestas (*Laguncularia racemosa*, coexistência de espécies e *Rhizophora mangle*). Os atributos químicos e físicos determinados foram: Eh, CE, pH, granulometria, matéria orgânica (MO), C e N. Além disto, foram determinados os teores totais de Na, Ca, Mg, Al, Si, Fe, S, Cl, e metais pesados: Mn, Ni, Cu, Zn, As, Cd, Pb, and Hg. Os solos apresentaram teor de MO e C semelhante, com diferença apenas na seção próximo a foz, devido a contribuição de carbonatos. Em ordem decrescente, os teores médios, mg kg^{-1}, dos metais foram: Mn (179,43); >Cr (96,43) >Zn (79,87) >Ni (60,57) >Pb (42,57) >Cu (28,73) >Hg (14,3)>As (4,23) >Cd (0,67). Todos os metais obtiveram concentração superior ao background local, com destaque para o Hg que teve concentração 161 vezes superior. Considerando o efeito tóxico destes metais, a contaminação enfatiza o alerta para biota e população local, ressaltando a necessidade de constantes monitoramentos ambientais com o intuito de se avaliar os níveis de contaminação nestas areas.

Palavras-chave: Poluição. Rio Botafogo. Metais pesados.

CHEMICAL AND PHYSICAL CHARACTERIZATION OF MANGROVE SOIL CONTAMINATED BY Hg

Abstract

The Botafogo River estuary, located on the north coast of Pernambuco, is one of Brazil's most important biological systems. The Botafogo watershed contributes to the drinking water supply of the entire metropolitan region of Recife, the state capital. However, for decades, human activities, such as: chemical industries, sugarcane cultivation, and shrimp farming have been causing the release of highly toxic contaminants, such as mercury, into the Botafogo River. The objectives were: 1) determine the soil chemical and physical attributes of different mangrove forests; 2) determine the levels of heavy metals in the soil; 3) establish the relationship between soil attributes and Hg contamination and 4) evaluate Hg contamination by comparing with environmentally available and background values. Soil samples were collected in forest areas and the sampling considered the vegetal variability, collected in soils from different forests (*Laguncularia racemosa*, coexistence of species and *Rhizophora mangle*). The chemical and physical attributes determined were: Eh, EC, pH, granulometry, organic matter (MO), C, and N. In addition, the total contents of Na, Ca, Mg, Al, Si, Fe, S, Cl, and heavy metals: Mn, Ni, Cu, Zn, As, Cd, Pb, and Hg were determined. The soils had similar OM and C content, with differences only in the section close to the mouth, due to the contribution of carbonates. In decreasing order, the average levels, mg kg^{-1}, of metals were: Mn (179.43); >Cr (96.43) >Zn (79.87) >Ni (60.57) >Pb (42.57) >Cu (28.73) >Hg (14.3) >As (4.23) >Cd (0.67). All metals obtained a concentration higher than the local background, especially Hg, which obtained a concentration 161-fold higher. Considering the toxic effect of these metals, contamination emphasizes the alert for biota and the local population, highlighting the need for constant environmental monitoring to assess contamination levels in these areas.

Keywords: Pollution. Botafogo River. Heavy metals.

3.1. Introduction

Uncontrolled growth of anthropogenic activities and urbanization without environmental protection planning have generated impacts on coastal ecosystems. For environments, such as mangrove forests, wastes produced by different point and diffuse sources, mainly sewage, industrial effluents, and agricultural chemicals runoff have raised concerns about its preservation and human health (ARAÚJO et al., 2019; LI et al., 2022).

Mangroves are in a transitional zone between land and marine environments, thus making it a deposition ecosystem. Therefore, besides the sediments resulting from weathering and erosion, numerous contaminants, such as heavy metals are deposited in mangrove soils (PASSOS et al., 2022). Globally, heavy metals represent a significant threat to this ecosystem and many studies have related contamination events around the world, such as China (CHAI et al., 2019); India (CHOUDHURY et al., 2021); Caribbean Sea (FUENTES-GANDARA et al., 2021); Red Sea (ALHARBI et al., 2019); Central Africa (AFONSO et al., 2023) and Brazil (ARAÚJO et al., 2022). All reports had heavy metals pollution due to agricultural runoff, industrial and urban effluents, and chemical spills activities as mainly contributors.

In this context, Hg is one of the main threats due to its long persistence and toxicity, capable to produce damage for all food chain (VIANA et al., 2023). The main anthropogenic sources are gold mining (PALACIOS-TORRES; CABALLERO-GALLARDO; OLIVERO-VERBEL, 2018) and chemical industries, such chlor-alkali plant (ARAÚJO et al., 2019). After its release, Hg ions achieve soil, water bodies, and air, being deposited on mangrove sediments, where it is converted to methylmercury (MeHg) (OLIVEIRA et al., 2015). Once there, MeHg is consumed by predator species, including humans. Hg causes several damages for nervous system: causing sensory and mental disturbances, motor and cognitive dysfunction, ataxia, constriction of the visual field, audition problems (BECKERS; RINKLEBE, 2017), as well as deleterious effects on the renal, pulmonary, cardiovascular, digestive, and immune system (BECKERS; RINKLEBE, 2017).

In this environmental framework, the coast of northeastern Brazil holds a Hg history of contamination caused by a mercury-cell chlor-alkali plant. About 22 to 35 tons of effluent containing Hg were released on the Botafogo River, located in Pernambuco state, between 1960 and 1980 (MEYER, 1996; 1998). The plant is located 8 km away from the mangrove evaluated. After geochemical evaluations, the Hg content was considered the highest concentration on the Brazilian coast (ARAÚJO et al., 2019).

The aims of this study were: 1) determine soil chemical and physical attributes and associate it with the estuary location; 2) determine total content of heavy metals; 3) establish the relationship between soil attributes and Hg contamination, and 4) compare the total content of heavy metal with environmentally available and local background values.

3.2. Material and methods

3.2.1. Study area

The mangrove area evaluated is located on the limits of the Botafogo River estuary, Goiana, north coast of Pernambuco state (Figure 2).

Figure 2 - Location of the study area and indication of sampling sites.

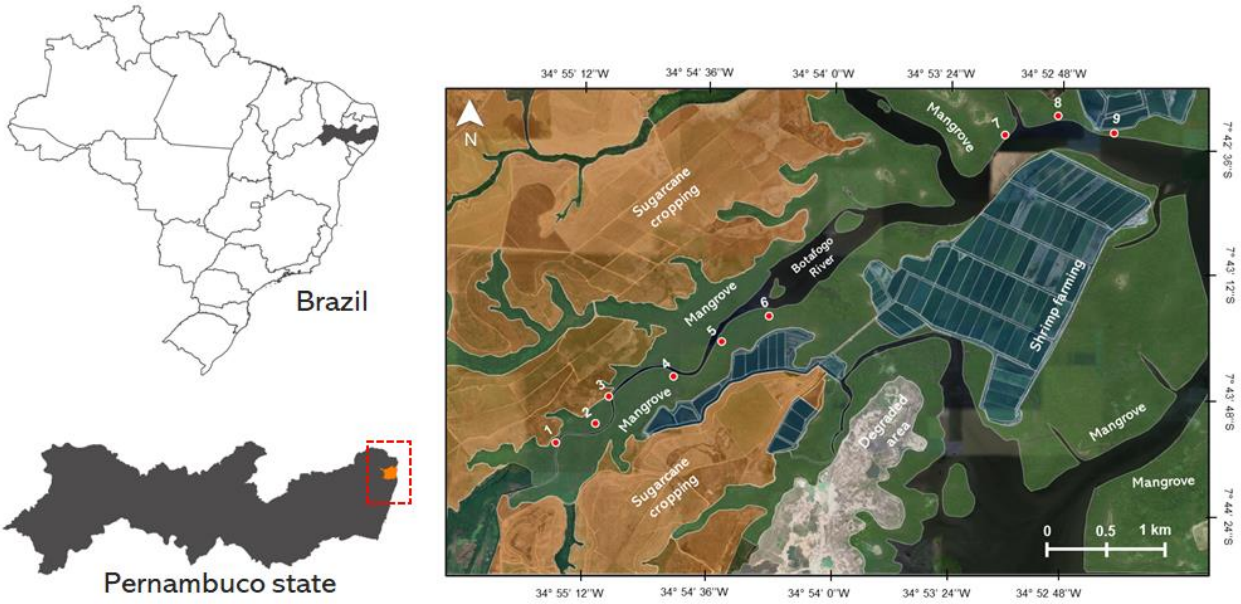

The areas in green represent the mangrove forests. Orange, blue, and white colors indicate the anthropic activities (Sugarcane cropping and shrimp farming) and degraded area, respectively. Red dots represent the sampling sites.

The Botafogo River is the largest river that flows into the Santa Cruz Channel, being formed by the union of several rivers, among the main ones, the Catucá, Itapirema, and Arataca. The Botafogo watershed is part of the "Sistema Botafogo", which is a potable water supplement system for the metropolitan region of Recife, capital of the state (CPRH, 2003; SRH, 2001).

According to the Köppen classification, the study area has a hot and humid climate, classified as type As', with an average temperature ranging between 24ºC and 31ºC, and precipitation between 1.300 and 2.200 mm per year (INPE, 2023). The studied area is inserted between the geological units, Beberibe Formation (Kb), Gramame Formation (Kg), and Maria Farinha Formation (Emf), having as local geology mangrove sediment, arising from the crystalline basement, and covering of medium-grained sandstones (CPRH, 2003).

The Botafogo mangrove forests are essentially composed of three species of tree. In the upper section (5.0 to 7.5 km from the following), there is a domain of *Laguncularia racemosa*; the middle section (2.5 to 5.0 km from the following) has a coexistence of *Rhizophora mangle*, *Laguncularia racemosa*, and *Avicennia shaueriana*; and in the lower section (0.0 to 2.0 km from the following), there is a domain of *Rhizophora mangle*. These areas are influenced by semi-diurnal tides, which have a maximum amplitude of 1.8 m, reaching a height of 2.2 m in spring tides, and 1.1 m in neap tides (PELAGE et al., 2021).

Anthropic activities surround the mangrove area, including sugarcane cultivation, the predominant economic activity in the Botafogo River basin. Some industries of the chemical sector are installed in the upper stretch of the river, as the chlor-alkali plant, located 8.5 km from the study area and have been working since the beginning of the 60s. It was considered the main polluting source of Hg in the region (ARAÚJO et al., 2019). Shrimp farming is also a local important activity located mainly in the middle and lower section of the mangrove. These economic activities cause the constant release of pollutants from industrial waste, phytosanitary products, and fertilizers. Furthermore, domestic waste disposed of through the sewers of small population centers living in the basin.

3.2.2. Sampling and sample preparation

The evaluations were made due to the sampling performed in three contaminated mangrove forests (*L. racemosa*, coexistence, and *R. mangle*), defined based on a previous study carried out by Araújo et al (2019). Soil samples were collected from areas adjacent to the tree roots (OLIVEIRA et al., 2015). Three sites were selected to represent each mangrove forest section (Figure 3).

Figure 3 - Sampling scheme along the Botafogo river mangrove.

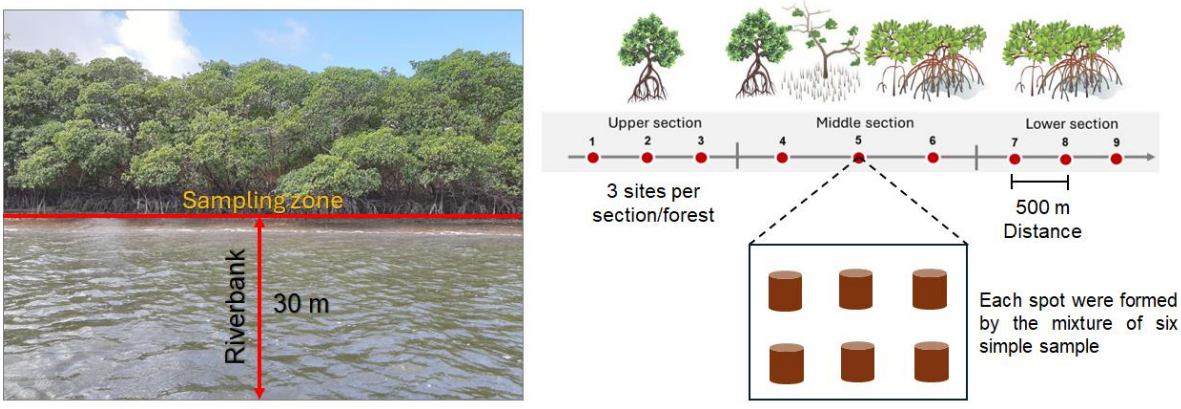

Source: mangrove photo - Personal archive; *R. mangle* - Kevin Songer (2024); *A. shaueriana* – vecta.io (2024); *L. racemosa* – pt.pngtree (2024).

The sampling zone in each section was 30 meters distant from the riverbank. In the end, we had 9 samples in total. The sampling was realized with the use of a specific sampler for flooded soils composed by PVC tubes with 50 mm of diameter and 10 cm of length. Then, the tubes containing the soil samples were transported in a thermal box with ice to avoid chemical and biological alterations to the samples.

The sampling was carried out during the dry season (summer), which corresponds to December to March, season when low quadrature tides are frequent. The selected sites were geo-referenced.

In the laboratory, soil samples were separated into layers. The study was performed using surface layer 0-10 cm. After that, the samples were homogenized, stored in plastic pots, and kept under refrigeration (-18 ºC) in a freezer.

3.2.3. Chemical and physical characterization of the soil

Some parameters could be determined in the field, such as the pH (H_2O) and oxidation-reduction (Eh) potentials. The Eh was measured using portable ORP equipment containing a previously calibrated platinum electrode. The soil pH was also determined using a calibrated portable pH meter.

The electrical conductivity (EC) of the soil was determined in ultrapure soil: water suspension (1:5), with prior preference in a centrifuge (BIRCH et al., 2011).

Soil organic matter (SOM) was determined by thermogravimetry, according to the methodology proposed by Davies (1974). 5 grams of soil were needed, previously dried in an oven (60ºC), and added in a muffle furnace at 450ºC for 2 hours. Total SOM results from the difference in mass observed when comparing the values weighed before and after combustion.

The particle size distribution was determined according to the methodology proposed by Donagemma et al (2017), previously following the recommendation to remove the salts, wash with 60% ethyl alcohol, and the organic matter, through oxidation with 17,5% hydrogen peroxide.

3.2.4. Elementary composition – CN elemental analyzer

The total content of C and nitrogen (N) of soil samples were determined via dry combustion. In this procedure, 1 g of air-dried soil was used, previously grounded in a mortar, and passed through a 0.2 mm mesh sieve. Total C and N were determinated in an elemental analyzer (CN), model Perkin Elmer, PE-2400 Series II.

3.2.5. Total content of elements – X-ray fluorescence (XRF)

The total content of the main elements (abundant ones), such as sodium (Na), calcium (Ca), magnesium (Mg), aluminum (Al), silicon (Si), iron (Fe), sulfur (S), chlorine (Cl), and the heavy metals: manganese (Mn), nickel (Ni), copper (Cu), zinc (Zn), arsenic (As), cadmium (Cd), lead (Pb), and mercury (Hg) was measured by XRF analysis. The samples were prepared by the loose-powder method and were analyzed using an ED-XRF (Spectro Xepos HE). Between 4.0 and 5.0 g of ground soil was placed in a plastic cup fitted with a thin layer of polypropylene Prolene film (Chemplex). X-rays were generated with a 50-watt X-ray tube. Measurements were performed in a He atmosphere to minimize X-ray attenuation. Bulk elemental abundance was calculated based on the intensity of the characteristic fluorescent X-rays of each element (SCHAEFER et al., 2017).

3.2.6. Data analysis

Mean, standard deviation (SD), and coefficient of variation (CV) were performed to describe soil physical and chemical characteristics and total metal concentrations. The spatial distribution of Hg concentrations was mapped using a geoinformation system by QGIS3 (v. 3.4.3). Soil contamination was evaluated by comparing total concentrations with environmentally available and geochemical background metal values (ARAÚJO et al., 2022).

3.3. Results and discussions

3.3.1. Soil characteristics

pH values remained in the neutral range (Table 1). For the three sections evaluated, pH did not exceed values greater than 7.5. Nevertheless, there is an increase trend of the values in the direction of the river mouth (4 to 8 site).

Table 1 - Chemical and physical characteristics in mangrove soils of the Botafogo river, Brazil.

Location	pH	Eh mV	EC dS m^{-1}	SOM	Sand	Silt	Clay
				---------- g kg^{-1} ----------			
Upper section							
1	6.9	143.5	10.5	228.1	172	315	514
2	6.6	123.5	12.6	278.1	72	338	591
3	6.8	152.5	13.6	254.7	174	284	542
Mean	6.8	140	12.2	257	139	312	549
SD	0.1	14.8	1.5	25.0	58.3	27.0	38.8
CV (%)	2.1	10.6	12.6	9.7	41.9	8.6	7.1
Middle section							
4	6.9	169	13.7	238.9	75	229	696
5	6.9	80	18.1	277.5	41	283	645
6	7.2	23	19.2	255.1	35	196	768

Mean	7.0	91	17.0	257	50	236	703
SD	0.2	73.6	2.9	19.4	21.3	43.8	61.9
CV (%)	2.6	81.2	17.0	7.5	42.4	18.5	8.8
Lower section							
7	7.4	72.5	17.2	251.6	323	221	457
8	7.0	26.5	20.0	301.2	119	351	530
9	6.8	-28.5	14.6	194.1	634	92	275
Mean	7.0	24	17.3	249	359	221	420
SD	0.3	50.6	2.7	53.6	259.4	129.9	131.4
CV (%)	4.4	215.2	15.5	21.5	72.4	58.7	31.3

SD – Standard deviation; CV – Coefficient of variation; SOM – Soil organic matter; EC – electric conductivity.

Neutrality reactions observed can be explained by the long periods mangrove areas stay flooded with river and seawater, significantly reducing O_2 diffusion into the soil. This process stimulates anaerobic respiration that consumes H^+ during the oxidation process following an Eh status (OTERO et al., 2017; ARAÚJO et al., 2019). The main oxidized elements are O_2, NO_3, Mn^{4+}, Fe^{3+}, and SO_4^{2-}.

In terms of pH influence of heavy metals availability, pH doesn't have direct correlation with these contaminants, however, it affects SOM dynamic and mineral stability in mangrove soils, both responsible to retain heavy metals (ARAÚJO et al., 2019; HU et al., 2021).

Most parts of the sites evaluated showed anoxic conditions (Eh < 100 mV) and became negative at site 9. It highlights the decreasing gradient of O_2 diffusion along the sections towards the river mouth. The lower section presents drainage even more incipient, showing negative Eh, probably due to tidal contribution and lower topographic elevation, maintained this zone flooded for a longer time compared to superior sections. Moreover, two factors contribute to O_2 depletion: 1) *R. mangle* roots can promote morpho-anatomical adaptations, such as new roots, which could maintain its productivity, and consequently, O_2 depletion; 2) O_2 consumption needed for organic matter decomposition by the microbiota (OKELLO et al., 2020; PEZESHKI; DELAUNE, 2012). Negative Eh was not the domain in all forest because only the superficial layer (0-10 cm) was evaluated. The opposite is observed evaluating deeper layers, which are more reduced zone (OTERO et al., 2009).

SOM content was similar in all three sections. The decrease observed was only in site 9. The organic matter comes mainly from the river sediments (allochthonous source) and tree tissues (autochthonous source). It indicates few differences comparing tree species domain, representing incipient variation in organic matter content. At this case, SOM seems to follow clay content (KIDA; FUJITAKE, 2020). Where texture becomes sandier (site 9), SOM consequently was lower than other sites. Clay content is a relevant factor in the maintenance of organic matter. An important mechanism in estuarine environments is Van der Waals forces

promoted by clay particles. This bond type protects organic matter against microbial degradation and mineralization (KIDA; FUJITAKE, 2020).

The SOM content discussion highlights the need to evaluate its quality characteristics, such as origin, stability, and molecular composition along the estuaries. Despite the similarity on SOM content, each section present different tree domain, also their distribution at the Botafogo estuary is different, where the sections show a unique soil chemical scenario condition. Chemical parameters such Eh and EC are determinants on SOM quality, especially in anaerobic soils. Once these parameters show variation along the mangrove, the SOM is also heterogeneous, and taking the area contamination historic in consideration, a deeper assessment about SOM quality may provide the influence of soil matrix on contaminants retention, such Hg.

C contents varied from 5.10 (middle section) to 8.13 (lower section) (Figure 4). The lower section presents 1.91% more C than the middle section and 1.22% than the middle and upper sections, respectively. As regards the C productivity, *L. racemosa* and *R. mangle* are more productive than *Avicennia* plants, mainly due to fine root decomposition (BARRETO et al., 2016; OCHOA-GÓMEZ et al., 2019).

Figure 4 - Total C and N content of soil in different sections of the Botafogo River.

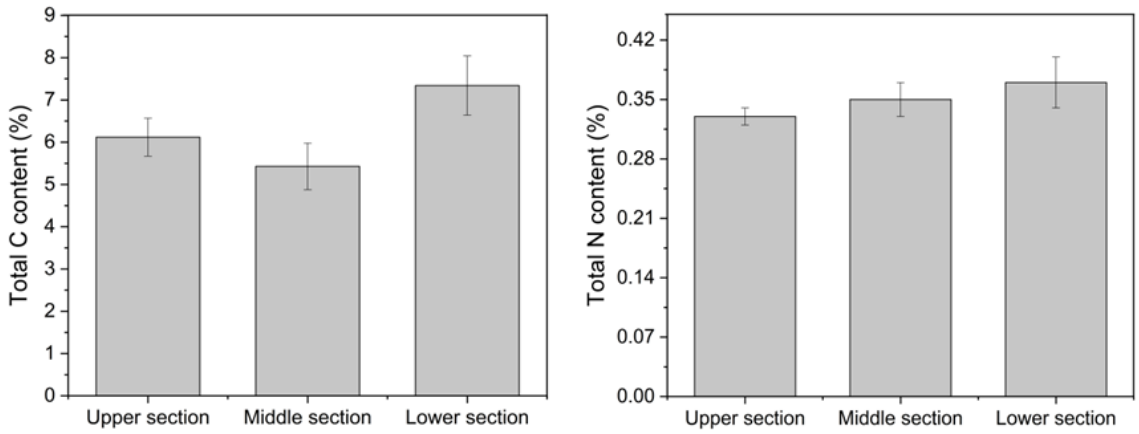

However, it is also relevant to highlight the higher C content identified in the lower section. It represents not only the *R. mangle* contribution but also the carbonates influence. This section receives significant influence from biogenic carbonate, derived from molluscs. *C. rhizophorae* is a common oyster that lives associated with *R. mangle* roots. It lives more on *R. mangle* roots than any other tree species at the studied mangrove. The local lithology act as second contributor. Local lithology shows a carbonate platform composed of calcarenites, siliciclastic limestones, and marly calcilutites that provide carbonate sediments. The platform is distributed mainly at Beberibe Formation (Kb), Gramame Formation (Kg), and Itamaracá

Formation (K2it) (VALENÇA; SOUZA, 2017). However, probably biogenic overcome lithology contribution because despite the presence of calcareous materials in the local lithology, mineral carbonate supply requires rocky outcrop, so the rocks can be able to be weathered and provide its chemical compounds, not identify along the estuary. This discussion will be better discussed at the last chapter.

N content values were similar between the sections with a slight increase trend towards the lower section. This increment indicates the dissolved organic nitrogen (DON) originating from tidal waters (ALONGI, 2020).

3.3.2. Heavy metals distribution in mangrove soil

Hg content varied from 2.8 (lower section) to 14.3 mg kg^{-1} (upper section) (Figure 5). According to the values it represents a decreasing gradient concentration with high levels closer to the chlor-alkali plant and low levels next to the river mouth. The first responsible factor for creating this gradient is the distance to the old chlor-alkali plant discharge point, where there is a reduction of the concentration as the distance from the polluting source increases (ARAÚJO et al., 2019).

Figure 5 - Hg total content in different sections of the Botafogo River mangrove.

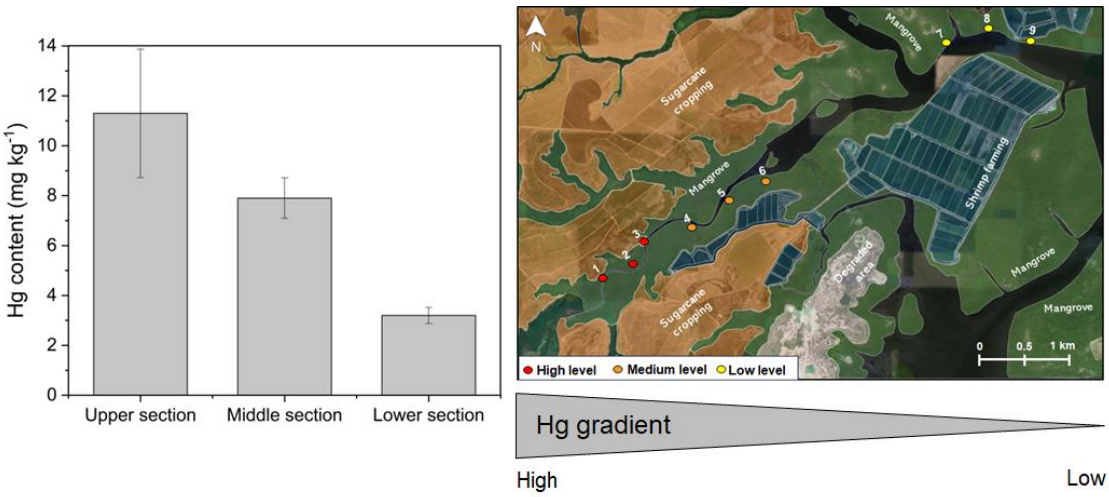

Upper section – 5.0 to 7.5 km; Middle section – 2.5 to 5.0; Lower section – 0.0 to 2.5 km to the river mouth. Detection limit: 0.7 µg kg^{-1}.

Besides the distance between the polluting source and the mangrove, Hg is a contaminant that has an affinity with soil organic phase, especially the material produced in situ (autochthonous) (DUAN et al., 2021).

The tree species domains are different along the Botafogo mangrove, which implies that the organic compounds produced are heterogeneous in terms of molecular characteristics,

stability, and dynamics. In this case, the Hg retention and availability are distinct along the mangrove. This context will be discussed in the next chapter.

Elements, such as Na, Cl, and Mg are found in higher levels in the middle and lower sections (Table 2). Comparing the Na, Cl, and Mg content between the upper and lower sections, mean values were 0.33%, 3.59%, and 0.43% higher in the lower section. These elements constitute the dissolved salts more concentrated near the river mouth. It corroborates with the higher values EC, identified at the lower section. Added to carbonates, they associate and form salts, such as sodium chloride, and remain partially precipitated on the soil mineral's surface (Identified using SEM/EDS - chapter 3).

Fe content also followed a gradient with the highest mean at the middle section, 5.16% and it reduces to 3.30% at the lower section. It indicates a higher input of Fe and probably its stabilization in the coexistence and *L. racemosa* forest compared to the *R. mangle* forest. It shows the relation with the estuary position, where upper zones receive greater sediments contribution. Clay particles becomes enriched (Table 1), and the Fe is founded associated with it. On other hand, the lower section showed a sand content domain, and generally this is negatively correlated with Fe concentration (OTERO et al., 2009). Furthermore, lower section presents higher reductive conditions, and the reductive dissolution of Fe (III) increases its solubility and mobility in suboxic pore water, resulting in its loss due to tidal fluctuation (OTERO et al., 2009). Based on Hg content gradient, this higher accumulation of Fe can provide the increase of reduced minerals, such pyrite, responsible to Hg retention in mangrove soils (SUN et al., 2017). This Fe/clay pattern may be lined with other heavy metal concentrations considering their affinity with clay-Fe forms (ARAÚJO et al., 2022).

Table 2 - Total metal content in mangrove soils of the Botafogo River, Brazil.

Location	Na	Ca	Mg	Al	Si	Fe	S	Cl	Cr	Mn	Cu	Zn	As	Cd	Pb	Ni
	----------%----------								----------mg kg^{-1}----------							
Upper section																
1	0.78	0.53	0.39	8.95	20.92	4.28	2.73	0.85	88.30	182.30	26.30	77.10	3.60	0.90	38.40	58.10
2	0.78	0.47	0.35	9.55	17.60	5.03	2.76	0.85	105.70	186.30	29.90	87.40	5.20	0.30	46.10	60.90
3	1.19	0.42	0.38	9.30	19.45	4.69	2.54	1.35	95.30	169.70	30.00	75.10	3.90	0.80	43.20	62.70
Mean	0.91	0.48	0.38	9.27	19.32	4.67	2.68	1.02	96.43	179.43	28.73	79.87	4.23	0.67	42.57	60.57
SD	0.24	0.06	0.02	0.30	1.66	0.38	0.12	0.29	8.76	8.66	2.11	6.60	0.85	0.32	3.89	2.32
CV (%)	25.84	11.67	5.56	3.23	8.61	8.05	4.46	28.39	9.08	4.83	7.34	8.26	20.09	48.22	9.14	3.83
Middle section																
4	0.93	0.34	0.46	10.82	19.23	4.95	1.57	1.31	113.20	169.60	29.90	85.20	6.60	0.20	52.10	62.40
5	1.12	0.42	0.47	10.25	18.51	5.16	2.48	1.59	110.20	171.90	27.90	85.90	8.10	0.50	47.90	61.60
6	1.15	0.38	0.49	10.61	17.89	5.36	2.25	1.16	113.30	172.20	27.90	91.80	6.60	0.60	50.00	67.80
Mean	1.06	0.38	0.47	10.56	18.54	5.16	2.10	1.35	112.23	171.23	28.57	87.63	7.10	0.43	50.00	63.93
SD	0.12	0.04	0.02	0.29	0.67	0.21	0.47	0.22	1.76	1.42	1.15	3.63	0.87	0.21	2.10	3.37
CV (%)	11.10	9.78	3.30	2.73	3.62	3.98	22.53	16.13	1.57	0.83	4.04	4.14	12.20	48.04	4.20	5.27
Lower section																
7	1.46	2.99	0.73	6.91	18.03	3.22	2.1	1.87	75.30	165.80	13.10	57.10	12.30	0.80	35.80	54.00
8	1.80	4.66	0.90	6.72	15.83	3.43	2.42	2.18	78.70	181.40	11.90	60.30	13.10	0.30	37.70	54.80
9	1.30	4.56	0.81	6.88	17.08	3.25	1.52	1.59	77.90	163.30	14.60	56.00	10.60	0.30	35.20	53.50
Mean	1.52	4.07	0.81	6.84	16.98	3.30	2.01	1.88	77.30	170.17	13.20	57.80	12.00	0.47	36.23	54.10
SD	0.26	0.94	0.09	0.10	1.10	0.11	0.46	0.30	1.78	9.81	1.35	2.23	1.28	0.29	1.31	0.66
CV (%)	16.96	23.01	10.73	1.49	6.50	3.44	22.66	15.70	2.30	5.76	10.25	3.86	10.64	61.86	3.60	1.21

SD – Standard deviation; CV – Coefficient of variation. All elements analyzed by ED-XRF following Schaefer et al. (2017) protocol. Detection limits: Na = 10.0 µg kg^{-1}; Mg = 20.0 µg kg^{-1}; Al = 20.0 µg kg^{-1}; Si = 5.0 µg kg^{-1}; Fe = 1.0 µg kg^{-1}; S = 2.0 µg kg^{-1}; Cl = 2.0 µg kg^{-1}; Cr = 1.0 µg kg^{-1}; Mn = 1.0 µg kg^{-1}; Cu = 0.5 µg kg^{-1}; Zn = 0.5 µg kg^{-1}; As = 0.5 µg kg^{-1}; 0.3 µg kg^{-1}; Pb = 0.6 µg kg^{-1}; Ni = 0.5 µg kg^{-1}.

The evaluation of S content permitted to identify a similar behavior. The values varied from 1.52 (lower section) to 2.76% (upper section), with a 0.67% difference when means were compared between these two areas. Higher S content in the upper section indicates similar pattern as Fe content, which had the content followed by clay content. Besides the Fe sulfides minerals such pyrite, S is component of sulfide bound Hg, which also act as geochemistry filters in the mangrove soils such as cinnabar and metacinnabar (HgS) (ARAÚJO et al., 2019). Furthermore, S derived from organic materials contributes to the formation of important functional groups capable to retain Hg in these soils, thiol (C-S-C) as the main of them (DING et al., 2017).

Most metals contents (Cr, Mn, Cu, Zn, Cd, Pb, and Ni) also follow the decreasing gradient toward the river mouth. The average metal concentrations considering all sections had the following sequence: Mn>Cr>Zn>Ni>Pb>Cu>As>Cd. Only As obtained opposite behavior, achieving the highest average value, 12.00 mg kg^{-1}, at the lower section. Local lithology reveals metals' contribution to mangrove sections. The higher Mn, Cr, Zn, and Ni contribution comes from the weathering process of metamorphic rocks, such as gneiss and migmatites (VALENÇA; SOUZA, 2017). In addition, local anthropic activities may contribute to metal contamination. Sugar cane cropping is installed around the sections and its management requires fertilizers and pesticides; both have residual concentration of heavy metal, such Cr and Pb accumulation due to phosphate fertilization and As due to insecticides and herbicides applications (SILVA et al., 2016; QUINTEROS et al., 2017). Same scenario can be applied to shrimp farming, located mostly around the middle and lower section. According to Lacerda et al. (2021), this activity tends to increase Zn and Cu concentrations of local areas due to its effluents.

As showed a high concentration and relevant accumulation in the lower section. Besides the sedimentary contribution and anthropic activities, it seems the area around the river mouth has a specific geochemical condition responsible for maintaining As at such level. As association with carbonates and manganese (hydro)oxides and iron crystalline fractions are essential reactions in aquatic systems such as mangroves (VAN THINH et al., 2018). However, the low stability of Mn and Fe crystalline forms in this Eh level makes the As fate controlled by the carbonates (CO_2 + H_2CO_3 and HCO_3^-). Another factor is root contribution. Some species, such as Avicennia trees, can sequestrate As in their roots. These plants accumulate As into the root tissues due to the reduction of As(V) that blocks the xylem transport of As. Therefore, As tends to exist as As (III) in roots having greater concentration over aerial tissues (MANDAL et al., 2019).

Metal concentrations seem to be similar to other contaminated mangroves around the world, such as in China, India, Malaysia, and Colombian (CASTRO et al., 2022; ELTURK et al., 2018; KALAIVANAN et al., 2017; SHI et al., 2019).

For Cr, Mn, Cu, Zn, As, Cd, Pb, and Ni, 40% to 60% of the total metal concentrations are considered environmentally available (Table 3) (ARAÚJO et al., 2022). Comparing total concentration with the local background, only Cu showed a similar concentration. Cr, Cd, and Pb values were at least 2-fold greater, but Ni values were 6-fold greater. Substantial contamination was observed comparing Hg, in which the total concentration of the upper section was 161-fold higher than the local background, indicating severe contamination by the chlor-alkali plant effluent.

Table 3 - Total and environmentally available metal concentrations in mangrove soils of Botafogo river and comparison with local background.

Location	Cr	Mn	Cu	Zn	As	Cd	Pb	Ni	Hg
	----------mg kg^{-1}----------								
Total									
Upper section	96.43	179.43	28.73	79.87	4.23	0.67	42.57	60.57	11.33
Middle section	112.23	171.23	28.57	87.63	7.10	0.43	50.00	63.93	7.93
Lower section	77.30	170.17	13.20	57.80	12.00	0.47	36.23	54.10	3.16
Environmentally available									
Mean - three sections[1]	52.79	ND	15.88	40.77	ND	0.16	20.10	12.3	4.61
Local background									
Jaguaribe river mangrove[1]	30.1	ND	19.3	38.3	ND	0.17	18.6	8.7	0.07

[1]Araújo et al., 2022. ND – Not determined.

3.4. Conclusions

Regarding soil attributes, the soil contamination by heavy metals in the Botafogo mangroves varies and depending on clay content, as well Fe and S concentration. Upper zones were considered greater sediment input areas, and it was essential for clay particles and Fe accumulation. On the other hand, at the *R. mangle* forest, close to the river mouth, the areas were considered sandier, more reduced and suffers carbonate influence.

All forests were considered contaminated by heavy metals, especially Hg, which achieved a concentration 161-fold higher than the local background. The similarity in SOM content indicates that its quality is more important in the performance of processes that complex or release Hg and other contaminants, requiring investigation.

In terms of the other metals, As was the unique exception, presenting higher concentration at the *R. mangle* forest. The source is probably connected with local anthropic activities and its

maintenance is governed by carbonate influence. Considering the proximity, others heavy metals must be derived from local activities, such Cr, Pb, and Zn.

Hg and As are potentially toxic and carcinogens for humans, demonstrating to be a significant alert for local biota and population. Furthermore, all metal contents evaluated were higher than the local background, indicating not only near lithology, but also anthropogenic influence. Considering the proximity, sugarcane production and shrimp farming may have contributed for metals release. Among all metals, Hg content showed severe local contamination, highlighting the adverse effects caused by the chlor-alkali plant effluent.

References

AFONSO, F.; PALMA, C.; BRITO, A. C.; CHAINHO, P.; DE LIMA, R.; HEUMÜLLER, J. A.; FÉLIX, P. M. Metal and semimetal loadings in sediments and water from mangrove ecosystems: A preliminary assessment of anthropogenic enrichment in São Tomé island (central Africa). **Chemosphere**, v. 334, p. 138973, 2023. https://doi.org/10.1016/j.chemosphere.2023.138973

AGÊNCIA ESTADUAL DE MEIO AMBIENTE (CPRH). **Diagnóstico Socioambiental do Litoral Norte de Pernambuco**. Recife, 2003. 214p.

ALHARBI, O. M.; KHATTAB, R. A.; ALI, I.; BINNASER, Y. S.; AQEEL, A. Assessment of heavy metals contamination in the sediments and mangroves (*Avicennia marina*) at Yanbu coast, Red Sea, Saudi Arabia. **Marine Pollution Bulletin**, v. 149, p. 110669, 2019. https://doi.org/10.1016/j.marpolbul.2019.110669

ALONGI, D. M. (2020). Nitrogen cycling and mass balance in the world's mangrove forests. **Nitrogen**, v.1, p. 167–189, 2020. https://doi.org/10.3390/nitrogen1020014

ARAÚJO, P. R. M.; BIONDI, C. M.; DO NASCIMENTO, C. W. A.; DA SILVA, F. B. V.; ALVAREZ, A. M. Bioavailability and sequential extraction of mercury in soils and organisms of a mangrove contaminated by a chlor-alkali plant. **Ecotoxicology and Environmental Safety**, v. 183, p. 109469, 2019. https://doi.org/10.1016/j.ecoenv.2019.109469

ARAÚJO, P. R. M.; BIONDI, C. M.; DO NASCIMENTO, C. W. A.; DA SILVA, F. B. V.; DA SILVA, W. R.; DA SILVA, F. L.; DE MELO FERREIRA, D. K. Assessing the spatial distribution and ecologic and human health risks in mangrove soils polluted by Hg in northeastern Brazil. **Chemosphere**, v. 266, p. 129019, 2021 https://doi.org/10.1016/j.chemosphere.2020.129019

ARAÚJO, P. R. M.; BIONDI, C. M.; DO NASCIMENTO, C. W. A.; DA SILVA, F. B. V.; FERREIRA, T. O.; DE ALCÂNTARA, S. F. Geospatial modeling and ecological and human health risk assessments of heavy metals in contaminated mangrove soils. **Marine Pollution Bulletin**, v. 177, p. 113489, 2022. https://doi.org/10.1016/j.marpolbul.2022.113489

BARRETO, M. B.; MÓNACO, S. LO; DÍAZ, R.; BARRETO-PITTOL, E.; LÓPEZ, L.; PERALBA, M. DO C. R. Soil organic carbon of mangrove forests (*Rhizophora* and *Avicennia*) of the Venezuelan Caribbean coast. **Organic Geochemistry,** v. 100, p. 51–61, 2016. https://doi.org/10.1016/j.orggeochem.2016.08.002

BECKERS, F.; RINKLEBE, J. Cycling of mercury in the environment: Sources, fate, and human health implications: A review. **Critical Reviews in Environmental Science and Technology**, v. 47, p. 693–794, 2017. https://doi.org/10.1080/10643389.2017.1326277

BIRCH, G. F.; VANDERHAYDEN, M.; OLMOS, M. The Nature and Distribution of Metals in Soils of the Sydney Estuary Catchment, Australia. **Water, Air, & Soil Pollution**, v. 216, p. 581–604, 2011. https://doi.org/10.1007/s11270-010-0555-1

CASTRO, E.; PINEDO, J.; MARRUGO, J.; LEÓN, I. Retention and vertical distribution of heavy metals in mangrove sediments of the protected area swamp of Mallorquin, Colombian Caribbean. **Regional Studies in Marine Science**, v. 49, p. 102072, 2022. https://doi.org/10.1016/j.rsma.2021.102072

CHAI, M.; LI, R.; DING, H.; ZAN, Q. Occurrence and contamination of heavy metals in urban mangroves: A case study in Shenzhen, China. **Chemosphere**, v. 219, p. 165-173, 2019. https://doi.org/10.1016/j.chemosphere.2018.11.160

CHOUDHURY, T. R.; ACTER, T.; UDDIN, N.; KAMAL, M.; CHOWDHURY, A. S.; RAHMAN, M. S. Heavy metals contamination of river water and sediments in the mangrove forest ecosystems in Bangladesh: A consequence of oil spill incident. **Environmental Nanotechnology, Monitoring & Management**, v. 16, p. 100484, 2021. https://doi.org/10.1016/j.enmm.2021.100484

DING, X.; WANG, R.; LI, Y.; GAN, Y.; LIU, S.; DAI, J. Insights into the mercury (II) adsorption and binding mechanism onto several typical soils in China. **Environmental Science and Pollution Research**, v. 24, p. 23607–23619, 2017. https://doi.org/10.1007/s11356-017-9835-2

DONAGEMMA, G. K. VIANA; J. H. M.; DE ALMEIDA, B. G.; RUIZ, H. A.; K. V. A., DECHEN, S. C. F.; FERNANDES, R. B. A. **Manual de Métodos de Análise de Solo**. Brasília: Embrapa, 2017. p. 95-124.

DUAN, D.; LEI, P.; LAN, W.; LI, T.; ZHANG, H.; ZHONG, H.; PAN, K. Litterfall-derived organic matter enhances mercury methylation in mangrove sediments of South China. **Science of the Total Environment**, v. 765, p. 142763, 2021. https://doi.org/10.1016/j.scitotenv.2020.142763

ELTURK, M.; ABDULLAH, R.; ROZAINAH, M. Z.; BAKAR, N. K. A. Evaluation of heavy metals and environmental risk assessment in the Mangrove Forest of Kuala Selangor estuary, Malaysia. **Marine Pollution Bulletin**, v. 136, p. 1–9, 2018. https://doi.org/10.1016/j.marpolbul.2018.08.06

FUENTES-GANDARA, F.; PINEDO-HERNÁNDEZ, J.; GUTIÉRREZ, E.; MARRUGO-NEGRETE, J.; DÍEZ, S. Heavy metal pollution and toxicity assessment in Mallorquin swamp: A natural protected heritage in the Caribbean Sea, Colombia. **Marine pollution bulletin**, v. 167, p. 112271, 2021. https://doi.org/10.1016/j.marpolbul.2021.11227

HU, B.; GUO, P.; WU, Y.; DENG, J.; SU, H.; LI, Y.; NAN, Y. Study of soil physicochemical properties and heavy metals of a mangrove restoration wetland. Journal of cleaner production, v. 291, p. 125965, 2021. https://doi.org/10.1016/j.jclepro.2021.125965

INSTITUTO NACIONAL DE PESQUISAS ESPACIAIS (INPE). **Centro de previsão de tempo e estudos climáticos**. Disponível em <http:// http://www.cptec.inpe.br/>. Acesso em 8 de dezembro de 2023.

KALAIVANAN, R.; JAYAPRAKASH, M.; NETHAJI, S.; ARYA, V.; GIRIDHARAN, L. Geochemistry of core sediments from tropical mangrove region of Tamil Nadu: implications on trace metals. **Journal of Earth Science and Climate Change**, v. 8, p. 2, 2017. https://doi.org/10.4172/2157-7617.1000385

KEVIN SONGER. **Red mangrove, *Rhizophora mangle***. Disponível em: < https://pixels.com/featured/red-mangrove-rhizophora-mangle-kevin-songer.html> Acesso em 28 fevereiro de 2024.

KIDA, M.; FUJITAKE, N. Organic carbon stabilization mechanisms in mangrove soils: a review. **Forests**, v. 11, p. 981, 2020. https://doi.org/10.3390/f11090981

LACERDA, L. D.; WARD, R. D.; GODOY, M. D. P.; DE ANDRADE MEIRELES, A. J.; BORGES, R.; FERREIRA, A. C. 20-years cumulative impact from shrimp farming on mangroves of Northeast Brazil. **Frontiers in Forests and Global Change**, v. 4, p. 653096, 2021. https://doi.org/10.3389/ffgc.2021.653096

LEÃO, Z. M. A. N.; KIKUCHI, R. K. P.; OLIVEIRA, M. D. M. **The Coral Reef Province of Brazil**. *In:* Sheppard*, C.* World Seas: an Environmental Evaluation. United Kingdom: Academic Press, 2019. p 813–833. 2019 Academic Press. https://doi.org/10.1016/B978-0-12-805068-2.00048-6

LI, P.; LI, X.; BAI, J.; MENG, Y.; DIAO, X.; PAN, K.; ZHU, X.; LIN, G. Effects of land use on the heavy metal pollution in mangrove sediments: Study on a whole island scale in Hainan, China. **Science of The Total Environment**, p. 824, p. 153856, 2022. https://doi.org/10.1016/j.scitotenv.2022.15385

MACHADO, W.; SANDERS, C. J.; SANTOS, I. R.; SANDERS, L. M.; SILVA-FILHO, E. V.; LUIZ-SILVA, W. Mercury dilution by autochthonous organic matter in a fertilized mangrove wetland. **Environmental Pollution**, v. 213, p. 30–35, 2016. https://doi.org/10.1016/j.envpol.2016.02.002

MANDAL, S. K., RAY, R., GONZÁLEZ, A. G., POKROVSKY, O. S., MAVROMATIS, V., JANA, T. K. Accumulation, transport and toxicity of arsenic in the Sundarbans mangrove, India. **Geoderma**, v. 354, p. 113891, 2019. https://doi.org/10.1016/j.geoderma.2019.113891

MEYER, U. **On the fate of mercury in the Northeastern Brazilian: mangrove system, Canal de Santa Cruz, Pernambuco**. 1996. 105 f. Thesis. (PhD) Zentrum fur Marine Tropenokologie (ZMT), Bremen University, Germany, 1996.

MEYER, U.; HAGEN, W.; MEDEIROS, C. Mercury in a northeastern Brazilian mangrove area, a case study: potential of the mangrove oyster *Crassostrea rhizophorae* as bioindicator for mercury. **Marine Biology**, v. 131, p. 113–121, 1998. https://doi.org/10.1007/s002270050302

OCHOA-GÓMEZ, J. G.; LLUCH-COTA, S. E.; RIVERA-MONROY, V. H.; LLUCH-COTA, D. B.; TROYO-DIÉGUEZ, E.; OECHEL, W.; SERVIERE-ZARAGOZA, E. Mangrove wetland productivity and carbon stocks in an arid zone of the Gulf of California (La Paz Bay, Mexico). **Forest Ecology and Management**, v. 442, p. 135–147, 2019. https://doi.org/10.1016/j.foreco.2019.03.059

OKELLO, J. A.; KAIRO, J. G.; DAHDOUH-GUEBAS, F.; BEECKMAN, H.; KOEDAM, N. Mangrove trees survive partial sediment burial by developing new roots and adapting their root, branch and stem anatomy. **Trees**, v. 34, p. 37–49, 2020. https://doi.org/10.1007/s00468-019-01895-6

OLIVEIRA, D. C. M.; CORREIA, R. R. S.; MARINHO, C. C.; GUIMARÃES, J. R. D. Mercury methylation in sediments of a Brazilian mangrove under different vegetation covers and salinities. **Chemosphere**, p. 127, p. 214–221 2015. https://doi.org/10.1016/j.chemosphere.2015.02.009

OTERO, X. L.; FERREIRA, T. O.; HUERTA-DÍAZ, M. A.; PARTITI, C. S. DE M., SOUZA JR, V.; VIDAL-TORRADO, P.; MACÍAS, F. Geochemistry of iron and manganese in soils and sediments of a mangrove system, Island of Pai Matos (Cananeia—SP, Brazil). **Geoderma**, v. 148, p. 318–335, 2009. https://doi.org/10.1016/j.geoderma.2008.10.016

OTERO, X. L.; MÉNDEZ, A.; NÓBREGA, G. N.; FERREIRA, T. O.; MELÉNDEZ, W.; MACÍAS, F. High heterogeneity in soil composition and quality in different mangrove forests of Venezuela. **Environmental Monitoring and Assessment**, v. 189 p. 511, 2017. https://doi.org/10.1007/s10661-017-6228-4

PALACIOS-TORRES, Y.; CABALLERO-GALLARDO, K.; OLIVERO-VERBEL, J. MERCURY pollution by gold mining in a global biodiversity hotspot, the Choco biogeographic region, Colombia. **Chemosphere**, v. 193, p. 421-430, 2018. https://doi.org/10.1016/j.chemosphere.2017.10.160

PASSOS, T.; SANDERS, C. J.; BARCELLOS, R.; PENNY, D. Assessment of the temporal retention of mercury and nutrient records within the mangrove sediments of a highly impacted estuary. **Environmental Research,** v. 206, p. 112569, 2022. https://doi.org/10.1016/j.envres.2021.11256

PELAGE, L.; GONZALEZ, J. G.; LE LOC'H, F.; FERREIRA, V.; MUNARON, J.M.; LUCENA-FRÉDOU, F.; FRÉDOU, T. Importance of estuary morphology for ecological connectivity with their adjacent coast: A case study in Brazilian tropical estuaries. **Estuarine, Coastal and Shelf Science**, v. 251, p. 107184, 2021. https://doi.org/10.1016/j.ecss.2021.107184

PEZESHKI, S. R.; DELAUNE, R. D. Soil oxidation-reduction in wetlands and its impact on plant functioning. **Biology**, v. 1, p. 196–221, 2012. https://doi.org/10.3390/biology1020196

PT.PNGTREE. ***Laguncularia racemosa***. Disponível em: < https://pt.pngtree.com/freepng/mangrove-tree-vector-illustrations-hand-drawn-art-isolated-on-white_8799817.html> Acesso em 28 de fevereiro 2024.

QUINTEROS, E.; RIBÓ, A.; MEJÍA, R.; LÓPEZ, A.; BELTETON, W.; COMANDARI, A.; ORANTES, C. M.; PLEITES, E. B.; HERNÁNDEZ, C. E.; LÓPEZ, D. L. Heavy metals and pesticide exposure from agricultural activities and former agrochemical factory in a Salvadoran rural community. **Environmental Science and Pollution Research**, v. 24, p. 1662–1676, 2017. https://doi.org/10.1007/s11356-016-7899-z

SCHAEFER, M. V.; GUO, X.; GAN, Y.; BENNER, S. G.; GRIFFIN, A. M.; GORSKI, C. A.; WANG, Y.; FENDORF, S. Redox controls on arsenic enrichment and release from aquifer sediments in central Yangtze River Basin. **Geochimica et Cosmochimica Acta**, v. 204, p. 104–119, 2017. https://doi.org/10.1016/j.gca.2017.01.035

SECRETARIA ESTADUAL DE RECURSOS HÍDRICOS (SRH). **Plano Estadual de Recursos Hídricos – Documento Síntese**. Recife, 2001. 215p.

SHI, C.; DING, H.; ZAN, Q.; LI, R. Spatial variation and ecological risk assessment of heavy metals in mangrove sediments across China. **Marine Pollution Bulletin**, v. 143, p. 115–124, 2019. https://doi.org/10.1016/j.marpolbul.2019.04.043

SILVA, F. B. V.; DO NASCIMENTO, C. W. A.; ARAÚJO, P. R. M.; DA SILVA, L. H. V.; DA SILVA, R. F. Assessing heavy metal sources in sugarcane Brazilian soils: an approach using multivariate analysis. **Environmental Monitoring and Assessment**, v. 188, p. 1–12, 2016. https://doi.org/10.1007/s10661-016-5409-x

SUN, Y.; LV, D.; ZHOU, J.; ZHOU, X.; LOU, Z.; BAIG, S. A.; XU, X. Adsorption of mercury (II) from aqueous solutions using FeS and pyrite: a comparative study. **Chemosphere**, v. 185, p. 452–461, 2017. https://doi.org/10.1016/j.chemosphere.2017.07.047

VALENÇA, L. M. M.; SOUZA, N. G. A. **Unidades estratigráficas**. Geologia e recursos minerais da folha Itamaracá SB. 25-YC-VI: estados de Pernambuco e Paraíba. *In*: VALENÇA, L. M. M.; SOUZA, N. G. A. Recife: CPRM, 2017. p. 23-41.

VAN THINH, N.; OSANAI, Y.; ADACHI, T.; THAI, P. K.; NAKANO, N.; OZAKI, A.; KUROSAWA, K. Chemical speciation and bioavailability concentration of arsenic and heavy metals in sediment and soil cores in estuarine ecosystem, Vietnam. **Microchemical Journal**, v. 139, p. 268-277, 2018. https://doi.org/10.1016/j.microc.2018.03.005

VECTA.IO. ***Avicennia* (Black Mangrove)**. Disponível em: <https://vecta.io/symbols/301/flora-mangroves/6/avicennia-germinans-black-mangrove-stress> Acesso em 28 de fevereiro 2024.

VIANA, A. P.; LE LOCH, F.; FRÉDOU, T.; LUCENA-FRÉDOU, F.; MÉNARD, F.; LAGANE, C.; MUNARON, J.M.; LIRA, A. S.; DOS SANTOS, Í. G. S.; FERREIRA, V.; GONZALEZ, J. G.; POINT, D. Mercury biomagnification and trophic structure patterns in neotropical coastal estuaries impacted by a Chlor-alkali plant in northeast Brazil. **Regional Studies in Marine Science**, v. 66, p. 103105, 2023. https://doi.org/https://doi.org/10.1016/j.rsma.2023.103105

4. ORIGEM, ESTABILIDADE E COMPOSIÇÃO QUÍMICA DA MATÉRIA ORGÂNICA EM SOLOS DE MANGUE CONTAMINADOS POR MERCÚRIO

Resumo

As investigações acerca da natureza da matéria orgânica do solo (MOS) em áreas de manguezais são essenciais para o entendimento de suas fontes, estabilidade e composição química em áreas de estuário. Além disto, pouco estudos são conduzidos em áreas contaminadas, onde estas informações podem ser utilizadas na predição da dinâmica de contaminantes nos solos. O objetivo desta pesquisa foi avaliar a MOS em diferentes domínios de vegetação em um manguezal contaminado por mercúrio (Hg). Nove locais ao longo do manguezal do Rio Botafogo foram selecionados para representar três seções, dominadas por diferentes espécies: *Laguncularia racemosa*, coexistência de espécies e *Rhizophora mangle*. A origem, estabilidade e composição molecular da MOS foram investigadas através dos seguintes procedimentos: $\delta^{13}C$ e $\delta^{15}N$; Calorimetria diferencial por varredura e termogravimetria (CDV-TG), relação C/N e espectroscopia no infravermelho por transformada de Fourier (FTIR), respectivamente. Os resultados isotópicos confirmaram a produção autóctone de MO nas seções superior e média, mas menores valores $\delta^{13}C$ em áreas próximas a foz. Os dados de CDV-TG e FTIR revelaram comportamento semelhante, com acúmulo de MO alifática na seção superior e média, contra o domínio de C aromático na floresta de *R. mangle*. A heterogeneidade nas características da MOS reflete as diferentes contribuições das espécies vegetais ligada às condições químicas do solo. Na retenção do Hg, esta heterogeneidade na qualidade da MOS demonstrou variações também no potencial de sequestro deste contaminante nos solos das diferentes seções do estuário do rio Botafogo. Nossos resultados contribuem para uma melhor compreensão das variações espaciais nas composições químicas da MOS criadas principalmente pelos domínios vegetais em áreas de mangue.

Palavras-chave: Isótopos estáveis. Decomposição. Variabilidade vegetal.

ORIGIN, DYNAMIC, AND CHEMICAL COMPOSITION OF ORGANIC MATTER IN CONTAMINATED MANGROVE SOILS BY MERCURY

Abstract

Investigations about the nature of soil organic matter (SOM) in mangrove areas are essential in understanding its sources, stability, and chemical composition in estuary areas. Furthermore, few studies are conducted in contaminated areas, where this information can be used to predict the dynamics of contaminants in soil. This study aimed to evaluate the SOM in different vegetation domains in a contaminated mangrove. Nine sites along the Botafogo River mangrove were selected to represent three sections, dominated by different species: *Laguncularia racemosa*, species coexistence, and *Rhizophora mangle*. The origin, stability and molecular composition of SOM were investigated due to the follow procedures: $\delta^{13}C$ and $\delta^{15}N$; differential scanning calorimeter and thermogravimetry (DSC-TG) and C/N, and Fourier transform infrared spectroscopy (FTIR), respectively. The isotopic results confirmed the autochthonous production of OM in the upper and middle sections, but lower δ13C values in areas close to the mouth. DSC-TG and FTIR revealed similar behavior, with an accumulation of aliphatic OM in upper and middle section, against aromatic C domain in *R. mangle* forest. In Hg retention, this heterogeneity in the quality of SOM also demonstrated variations in the potential for sequestration of this contaminant at the different sections of the Botafogo River estuary. Our results contribute to a better understanding of the spatial variations in SOM chemical compositions created mainly by plant domains in mangrove areas.

Keywords: Stable isotopes. Decomposition. Vegetable variability.

4.1. Introduction

Despite recent studies address SOM variability in mangrove soils, only a few have investigated it in contaminated areas and how these forests contribute to the quality of the organic matter in the sediments. Most of OM mangrove research focuses only on C sequestration and the impact of human activities on C losses (SANTOS-ANDRADE et al., 2021).

Besides the OM monitoring in pursuit of C losses and how it affects climate change control, the OM stocked in mangrove areas must be observed qualitatively because it provides countless ecosystem services for the fauna, flora, and population (ATWOOD et al., 2017). The protection role as biogeochemical filter is one of them, which acts retaining contaminants coming from urban and rural areas (CHAKRABORTY et al., 2015). Nevertheless, SOM variation along comprehension estuaries remains unclear and there is information lack about it, going even further in the contaminated areas context.

The SOM controls the fate variation of many inorganic contaminants such heavy metals (MARCHAND; ALLENBACH; LALLIER-VERGÈS, 2011). Among them, Hg is one of the heavy metals that constantly threats coastal ecosystems such mangroves, and it has highly affinity with organic compounds present in mangrove sediments (CHAKRABORTY et al., 2015). In this context, SOM characteristics are critical to predict the interactions with soil microbial communities, Hg, and consequently affect the production of even more toxic forms, such methylmercury (MeHg), in mangrove soils (DUAN et al., 2021).

SOM act as energy source to methylators bacteria such as sulfur reducing bacteria (SRB) and/or iron reducing bacteria (FeRB) (CORREIA; GUIMARÃES, 2017). However, this influence on Hg dynamic is rather complicated due to SOM variation composition along the estuaries. For example, OM stored in lower Eh soils stimulates the growth of methylators communities, and this process is also dependent on Hg input and more importantly, OM lability (LEI et al., 2019). Therefore origin, molecular composition, and stability of this phase on mangrove soils are relevant parameters responsible to provide not only information about its accumulation and stabilization, but also predictability of the action of organic compounds in face of contaminants association. The evaluation of these parameters can be performed using spectroscopic, thermodegradative, and isotopic techniques such as FTIR, DSC-TG, and isotopic $\delta^{13}C$ and $\delta^{15}N$ (GIOVANELA et al., 2004; KUSUMANINGTYAS et al., 2019; SANTOS-ANDRADE et al., 2021).

As the main autochthonous representative in mangrove soils, the tree species domain is one important factor controlling these OM characteristics in soils, especially at zones close to the forest (BARRETO et al., 2016). Previous studies revealed that species such as *Rhizophora mangle, Avicennia Shaueriana,* and *Laguncularia racemosa*, common halophytes in brazilian mangroves, release different C compounds on soil, especially through their leaves and roots (BARRETO et al., 2016; SILVA; MADUREIRA, 2012). In general, the species variation determines the relative proportion of refractory and aliphatic compounds in soil. For example, *R. mangle* leaves are very rich in tannin and this aromatic compound is known by decrease the activity of benthic organisms, responsible to SOM decomposition (LACERDA et al., 1995).

Therefore, the aim of this study was to evaluate the SOM origin, molecular composition, and thermal stability along the *Rhizophora mangle, Laguncularia racemosa, and Avicennia shaueriana* forests of the Botafogo estuary contaminated by mercury.

4.2. Material and methods

4.2.1. Study area

The mangrove area evaluated is located on the limits of the Botafogo River estuary, Goiana, north coast of Pernambuco state (Figure 6). The Botafogo River is the largest river that flows into the Santa Cruz Channel, being formed by the union of several rivers, among the main ones, the Catucá, Itapirema, and Arataca. The Botafogo watershed is part of the “Sistema Botafogo”, which is a potable water supplement system for the metropolitan region of Recife, capital of the state (CPRH, 2003; SRH, 2001).

Figure 6 - Location of the study area and indication of sampling sites.

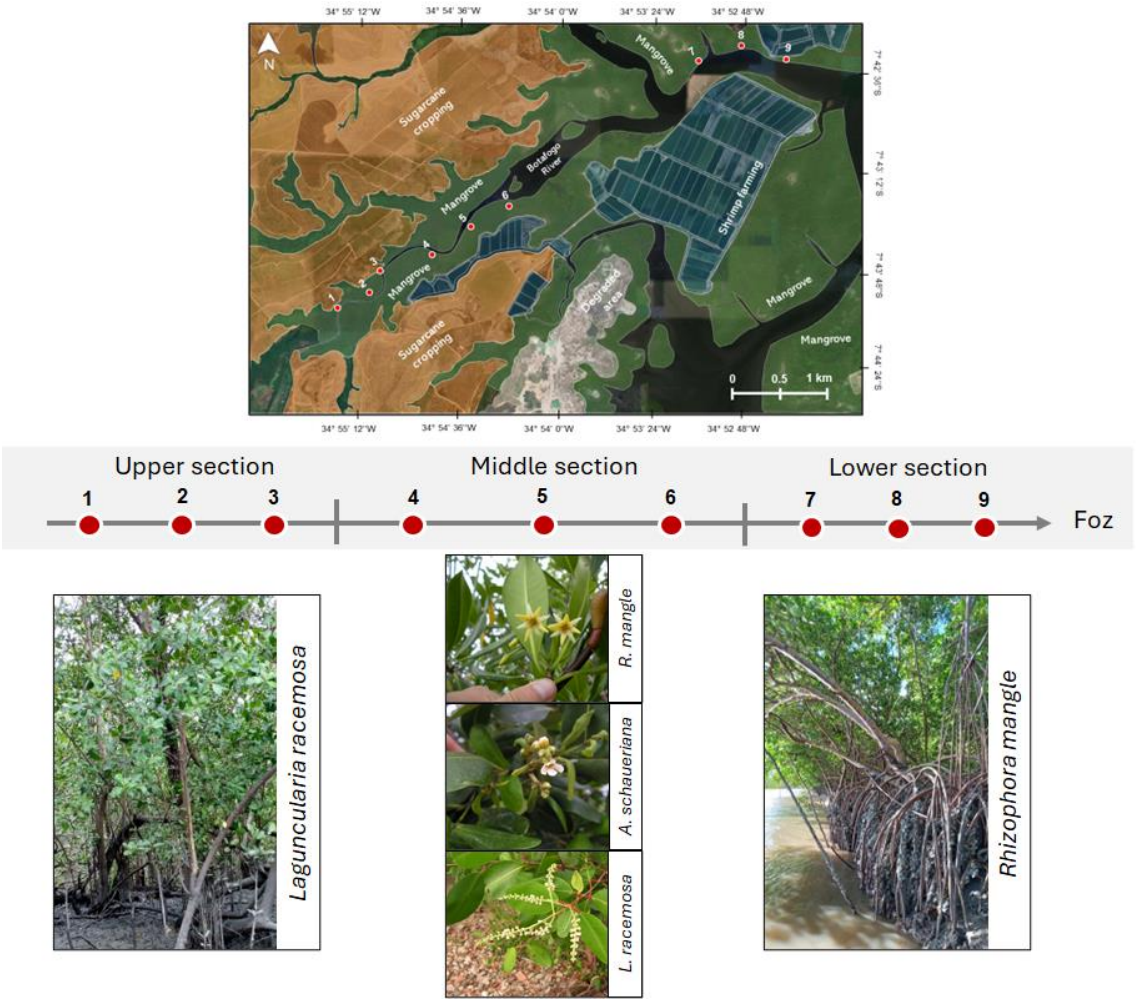

Each section shows a difference in species domain. Source: upper and lower section - personal archive. Middle section: *R. mangle* - Samuel Thomas (2024); *A. shaueriana* - Tarciso Leão (2024a); *L. racemosa* - Tarciso Leão (2024b).

The Botafogo mangrove forests are divided by three species domains. In the upper section (5.0 to 7.5 km from the following), there is a domain of *Laguncularia racemosa*; the middle section (2.5 to 5.0 km from the following) has a coexistence of *Rhizophora mangle*, *Laguncularia racemosa*, and *Avicennia shaueriana*; and in the lower section (0.0 to 2.5 km from the following), there is a domain of *Rhizophora mangle*. These areas are influenced by semi-diurnal tides, which have a maximum amplitude of 1.8 m, reaching a height of 2.2 m in spring tides, and 1.1 m in neap tides (PELAGE et al., 2021).

According to the Köppen classification, the study area has a hot and humid climate, classified as type As', with an average temperature ranging between 24ºC and 31ºC, and precipitation between 1.300 and 2.200 mm per year (INPE, 2023).

Anthropic activities surround the mangrove area, including sugarcane cultivation, the predominant economic activity in the Botafogo River basin. Some industries of the chemical

sector are installed in the upper stretch of the river, as the chlor-alkali plant, located 8.5 km from the study area and have been working since the beginning of the 60s. It was considered the main polluting source of Hg in the region (ARAÚJO et al., 2019). Shrimp farming is also a local important activity located mainly in the middle and lower section of the mangrove. These economic activities cause the constant release of pollutants from industrial waste, phytosanitary products, and fertilizers. Furthermore, domestic waste can be disposed of in rivers through the sewers of small population centers.

4.2.2. Sampling and samples preparation

The evaluation was performed due to the analysis of soil samples collected according to the sampling process discussed in the last chapter. The same 9 sites were evaluated, but the only difference was the pre-treatments requested by the procedures used to analyze the quality of the organic matter.

At the same spots where soil samples were taken, leaves samples from three trees were collected. About 30 and 50 leaves were removed from the canopy section of adult trees. The leaves were removed from the canopy of the trees. Then, the leaves were stored in plastic bags and transported to the laboratory to over dried at 60ºC. After identifying the achievement of constant weight, they were grounded in knife mills and stored in an airy place until the moment of analysis.

4.2.3. Characterization of soil organic matter

4.2.3.1. Identification of organic matter origin – $\delta^{13}C$ and $\delta^{15}N$

The geochemical technique used to identify the sources of SOM was the determination of isotopic composition of C and N ($\delta^{13}C$ and $\delta^{15}N$). Soil samples and fresh leaves were dried in an oven at 40 ºC, homogenized in an agate mortar and weighed in tin capsules. Approximately 3.5 mg of each sample was used to determine $\delta^{13}C$, $\delta^{15}N$, %C and %N. These elements were simultaneously determined by a continuous flow of isotopes of spectrometry ratio in an elementary combustion analyzer (EA-Carlo Erba), coupled in a Mass Spectrometer (Delta Plus, Finnigan Mat, San José, CA, EUA). The natural abundance of 13C and 15N is expressed in deviations (δ) per thousand (‰) from an international standard, the carbon standard being Pee dee Belemnite (PDB), and N being atmospheric air. The procedure was performed according to methodology proposed by Martins et al. (2015).

4.2.3.2. Soil pre-treatment with hydrofluoric acid (HF)

To better understand the isolate characteristics of OM molecular composition and stability, we removed the mineral phase of the samples (RUMPEL et al., 2006). According to this method, the minerals are removed due to a washing process using HF (10%), adding 10 ml HF to the previous ground samples. The suspensions were shaken for 2h at room temperature centrifuged and the supernatant removed. The procedure was repeated five times. The residue was washed five times with deionized H_2O to remove salts and residual HF. After that, the samples were oven dried (45ºC) and sieved (Ø – 0.200 mm). When the HF treatment was completed, the samples were able to be analyzed at the DSC-TG and FTIR.

4.2.3.3. Organic matter thermal stability – DSC-TG

Thermal measurements were performed simultaneously on soil samples by Differential Scanning Calorimetry (DSC) and Thermogravimetry (TG), using the Netzsch STA 449 thermal analyzer. The samples were heated from room temperature (approximately 25° C) at 950°C at a heating rate of 10°C min^{-1} in a furnace atmosphere consisting of synthetic air (80% N_2 and 20% O_2) flowing at 50 mL min^{-1} and shield gas N_2 flowing at 20 mL min^{-1}. 20 mg of ground soil sample were used, and an empty alumina crucible was used as a sample reference. These measurements quantified different thermal stability fractions, according to Dell' Abate et al. (2002); Dell' Abate; Benedetti; Brookes (2003). Considering the similarity of OM stability data inside the area sections, only one sample was chosen to represent the section.

4.2.3.4. Identification of organic functional groups – FTIR

The Infrared spectra of raw soil previously treated with HF were obtained in the range of 4000 – 400 cm^{-1} using a Fourier transform infrared spectrometer (FTIR). Each spectrum was obtained from 100 scans, calculated and corrected against ambient air (H_2O and CO_2) as background and with a resolution of 16 cm^{-1}. The baseline was corrected for all spectra. KBr pellets were obtained by mixing and grinding 1 mg of raw soil and 200 mg of potassium bromide (KBr). Readings were taken in absorbance versus wavenumber (cm^1). The spectras were interpretated due to the follow studies: Silverstein; Webster; Kiemle (2005); Stevenson (1994). Similar to DSC-TG samples, only three sites were evaluated due to the similarity of OM molecular composition inside of each section.

4.2.3.5. C/N ratio

The total content of C and nitrogen (N) of soil samples were determined via dry combustion. In this procedure, 1 g of air-dried soil was used, previously grounded in a mortar, and passed through a 0.2 mm mesh sieve. Total C and N were determined in an elemental analyzer (CN), model Perkin Elmer, PE-2400 Series II. Using the total C and N content was possible to calculate the C/N ratio. This ratio provides more information about the OM characterization, contributing on sources and decomposition investigations (KUSUMANINGTYAS et al., 2019). Only the soil and plant C/N ratio values were showed by graphics.

4.2.4. Data analysis

Mean, standard deviation (SD), and coefficient of variation (CV) were performed to describe isotopic $\delta^{13}C$ and $\delta^{15}N$. Geoinformation system was used by the software QGIS3 (v. 3.4.3).

4.3. Results and discussions

The soil $\delta^{13}C$ signal of C varied from -27.35 ‰ to -19,39 ‰, a difference of 7.96 ‰ (Table 4). It is possible to observe a decreasing gradient with the mean values toward to the river mouth, starting with -27.20 ‰ at the upper section to -21.99 ‰ at the lower section. The $\delta^{13}C$ values of species leaves were similar to other studies: *L. racemosa* (WOOLLER et al., 2003); *R. mangle* (SMALLWOOD et al., 2003); *A. shaueriana* (LARCHER; BOEGER; O'REILLY, 2016). The soil $\delta^{13}C$ reveals a close signature with plant $\delta^{13}C$ values at the upper and middle section, indicating most of SOM is autochthonous (C3 plants).

Table 4 - Isotopic 13C and 15N in soils and plants of Botafogo river mangrove.

Location	$\delta^{13}C$	$\delta^{15}N$
	----------‰----------	
	Upper section – *L. racemosa*	
1	-27.32	5.49
2	-26.92	5.09
3	-27.35	5.29
Mean	-27.20	5.29
SD	-0.24	0.20
CV	-0.89	0.03
	Middle section – coexistence	
4	-26.43	5.11
5	-26.87	4.84
6	-26.03	4.93
Mean	-26.44	4.96
SD	-0.42	0.13
CV	-1.59	0.02
	Lower section – *R. mangle*	

7	-25.17	4.39
8	-21.41	4.42
9	-19.39	5.01
Mean	-21.99	4.61
SD	-2.93	0.35
CV	-13.34	0.07
Species		
L. racemosa	-28.92	5.30
A. shaueriana	-28.93	3.99
R. Mangle	-29.13	3.87

SD – Standard deviation and CV – Coefficient of variation.

Once the SOM origin is predominantly autochthonous, it has some implications related to the Hg contamination historic as well as the SOM utilization as substrate by the methylators bacteria (SRB and FeRB) (CORREIA; GUIMARÃES, 2017). First, besides the domain of autochthonous OM in each forest, $\delta^{13}C$ signatures varied along the estuary. Consequently, each forest may present a different potential to retain inorganic Hg and the potential for methylmercury formation. This is corroborated by the De Oliveira et al. (2015) data, which they studied MeHg formation in mangroves soils under different vegetations. The authors identified *R. mangle* forest had lower MeHg formation (0.018–2.23%) than under *A. shaueriana* (0.2–4.63%) and *L. racemosa* (0.08–7.82%). Soil chemical conditions must be also considered, especially Eh, pH and salinity because these are parameters that affect OM nature (KIDA; FUJITAKE, 2020).

On other hand, lower $\delta^{13}C$ values occurred at the lower section (site 7 to 9). Despite the influence of shrimp farming activity, stimulating phytoplankton production around (e.g., seagrass and algae) (SANTOS-ANDRADE et al., 2021), the lower section is located closer to the ocean in comparison to other areas (figure 7). The *R. mangle* forest acted as a deposition zone of inorganic C due to carbonate supply from oyster (*Crassostrea rhizophorae*). This biogenic carbonate $\delta^{13}C$ signature usually is lower than those identified in C3 plants (LIN; BANKS; STERNBERG, 1991). This soil samples were not HCL treated to confirm the biogenic C presence in this estuary section.

$\delta^{15}N$ values also followed the decreasing gradient along the areas. The maximum and minimum signal observed was 5.49‰ (upper section) and 4.39‰ (lower section), respectively. The soil and fresh leaves $\delta^{15}N$ signature showed a close relation, especially at the upper section (soil $\delta^{15}N$ – 5.29 ‰ and fresh leaves $\delta^{15}N$ – 5.30 ‰). Nevertheless, in this context, an increment of N was observed at the lower section because the values were higher than those observed at the leaves of *R. mangle*. Based on the distance from the shrimp farms, this forest may be assimilating heavier nitrogen from algal-derived organic matter (PÉREZ et al., 2020). Shrimp

farming effluents stimulate the growth of algae, and these organisms present a natural higher $\delta^{15}N$ signature (PÉREZ et al., 2020).

Figure 7. Location of the study area.

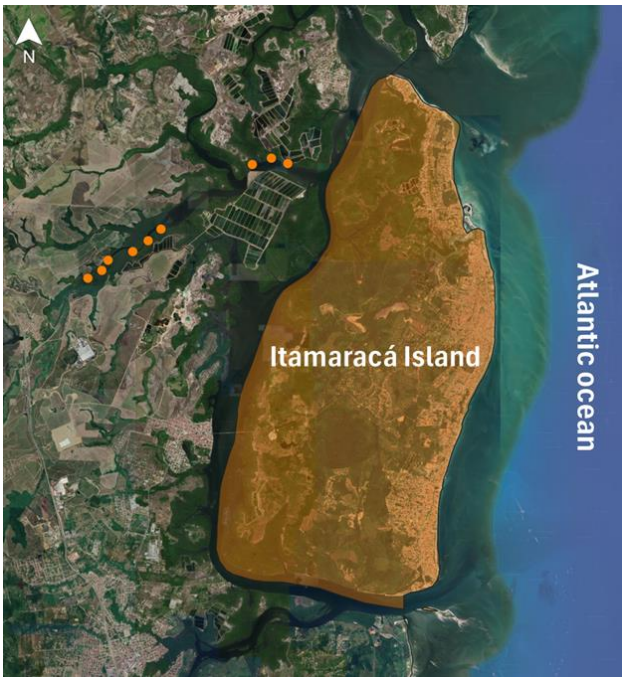

Orange dots indicate the evaluated sites. The figure shows the proximity between the study area and the ocean.

C/N ratio was also used to identify potential sources of OC (Figure 8). It showed significant differences between soils C/N and C/N of trees leaves. The values varied along the sections, achieving the lowest average at the middle section (C/N - 16.54).

Figure 8 - C/N ratio values of soil and leaves (in colors) from mangrove species in different sections.

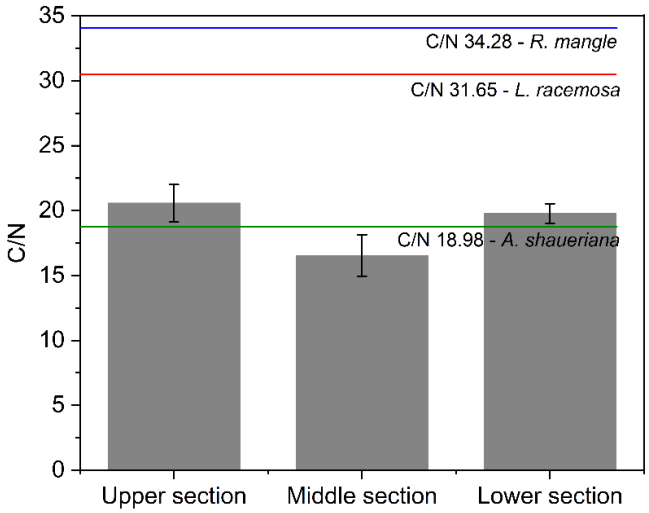

The decreasing order of leaves C/N values of the species were: *R. mangle>L. racemosa>A. shaueriana.* In relation to middle and lower section, C/N values at the upper

section shows the *L. racemosa* leaves C contribution. At this section, soil C/N was high due to the high C content of the *L. racemosa* leaves (44.38%), being the highest one in comparison to other species (*R. mangle* = 44.04%; *A. shaueriana* = 40.46%). A similar effect apparently occurred at the lower section based on the *R. mangle* leaves also show a high content of C. In addition, it represents not only the *R. mangle* contribution but also the carbonates influence discussed in the last chapter (VALENÇA; SOUZA, 2017). Two sources contribute to carbonate accumulation, 1) around the mangrove sediments (Q2m), local formations: Beberibe (Kb), Gramame (Kg), and Itamaracá Formation (K2it) represent the mineral sources of carbonate in the whole region. All geological formation present carbonate materials. However, 2) biogenic carbonate probably could be the main Ca and C source. Oyster species, such *Crassostrea rhizophorae* live associated with *R. mangle* roots. Considering mineral supply requires rocky outcrop, the high content of carbonate is more associated with biological contribution in this section. This discussion will be better detailed at chapter 4. *A. shaueriana* leaves show a lower C/N value, it suggests an influence in soil C/N decrease at the middle section. Therefore, *A. shaueriana* presence at the coexistence section contributed to the release of unstable C in the soil, making the OM more easily to be decomposed (LACERDA et al., 1995).

The last results are consistent with the DSC-TG data (Table 5). The first peak temperature (between 80 – 100 ºC) corresponds the loss of water reaction. After that two exothermic reactions were registered by the peaks of temperature 277 - 286 ºC and 351 - 369 ºC. 1) first reaction represents the decomposition of aliphatic chains and functional groups, revealing an exothermic peak with a maximum of 290.5 °C; 2) the second exothermic reaction began from the last peak, indicating the decomposition of aromatic structures such as lignin and other polyphenols with maximum temperature of 369.0 ºC.

Table 5 - DSC-TG data of OM extracted from surface layer (0-10cm).

Site	DSC					TG		1ºExo%
	Peak temperature (°C)			Energy (µV/min)		Mass loss (%)		
	1°End	1°Exo	2°Exo	1°Exo	2°Exo	1ºExo	2ºExo	
Upper section	82.5	286.7	363.8	1.01	0.64	20.64	11.66	63.9
Middle section	82.3	290.5	369.0	0.81	0.62	21.38	9.50	69.2
Lower section	101.2	277.4	351.1	0.85	0.27	7.97	20.26	28.23

Bulk soil DSC-TG parameters: temperature peaks (ºC) related to DSC; and mass loss (%) related to TG. First endothermic reaction (1°End), first exothermic reaction (1°Exo) and second exothermic reaction (2°Exo). Relative percentage of first weight loss in relation to total weight loss (1Exo%).

The lower section shows the prevalence of aromatic C (71.77%). However, the middle section and upper section had the opposite characteristic, which presented more than 60% of C in aliphatic form. Lower section represents a refractory compounds pool, such as tannins and

lignin, derived from *R. mangle* trees and it is maintained by the low-rate decomposition conditions associated to the lower soil Eh (chapter 2) (LACERDA et al., 1995).

Considering the soils role as biogeochemical filter, each forest can act differently in heavy metal retention. The degree of aromaticity of C helps to predict the contaminant retention on soil, which is represented mainly by the accumulation of less reactive compounds, such lignin and tannin groups. The *R. mangle* forest soil, in terms of hydrocarbons, shows the lowest potential to complex metals, especially Hg. Correlated with it, this section presented the lowest Hg concentration, indicating a weaker C contribution compared to *L. racemosa* and coexistence forest. In terms of soil functionality as filter, local areas tend to be safer with the act of *L. racemosa* in Hg complexation. Zhang et al. (2009) identified this functionality, after observing the high affinity Hg ions has with carboxylic and phenols groups, forming complex structures. However, Vasques et al. (2020) added that Hg-carboxylic complex can be less stable than those that would be formed with sulfhydryl, such thiol

Furthermore, this *R. mangle* forest is located next to the river mouth, closer to the sea. In this section, soils are sandier, and its mineralogy is dominated by quartz (chapter 4), which has low Hg retention capacity. Besides that, this zone has a high hydrological influence created by the tidal dynamics that constantly removes chemicals from soil particles and according to Van Santen et al. (2007), bare mudflat can show five to ten times less sedimentation rate when compared to densely vegetated area. Overall, *R. mangle* trees must be preserved, avoiding the loss of OM, which clearly is the main agent for Hg retention in this position of Botafogo estuary.

Overall, FTIR shows similar functional groups, however some differences were identified in the absorption intensities of the bands (absorbance), indicating variability in SOM dynamics (Table 6).

Table 6 - Absorption frequencies and assignment of functional groups by FTIR for the SOM in soils of mangroves forests.

Frequency (cm^{-1})	Assignment
3500 – 3200	Vibration of hydroxyl groups (O-H) of water molecules, alcohols, phenols, N-H groups, or vibrations of the OH of silicate octahedrons
2920 and 2850	Asymmetric and symmetric stretching vibration of C-H bonds of CH_2 and CH_3.
2360 and 2337	Carbon dioxide absorption indicating O=C=O stretching.
1720	Stretching vibrations of C=O bonds of carboxylic acids and ketones.
1630	vibrations of aromatic C=C bonds
1500 and 1450	vibrations of aromatic nuclei
1380	OH deformation, C-O stretching of alcohols and phenols, and C-H deformation of CH_2 and CH_3
1200	C-O stretching and O-H deformation of COOH. 1100 - 1030 cm^{-1}: stretching vibrations of C–O–C bonds in polysaccharides or polysaccharide-like substances, stretching of C−O of primary and secondary alcohols and of inorganic Si–O–Si.

The FTIR spectra from the upper and middle section indicate markedly more aliphatic organic compounds, especially in the upper section (Figure 9). This is shown by the evident aliphatic bands around 1080 cm^{-1} (stretching of C−H groups) and with a greater diversity of these structures, including peaks at approximately 1220 cm^{-1} and 1033 cm^{-1}, which correspond to the C−O stretch, as primary and secondary alcohols.

Figure 9 - FTIR spectra of organic matter extracted from surface layer (0-10 cm).

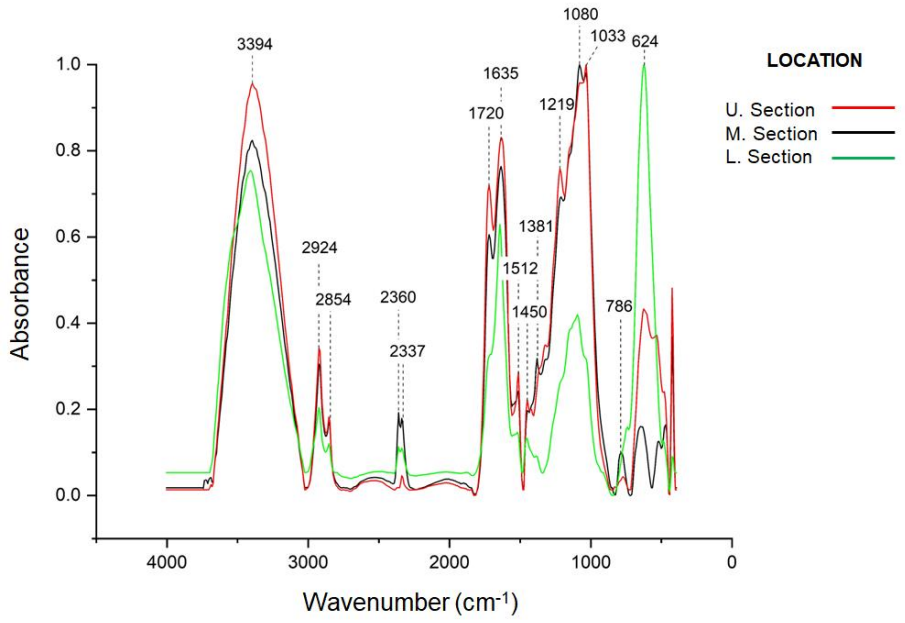

Other aliphatic groups are indicated by the frequencies 2920 cm^{-1} and 2851 cm^{-1}, assigned to methylene and methyl, and to C-H stretch, CH_2 groups such as alkanes, respectively (BARRETO et al., 2016). All soil samples showed a broad band around 3400 cm^{-1}, referring mainly to the OH vibration of the water. While the region between 3800 and 3600 cm^{-1}, more expressive in the middle and upper section, possibly suggests the presence of alcohols, phenols, and inorganic impurities.

Upper and middle section showed a greater hydrophilic character due to the greater intensity of absorption around 1700 cm^{-1}, representing the stretching of C=O functional carboxylic groups (BARRETO et al., 2016). These profiles also showed a greater contribution of lignin/phenolic compounds, by absorption at 1200 cm^{-1}.

On other hand, soil from lower section showed significant loss of structures such as polysaccharides (1080 cm^{-1}) and carboxylic groups (1720 cm^{-1}), in addition to the enrichment of aromatic groups in the region of 620 cm^{-1} (C-H). Under anaerobic conditions C=O groups can be used as sources of oxygen, resulting in an increase in C-H groups.

FTIR confirms DSC-TG data, and based on the groups identified, it seems the sites located away from river mouth concentrates more reactive C groups, such as carboxylic acids, alcohols, and phenols. Besides sulfur reduced groups, such thiols, oxygen-containing functional groups are important C components in Hg complexation (RAVICHANDRAN, 2004). Considering the history of contamination, especially by Hg, the variation in OM quality along the area may contribute to explaining the Hg concentration gradient, which until now has only been related to the distance from the polluting source, OM content, and the mineral contribution. (clay content) (ARAÚJO et al., 2019).

Comparing the forests, two points must be highlighted: 1) upper and middle section showed greater contribution on aliphatic C release, which was essential on Hg sequestration. However, 2) This upper forests may act as a "time-bomb" for the whole estuary. Hg can be more available if these tree species are not preserved, especially *L. racemosa* forest, where it holds the highest Hg concentration. The preservation extends to the soil conditions. Based on it, this information strengthens the need of preservation. Botafogo river mangroves has been threatened by local anthropic activities and it must be monitored, considering the possibility of drainage and deforestation. These practices accelerate OM decomposition, release CO_2 to the atmosphere, and more important, promote the loss of C forms, responsible for Hg retention.

4.4. Conclusions

With the use of spectroscopy and thermal techniques we were able to identify the variation of OM sources, composition, and stability. Soil $\delta^{13}C$ signature confirms the domain of autochthonous OM along the Botafogo mangrove. $\delta^{15}N$ signature indicates leaves contribution to the soil, but also introduction of heavier N at the *R. mangle* forest, which is located around the shrimp tanks, thus demanding constant monitoring.

Comparing the species, *R. mangle* also demonstrated to be the greatest producer of more resistant OM against decomposition. At the lower section, refractory C is released mainly by *R. mangle* leaves and roots tissues and the soil anaerobic conditions (Low Eh) maintains these C compounds. DSC-TG confirmed a greater stability of these OM, possible related to complex C substances, such as lignin and tannin.

Overall, taking distance from the river mouth it is possible to identify more aliphatic OM contribution originated from the species of tree, especially *L. racemosa*. It indicates a difference in organic compounds produced by the trees, and the maintenance by soil chemical conditions.

Considering the area contamination context, the environmental monitoring of OM quality is an essential and parameters used in this study demonstrated to be an important tool to

characterize it. The relevance of OM in contaminants retention, such Hg, can be natural affected by the species variation domain, soil chemical conditions, and human activities disturbance in mangrove forests. *L. racemosa* forest was responsible for the greater contribution on Hg sequestration at the Botafogo river mangrove. However, it must be well monitored because the potential of methylation and the risks promoted by anthropogenic activities, responsible for SOM degradation and consequently, Hg release.

References

ARAÚJO, P. R. M.; BIONDI, C. M.; DO NASCIMENTO, C. W. A.; DA SILVA, F. B. V.; ALVAREZ, A. M. Bioavailability and sequential extraction of mercury in soils and organisms of a mangrove contaminated by a chlor-alkali plant. **Ecotoxicology and Environmental Safety**, v. 183, p. 109469, 2019. https://doi.org/10.1016/j.ecoenv.2019.109469

ATWOOD, T. B.; CONNOLLY, R. M.; ALMAHASHEER, H.; CARNELL, P. E.; DUARTE, C. M.; EWERS LEWIS, C. J.; LOVELOCK, C. E. Global patterns in mangrove soil carbon stocks and losses. **Nature Climate Change**, v. 7, p. 523–528, 2017. https://doi.org/10.1038/nclimate3326

BARRETO, M. B.; MÓNACO, S. LO; DÍAZ, R.; BARRETO-PITTOL, E.; LÓPEZ, L.; PERALBA, M. DO C. R. Soil organic carbon of mangrove forests (*Rhizophora* and *Avicennia*) of the Venezuelan Caribbean coast. **Organic Geochemistry,** v. 100, p. 51–61, 2016. https://doi.org/10.1016/j.orggeochem.2016.08.002

CHAKRABORTY, P.; SARKAR, A.; VUDAMALA, K.; NAIK, R.; NATH, B. N. Organic matter — A key factor in controlling mercury distribution in estuarine sediment. **Marine Chemistry**, v. 173, p. 302–309, 2015. https://doi.org/10.1016/j.marchem.2014.10.005

CORREIA, R. R. S.; GUIMARÃES, J. R. D. Mercury methylation and sulfate reduction rates in mangrove sediments, Rio de Janeiro, Brazil: the role of different microorganism consortia. **Chemosphere**, v. 167, p. 438-443, 2017. https://doi.org/10.1016/j.chemosphere.2016.09.15

DELL'ABATE, M. T.; BENEDETTI, A.; TRINCHERA, A.; DAZZI, C. Humic substances along the profile of two Typic Haploxerert. **Geoderma**, v. 107, p. 281–296, 2002. https://doi.org/10.1016/S0016-7061(01)00153-7

DELL'ABATE, M. T.; BENEDETTI, A.; BROOKES, P. C. Hyphenated techniques of thermal analysis for characterisation of soil humic substances. **Journal of Separation Science**, v. 26, p. 433–440, 2003. https://doi.org/10.1002/jssc.200390057

DUAN, D.; LEI, P., LAN, W.; LI, T.; ZHANG, H.; ZHONG, H.; PAN, K. Litterfall-derived organic matter enhances mercury methylation in mangrove sediments of South China. **Science of the Total Environment**, v. 765, p. 142763, 2021. https://doi.org/10.1016/j.scitotenv.2020.142763

GIOVANELA, M.; PARLANTI, E.; EJ, S. S.; MMD, S. Elemental compositions, FT-IR spectra and thermal behavior of sedimentary fulvic and humic acids from aquatic and terrestrial environments. **Geochemical Journal**, v. 38, p. 255–264, 2004. https://doi.org/10.2343/geochemj.38.255

KIDA, M.; FUJITAKE, N. Organic carbon stabilization mechanisms in mangrove soils: a review. **Forests**, v. 11, p. 981, 2020. https://doi.org/10.3390/f11090981

KUSUMANINGTYAS, M. A.; HUTAHAEAN, A. A.; FISCHER, H. W.; PÉREZ-MAYO, M.; RANSBY, D.; JENNERJAHN, T. C. Variability in the organic carbon stocks, sources, and accumulation rates of Indonesian mangrove ecosystems. **Estuarine, Coastal and Shelf Science**, v. 218, p. 310–323, 2019. https://doi.org/10.1016/j.ecss.2018.12.007

LACERDA, L. D.; ITTEKKOT, V.; PATCHINEELAM, S. R. Biogeochemistry of Mangrove Soil Organic Matter: a Comparison Between *Rhizophora* and *Avicennia* Soils in South-eastern Brazil. **Elsevier**, v. 40, p. 713–720, 1995. https://doi.org/10.1006/ecss.1995.0048

LARCHER, L.; BOEGER, M. R. T.; O'REILLY, L. DA S. L. Gas exchange and isotopic signature of mangrove species in Southern Brazil. **Aquatic botany**, v. 133, p. 62–69, 2016. https://doi.org/10.1016/j.aquabot.2016.06.001

LEI, P.; ZHONG, H.; DUAN, D.; PAN, K. A review on mercury biogeochemistry in mangrove sediments: hotspots of methylmercury production?. **Science of the total environment**, v. 680, p. 140-150, 2019. https://doi.org/10.1016/j.scitotenv.2019.04.451

LIN, G.; BANKS, T.; O'REILLY, L. D. S. L. Variation in $\delta^{13}C$ values for the seagrass *Thalassia testudinum* and its relations to mangrove carbon. **Aquatic Botany**, v. 40, p. 333-341, 1991. https://doi.org/10.1016/0304-3770(91)90079-K

MARCHAND, C.; ALLENBACH, M.; LALLIER-VERGÈS, E. Relationships between heavy metals distribution and organic matter cycling in mangrove sediments (Conception Bay, New Caledonia). **Geoderma**, v. 160, p. 444-456, 2011. https://doi.org/10.1016/j.geoderma.2010.10.015

MARTINS, S. C.; NETO, E. S.; DE CÁSSIA PICCOLO, M.; ALMEIDA, D. Q.; DE CAMARGO, P. B.; DO CARMO, J. B.; MARTINELLI, L. A. Soil texture and chemical characteristics along an elevation range in the coastal Atlantic Forest of Southeast Brazil. **Geoderma Regional**, v. 5, p. 106–116, 2015. https://doi.org/10.1016/j.geodrs.2015.04.005

PÉREZ, A.; MACHADO, W.; GUTIÉRREZ, D.; SALDARRIAGA, M. S.; SANDERS, C. J. Shrimp farming influence on carbon and nutrient accumulation within Peruvian mangroves sediments. **Estuarine, Coastal and Shelf Science**, v. 243, p. 106879, 2020. https://doi.org/10.1016/j.ecss.2020.106879

RAVICHANDRAN, M. Interactions between mercury and dissolved organic matter—a review. **Chemosphere**, v. 55, p. 319–331, 2004. https://doi.org/10.1016/j.chemosphere.2003.11.011

RUMPEL, C.; RABIA, N.; DERENNE, S.; QUENEA, K.; EUSTERHUES, K.; KÖGEL-KNABNER, I.; MARIOTTI, A. Alteration of soil organic matter following treatment with hydrofluoric acid (HF). **Organic Geochemistry**, v. 37, p. 1437–1451, 2006. https://doi.org/10.1016/j.orggeochem.2006.07.001

SAMUEL THOMAS. ***Rhizophora mangle* flowers in Jobos Bay National Estuarine Research Reserve, Aguirre, Puerto Rico.** Disponível em: < https://en.m.wikipedia.org/wiki/File:Rhizophora_mangle_flowers.JPG> Acesso em 11 de fevereiro de 2024.

SANTOS-ANDRADE, M.; HATJE, V.; ARIAS-ORTIZ, A.; PATIRE, V. F.; DA SILVA, L. A. Human disturbance drives loss of soil organic matter and changes its stability and sources in mangroves. **Environmental Research**, v. 202, p. 111663, 2021. https://doi.org/10.1016/j.envres.2021.111663

SILVA, C. A.; MADUREIRA, L. A. S. Source correlation of biomarkers in a mangrove ecosystem on Santa Catarina Island in southern Brazil. **Anais da Academia Brasileira de Ciências**, v. 84, p. 589–604, 2012. https://doi.org/10.1590/S0001-37652012005000042

SMALLWOOD, B. J.; WOOLLER, M. J.; JACOBSON, M. E.; FOGEL, M. L. Isotopic and molecular distributions of biochemicals from fresh and buried *Rhizophora mangle* leaves. **Geochemical Transactions**, v. 4, p. 38–46, 2003. https://doi.org/10.1039/B308902A
STEVENSON, F.J. **Humus chemistry: genesis, composition, reactions**. 2.ed. New York: Wiley, 1994. 496p.

TACIRSO LEÃO. Leaves and flower of *Avicennia cf. schaueriana*. Disponível em: < https://pt.wikipedia.org/wiki/Avicennia_schaueriana#/media/Ficheiro:Avicennia_cf._schaueriana_mangue-preto.jpg> Acesso em 11 de fevereiro de 2024a.

TARCISIO LEÃO. *Laguncularia racemosa*, mangue-branco. Disponível em: < https://www.flickr.com/photos/tarcisoleao/17429916883> Acesso em: 11 de fevereiro de 2024b.

VALENÇA, L. M. M.; SOUZA, N. G. A. **Unidades estratigráficas**. Geologia e recursos minerais da folha Itamaracá SB. 25-YC-VI: estados de Pernambuco e Paraíba. *In*: VALENÇA, L. M. M.; SOUZA, N. G. A. Recife: CPRM, 2017. p. 23-41.

VAN SANTEN, P.; AUGUSTINUS, P. G. E. F.; JANSSEN-STELDER, B. M.; QUARTEL, S.; TRI, N. H. Sedimentation in an estuarine mangrove system. Journal of Asian Earth Sciences, v. 29, p. 566-575, 2007. https://doi.org/10.1016/j.jseaes.2006.05.011

VASQUES, I. C.; EGREJA FILHO, F. B.; MORAIS, E. G.; LIMA, F. R.; OLIVEIRA, J. R.; PEREIRA, P.; MARQUES, J. J. Mercury fractionation in tropical soils: A critical point of view. **Chemosphere**, v. 257, p. 127114, 2020. https://doi.org/10.1016/j.chemosphere.2020.127114

WOOLLER, M.; SMALLWOOD, B.; JACOBSON, M.; FOGEL, M. Carbon and nitrogen stable isotopic variation in *Laguncularia racemosa* (L.) (white mangrove) from Florida and Belize: implications for trophic level studies. **Hydrobiologia**, v. 499, p. 13–23, 2003. https://doi.org/10.1023/A:1026339517242

ZHANG, J.; DAI, J.; WANG, R.; LI, F.; WANG, W. Adsorption and desorption of divalent mercury (Hg^{2+}) on humic acids and fulvic acids extracted from typical soils in China. **Colloids and surfaces A: physicochemical and engineering aspects**, v. 335, p. 194-201, 2009. https://doi.org/10.1016/j.colsurfa.2008.11.006

5. MINERALOGIA E ESPECIAÇÃO DE ENXOFRE DE SOLOS DE MANGUEZAL CONTAMINADOS POR INDÚSTRIA SODA-CLORO

Resumo

Os manguezais que cobrem o litoral Norte do estado de Pernambuco são zonas importantes para toda região costeira, porém devido ao descarte inadequado de resíduos industriais, estas áreas detêm atualmente a maior concentração de mercúrio (Hg) da costa brasileira. Neste contexto, investigações mineralógicas e quimica podem contribuir para a elucidação da dinâmica de Hg nestes ambientes. O trabalho teve como objetivo identificar a assembleia mineralógica e realizar a especiação de enxofre (S) nos solos em diferentes florestas de manguezais contaminados do Rio Botafogo. Para isto, foi realizado a identificação de silicatos da fração argila por difração de raio-x (DRX) e a fração areia analisada por microscopia óptica. Análises no MEV/EDS foram realizadas visando a identificação de minerais não silicatados, bem como a distribuição do Hg nestes componentes. Espécies de S foram também caracterizadas por espectroscopia de fotoelétrons de raio-x (XPS). A fração argila destacou a presença de caulinita, ilita, esmectita e quartzo. A fração areia é predominante quartzosa com presença também de muscovita, feldspato, fragmentos quartzo/muscovita e materiais opacos. Nas amostras frescas, foram identificados: pirita, quartzo, muscovita e carbonatos. O Hg se encontrou associado a pirita. Ademais, as espécies oxidadas de S predominaram, porém sulfetos orgânicos e dissulfetos foram identificados na maior parte do manguezal. Os resultados indicam a contribuição da litologia local (alóctone) e transporte de minerais como a caulinita, muscovita e quartzo, e a neoformação de outros: pirita, esmectita e carbonatos. A mineralogia e especiação de S revelaram a distribuição dos sulfetos ao longo das diferentes florestas de mangue, bem como a importância destes compostos na retenção de Hg em cada posição do estuário. Essa variação contribuiu para o gradiente de concentração de Hg no solo. Estes resultados possibilitaram o avanço nas discussões de caracterização de manguezais contaminados com ênfase na interação com Hg. Os resultados revelaram que estes solos desempenharam o papel de filtro geoquímico de Hg pela presença dos sulfetos minerais e orgânicos.

Palavras-chave: Contaminação. Rio Botafogo. Sulfetos.

SOIL MINERALOGY AND SULFUR SPECIATION OF MANGROVE SOILS CONTAMINATED BY CHLOR-ALKALI PLANT

Abstract

The mangroves that cover the northern coast of the state of Pernambuco are important areas for the entire coastal region, however, due to inadequate disposal of industrial waste, these areas currently have the highest concentration of mercury (Hg) on the Brazilian coast. In this context, mineralogical and chemical investigations contribute to the elucidation of Hg dynamics in these environments. The aim of this study was to identify the mineralogical assemblage and perform sulfur (S) speciation in soils from different contaminated mangrove forests on the Botafogo River. Considering it, silicates from the clay fraction were identified by x-ray diffraction (XRD) and the sand fraction was analyzed by optical microscopy. SEM/EDS analyzes were carried out to identify non-silicate minerals, as well as the distribution of Hg in these components. S species were also characterized by x-ray photoelectron spectroscopy (XPS). The clay fraction highlighted the presence of kaolinite, illite, smectite and quartz. The sand fraction is predominantly quartz with the presence of muscovite, feldspar, quartz/muscovite fragments and opaque materials. In the fresh samples, the following were identified: pyrite, quartz, muscovite, and carbonates. Hg was found associated with pyrite. Furthermore, oxidized S species predominated, but organic sulfides and disulfides were identified in most of the mangrove. The results indicate the contribution of local lithology (allochthonous) and transport of minerals such as kaolinite, muscovite and quartz, and the neoformation of others: pyrite, smectite and carbonates. S mineralogy and speciation revealed the distribution of sulfides along the different mangrove forests, as well as the importance of these compounds in Hg retention in each position of the estuary. This variation contributed to the Hg concentration gradient in the soil. These results made it possible to advance discussions on the characterization of contaminated mangroves with an emphasis on the interaction with Hg. The results revealed that these soils played the role of geochemical Hg filter due to the presence of mineral and organic sulfides.

Keywords: Silicates. Contamination. Botafogo River. Sulfides.

5.1. Introduction

The mineralogy assemblage of mangrove soils is mostly detrital, and consequently variable due to its characteristic as transition zone between the coast and the ocean (SOUZA-JÚNIOR et al., 2008). In this context, allochthonous minerals are derived from two flows, 1) terrestrial sediments transported in runoff process and transported to coastal areas, 2) marine sediments deposited during past transgressive events and tidal currents (WOODROFFE et al., 2016).

Silicates, such as montmorillonite, kaolinite, illite, chlorite, are common minerals in those environments. Most of them are originate from the weathering of local rocks (SOUZA-JÚNIOR et al., 2008). Besides the silicates, the redox conditions with the high concentration of Mn, Fe, and S, provide the formation of minerals such as pyrite, jarosite, manganese sulfides, and gibbsite (OTERO et al., 2009). Furthermore, other minerals can be formed by the salinity water contribution, such halite, and carbonates (BEHLING; DA COSTA, 2004).

The mineralogy associated with clay, sand, and silt at the Northeast of Brazil maintains a signature with the tertiary sediments originated from the "Barreiras formation", a geological structure, characterized by white to yellow claystones (or mudstones), siltstones, sandstones, and conglomeratic sediments. These soils are mostly highly weathered, kaolinite-dominated and with minor amounts of Fe oxyhydroxides (BEHLING; DA COSTA, 2004).

The mineralogical studies conducted in contaminated mangroves are essential considering the role these minerals act as geochemistry filter. A great example are the non-silicates such as Fe oxyhydroxides, carbonates, and pyrite, which are responsible to remove temporally some heavy metals out of the soil solution during the co-precipitation reactions (MACHADO et al., 2014). Nevertheless, the oxidation of the soil caused by the tidal fluctuation and progress of anthropogenic activities promote certain instability to these minerals-contaminants association and it must be well monitored (MACHADO et al., 2014).

Based on this, the mineralogical approach of contaminated soil, especially clay and sand fractions, is the first step in the prediction of heavy metals dynamics along different mangrove forests.

5.2. Material and methods

5.2.1. Study area

The mangrove area evaluated is located on the limits of the Botafogo River estuary, Goiana, north coast of Pernambuco state (Figure 10).

Figure 10 - Location of the study area and indication of sampling sites.

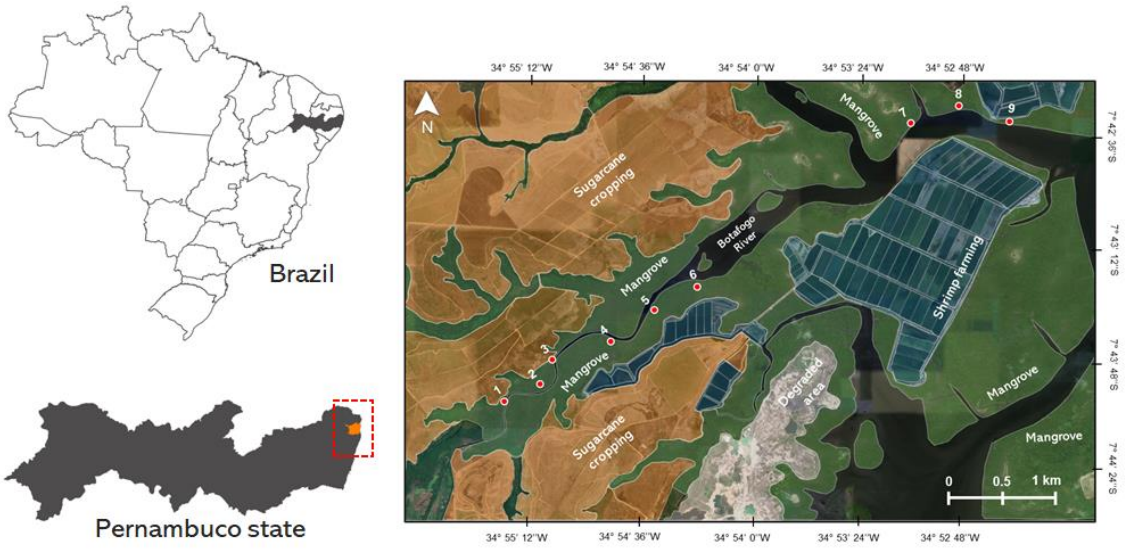

The areas in green represent the mangrove forests. Orange, blue, and white colors indicate the anthropic activities (Sugarcane cropping and shrimp farming) and degraded area, respectively. Red dots represent the sampling sites.

The Botafogo mangrove forests are divided by three species domains, all of them classified as riverine forests (LUGO; SNEDAKER, 1974). In the upper section (5.0 to 7.5 km from the following), there is a domain of *Laguncularia racemosa*; the middle section (2.5 to 5.0 km from the following) has a coexistence of *Rhizophora mangle*, *Laguncularia racemosa*, and *Avicennia shaueriana*; and in the lower section (0.0 to 2.5 km from the following), there is a domain of *Rhizophora mangle*. These areas are influenced by semi-diurnal tides, which have a maximum amplitude of 1.8 m, reaching a height of 2.2 m in spring tides, and 1.1 m in neap tides (PELAGE et al., 2021).

According to the Köppen classification, the area has a hot and humid climate, classified as type As', with an average temperature ranging between 24ºC and 31ºC, and precipitation between 1.300 and 2.200 mm per year (INPE, 2023).

Anthropic activities surround the mangrove area, including sugarcane cultivation, the predominant economic activity in the Botafogo River basin. Some industries of the chemical sector are installed in the upper stretch of the river, as the chlor-alkali plant, located 8.5 km from the study area and have been working since the beginning of the 60s. It was considered the main polluting source of Hg in the region (ARAÚJO et al., 2019). Shrimp farming is also a local important activity located mainly in the middle and lower section of the mangrove. These economic activities cause the constant release of pollutants from industrial waste, phytosanitary products, and fertilizers. Furthermore, domestic waste disposed of through the sewers of small population centers living in the basin.

5.2.2. Sampling and samples preparation

The evaluation was performed due to the analysis of soil samples collected according to the sampling process discussed in the last chapter. The same 9 sites were evaluated, but the only difference was the pre-treatments requested by the procedures used to analyze the mineralogical assemblage.

5.2.3. Samples preparation

Soil samples were previously treated for the processes of clay and sand separation and identification of silicates minerals by X-ray diffraction (XRD) and optical microscopy. Considering the high content of OM and dissolved salts, including carbonates, the samples were treated with hydrogen peroxide (17,5%), and alcohol (60%), respectively. Furthermore, taking into consideration the carbonate influence on soil (especially sites 8, 9, and 10), the samples were treated with sodium acetate after washing with alcohol (SOUKUP; BUCK; HARRIS, 2008). Then, the samples were air-dried, grounded, and sieved (2 mm).

The separation of fractions (sand and clay) process was performed due to a physical-chemical process using a Wagner shaker and a combined solution of sodium hexametaphosphate (0.5 mol L^{-1}) and sodium hydroxide (0.1 mol L^{-1}). Subsequently, the samples were transferred to a graduated cylinder, where 24h were waited to start collect the fractions. The sand fraction was collected using a 0.053 mm mesh sieve. Then, the clay particles were separated from the silt by siphonation process, according to the sedimentation time of the silt particle proposed by Stokes (1851). After that, the sand fraction was stored in Petri dish until the optical microscopy. The clay fraction was air-dried, grounded, and sieved (80 mesh).

Sulfides identification was performed using scanning electron microscope (SEM) with energy dispersive (EDS). The procedure described earlier is not adequate when reduced compounds and others non-phyllosilicates minerals, such pyrite and halite, must be identified. In this case, 10 g of wet soil samples from each section was freeze-dried for 48 h. After that, these subsamples were gently disaggregated using an agate mortar (OTERO et al., 2023). Then, they were kept in vacuum until the microscopy analyses (SEM/EDS).

Lyophilized samples were also used for S speciation (XPS). A subsample of 100 mg was separated and then ground (agate mortar) and sieved (0.2 mm). No pre-treatment was used in this samples.

5.2.4. Clay mineralogy – XRD

The oxide forms of iron have low stability in mangrove soils and these minerals can act as cementing agents capable to reduce the diffractograms quality. Considering it, the clay samples were treated with citrate bicarbonate dithionite (CBD) before the XRD scanning (JACKSON, 1975). Then, the samples were saturated with potassium chloride (1 mol L^{-1}) and magnesium chloride (1 mol L^{-1}), separately, with the purpose to provide variation on the minerals interplanar spacing and enable the identification of expansive phyllosilicates. The prior treatment was completed with the remotion of the salts excess using alcohol washing.

The oriented clay slides were prepared, and analyzed in a diffractometer model Shimadzu XRD 6000, operated with a Copper tube (Cu) at 40 kV (Kilovolts) and 30 mA (Milliampere). The samples were analyzed according to the following treatments: 1) heated initially at 25ºC and then, 2) heated to 550 ºC for 3 hours. The Mg slides were also saturated with ethylene glycol and maintained in a desiccator (60 ºC) for a night.

The interpretation of diffractograms was based on the behavior, shape, width, and intensity of the peaks, produced according the chemical and thermal treatments applied. For this purpose, we used the following the methodologies: Jackson (1975); Brown and Brindley (1980) and Moore and Reynolds (1989). Considering the similarity of XRD data in all samples analyzed, we selected only one sample (upper section) to represent the silicates identification in the graphic.

5.2.5. Sand mineralogy analysis – Optical microscopy

The description of the sand mineralogical assemblage was conducted by optical microscopy. We use a SMZ-171-Tled stereomicroscope with zoom Greenough optical system, MOTIC brand, coupled to a MOTIC Moticam Pros 5 Lite digital video camera with 1/3 CMOS sensor and primary color filter RGB. For the sand samples no pretreatment was necessary.

5.2.6. Soil microscopy analysis and elementary quantification - SEM/EDS

The scanning electron microscope (SEM) of the samples was obtained using a microscope VEGA3 (TESCAN). The instrument is equipped with secondary electron (SE), backscattered electron (BSE), cathodoluminescence (CL) detectors, and an X-act probe, these materials are needed for qualitative analysis of chemical composition using energy dispersive x-rays (EDX/EDS), also performed on these soil samples.

The first procedure was the stubs preparation, which they were used as platform to soil samples. After that, the samples were metallized with a thin layer of gold dust (0.5 – 15 nm),

trying to avoid electric charge accumulated by some materials present on the samples. The gold can neutralize them and improves the level of secondary electron emission. Then, the samples were transferred to the microscope to proceed with the identification of minerals.

5.2.7. Sulfur speciation – XPS

X-ray photoelectron spectroscopy (XPS) characterization was carried out by using a Kratos AXIS ULTRA^{DLD} XPS system equipped with an Al Kα mono chromated X-ray source and a 165 mm mean radius electron energy hemispherical analyzer with a slot and electrostatic lens mode. Vacuum pressure was kept below 3×10−9 torr during the acquisition, and a neutralizer was applied to compensate sample charging during the measurement.

5.3. Results and discussions

5.3.1. Clay mineralogy – XRD

The XRD of the clay fraction is shown in Figure 11. The minerals identified were smectite, interstrafied or interlayered illite-smectite, illite, kaolinite, and quartz.

Figure 11 - DRX of clay fraction from Botafogo mangrove river.

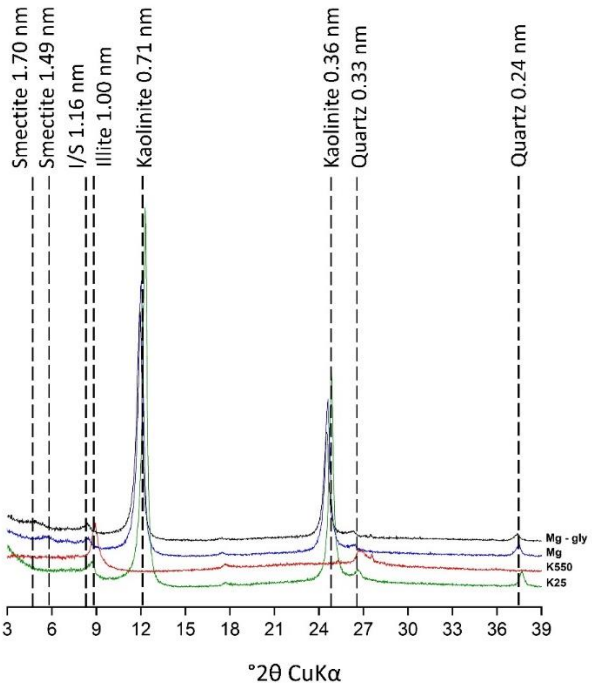

(I/S): Interstrafied or interlayered illite-smectite

The smectite were identified due to the expansion of the peak from the basal spacing from 1.49 to 1.70 nm after treatment with glycerol (Mg-gly). Overall, the intensity of the peaks was low. Illite-smectite interstratified by a slight expansion of the basal spacing peak from 1.00 to

1.16 nm after saturation with Mg (Mg) which expanded a little more with Mg + glycerol (Mg-gly). kaolinite was identified by peaks 0.71 and 0.36 nm that collapsed (disappeared) with treatment at 550°C (K550). Low intensity of quartz-related peaks was also verified due to the basal spacings at 0.33 and 0.24 nm in all chemical treatments.

The clay mineralogy shows similar pattern identified in others brazilian studies (ANDRADE et al., 2018; SOUZA-JÚNIOR et al., 2008; VILHENA; COSTA; BERRÊDO, 2010). The XRD revealed kaolinite as the main silicate mineral of the clay fraction in these soils (high intensity). Despite the geochemical conditions that support neogenesis, the kaolinite identified must have allochthonous origin, derived from local kaolinitic soils adjacent to the coastal plain.

Smectite, on other hand, probably presents autochthonous origin. The geology of the surrounding areas (Table 7) does not provide 2:1 minerals, and rarely contains smectite. Andrade et al. (2014) studying smectite transformation in some brazilian mangrove soils, identified an authigenic transformation process in response to the high Fe activity in solution (produced by the pyrite oxidation) and high salt content in the water, which produces transitory kaolinite–smectite and illite–smectite phases (also identified – Figure 10).

Quartz resisted in clay fraction, but its peak showed low intensity. The occurrence in clay fraction is related to the high resistance this tectosilicate has against chemical weathering. Most of the quartz is found at sand mineralogy composition (Table 8). Besides the local Holocene sediments contribution (SOUZA-JÚNIOR et al., 2008), this mineral is originated from the weathering of sedimentary rocks from the Beberibe formation, mainly sandstone (VALENÇA; SOUZA, 2017).

Overall, no differences were observed between the three mangrove forests. The whole area is inserted in the same mineralogical context. In terms of silicates, the present environmental conditions promote the maintenance of the same minerals along the mangrove.

5.3.2. Soil microscopy analysis and elementary quantification - SEM/EDS

5.3.2.1. Pyrite identification and Hg association

From the evaluation of SEM, we identified pyrite framboids (Figure 12). Pyrite is a common mineral in sedimentary environments, such mangrove forests, especially under suboxic and anoxic conditions. It is an iron disulfide (FeS_2) formed by the terrestrial contribution of Fe, reduced in those environments under anoxic conditions and then become associated with sulfate (SO_4^{2-}) (FERREIRA et al., 2015).

Figure 12 - SEM images of framboidal pyrite in the sediments and organic materials from the upper section.

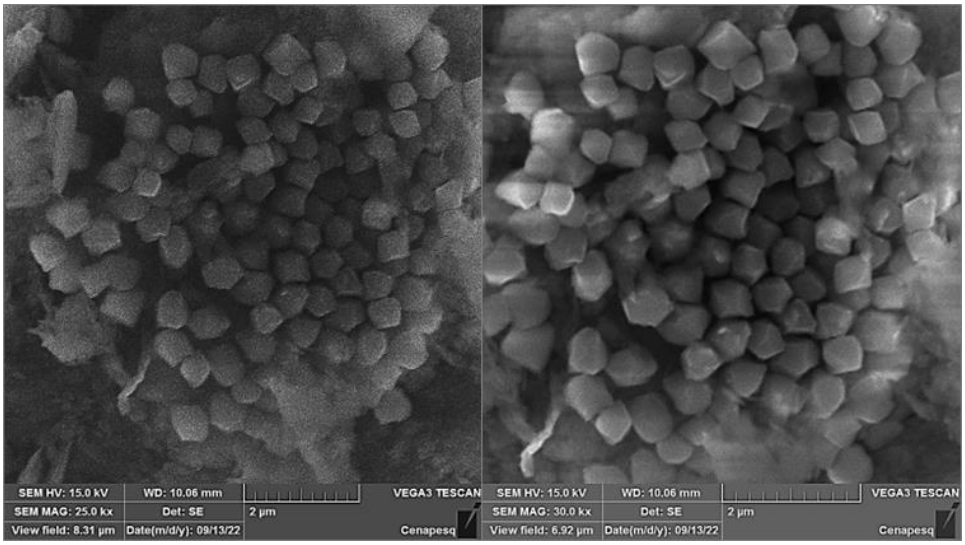

The pyrite was identified associated with Hg in the studied soils (Figure 13). It confirms the capacity of pyrite in Hg retention in coastal ecosystem, being considered one of the important ecological (HUERTA-DIAZ; MORSE, 1992).

Figure 13 - SEM and EDS map images of pyrite, and spectra of main elements in the upper section.

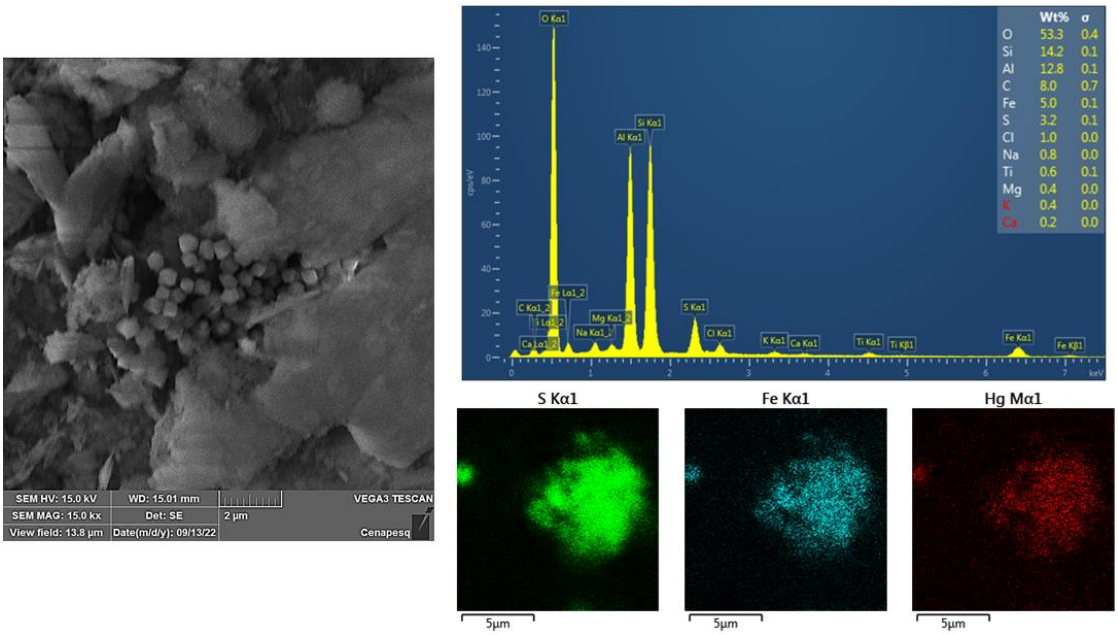

The EDS maps reveal the Hg associated with the pyrite.

The identification of Hg was possible due to the EDS mapping evaluation. Considering the EDS limit of detection for heavy elements, such Hg, we could identify mercury associated with framboidal pyrite due to its distribution along the microregions of the samples. Iron, sulfur

and Hg obtained similar distribution pattern, and Fe and S were considered one of the two elements most abundant in the system (Fe = 5% and S = 3.2%).

The Hg association with sulfide-Fe forms was also observed at the middle section (Figure 14). Environmentally speaking, we confirmed that iron sulfides are an important component in Hg occlusion. However, this occlusion presents a certain instability, since sulfide minerals, when in contact with atmospheric oxygen, can undergo oxidation and, consequently, favor the release of associated metals. This represents a potential release of inorganic Hg mainly during the dry period (low tide), when there is a reduction in the water level.

Although sulfides represent a threat as a source of Hg, we found that their oxidation occurs in parts, and new iron precipitates can also occlude Hg. Not representing a short-term problem in Hg release. It is important to note that the residence time of saturation in the upper and lower sections can lead to greater oxidation of the iron sulfides present. On the other hand, vegetation increases more labile compounds, which are essential for the processes of reducing and reformulating sulfides.

Figure 14 - SEM-EDS mapping showing the distribution of main elements among the sediments in the middle section.

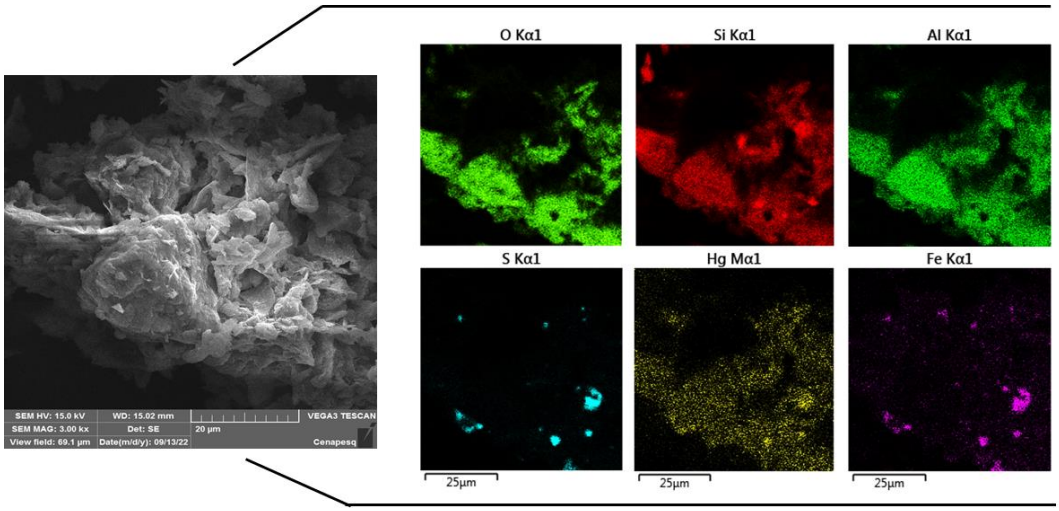

Pyrite surface has been described composed by two parts: a pyritic area and oxidized one with iron hydroxides. The Hg can be associated in both zones (EHRHARDT et al., 2000), Sun et al. (2017) corroborate it and added Hg^{2+} removal mechanisms on iron sulfides in aqueous solutions include precipitation (formation of HgS), ion exchange (formation of $[Fe_xHg_y]S$), surface complexation and adsorption.

Its oxidation and subsequent degradation represent a risk for this environment and the nature around (ARAÚJO et al., 2022). In terms of anthropic activities progress, the progress of

shrimp farming and sugarcane cultivation at the Botafogo river mangroves must be well monitored, avoiding any relevant disturbance in the anoxic conditions.

5.3.2.2. Silicates

In general terms, the SEM/EDS data shows the silicate mineralogy (Figure 15) is composed mainly by quartz, and muscovite, especially at the lower section, where the sand content is higher (Table 1 - chapter 2). Kaolinite is the most important mineral in this area, but it was better identified and described using XRD procedure.

Figure 15 - SEM image from soil collected at the lower section.

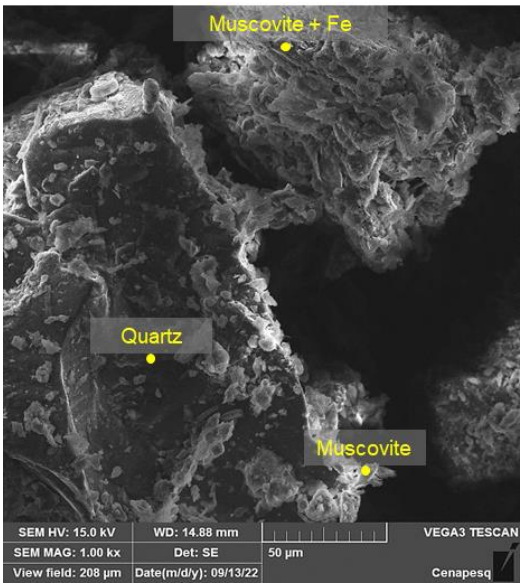

Quartz identified has sandy coastal sediments origin that was transported during the last Holocenic transgressive events (SOUZA-JÚNIOR et al., 2008). SEM also shows quartz particles covered by muscovite and muscovite associated with Fe, all of them confirmed by the EDS spectra (Figure 16).

Figure 16 - EDS spectra of quartz (A), muscovite (B) and muscovite associated to Fe-oxide (C).

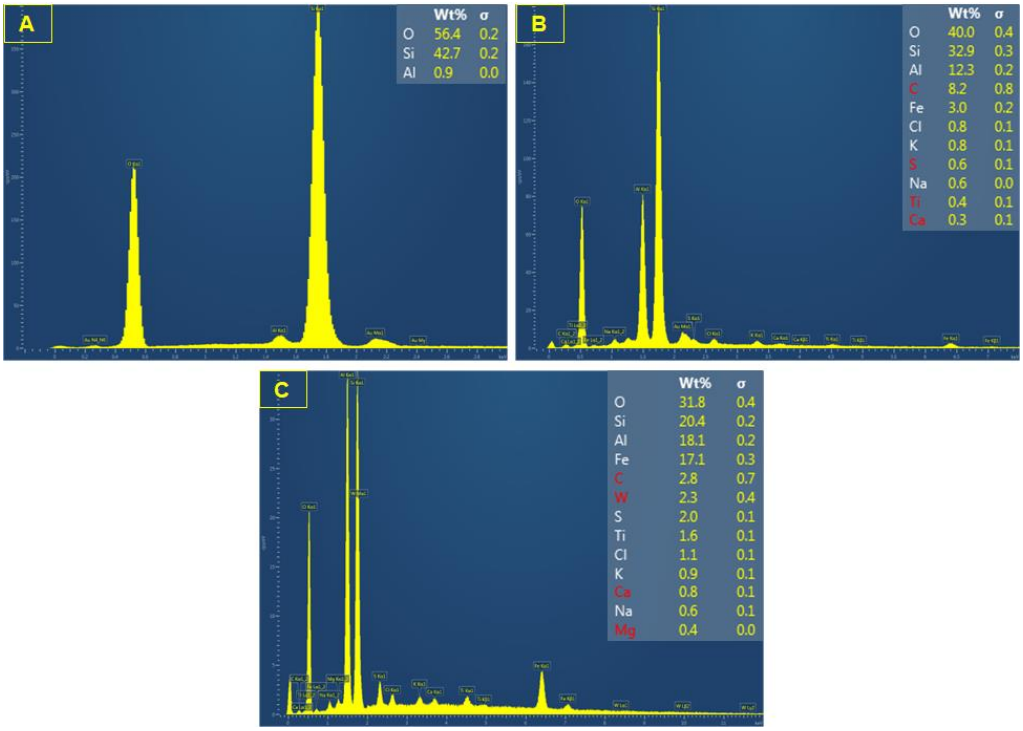

The spectra shows the Fe enrichment, which went from 3.0% at muscovite particles (B) to 17.1% when this mineral is surrounded by Fe (B). Considering the anaerobic conditions, the Fe around the muscovite is probably attributed to pyrite occurrence, as identified in the upper section (Figure 11).

The presence of muscovite is probable attributed to sediments that is transported and deposited in the mudbank close to the forests. The geology of the Botafogo river watershed provide this type of mica, which is represented by crystalline basement rocks, characterized by lithotypes of gneissic-migmatitic complexes (VALENÇA; SOUZA, 2017). Furthermore, muscovite is normally much more resistant to weathering than trioctahedral micas, such biotite, allowing it to be moved over long distances without significant alteration.

5.3.2.3. Carbonates

SEM/EDS data also made it possible to confirm the presence of carbonates (Figure 17). The occurrence of carbonates was exclusive to the lower section. At this zone, the Ca achieved about 18%, being the third element most abundant. Compared to spectra from the upper section (Figure 12) shown earlier (~0.2%), the Ca content increased almost 90 times.

Figure 17 - SEM image and EDS spectra of precipitates on sediments surface of soil from the lower section.

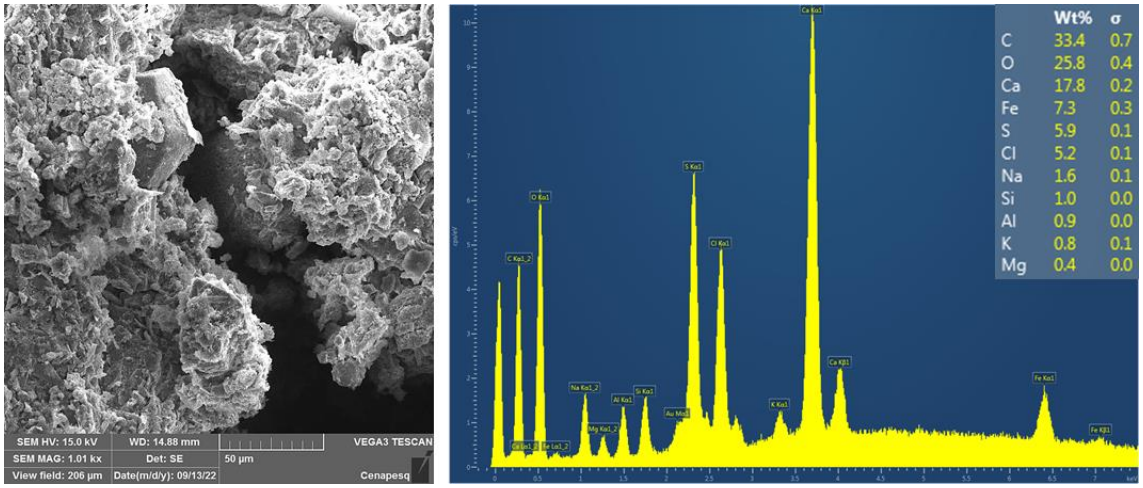

Carbonate presence must be biogenic derived from molluscs, which explains the Ca and C contribution. At the lower section, *C. rhizophorae* is a common oyster that lives associated with *R. mangle* roots (Figure 18). It lives more on *R. mangle* roots than any other tree species at the studied mangrove.

Figure 18 - Oyster (*Crassostrea rhizophorae*) living on *R. mangle* roots at the lower section.

Oyster shell represents a calcium carbonate source to mangrove soils. Source: Personal archive.

Moreover, as discussed earlier (chapter 2), around the mangrove sediments (Q2m), local formations: Beberibe (Kb), Gramame (Kg), and Itamaracá Formation (K2it) are sources of carbonate materials (table 7).

Table 7 - Local geology of the northern part of the Recife metropolitan region.

Unit acronym	Name of the stratigraphic unit	Lithology
Q2m	Mangrove sediments	Current floodplain sediments, channel bars and river channels, composed of gravels, sands and clays, semi-consolidated to unconsolidated.
K2be	Beberibe formation	Medium to coarse sandstone, locally fine, poorly sorted, with occasional conglomeratic fractions, which grade to carbonate sandstone towards the top of the unit.
E1mf	Maria Farinha formation	Marly limestones and marls, fossiliferous
K2g	Gramame formation	Fossiliferous limestone, marly limestone, marl and clay, containing phosphorite horizons interdigitated with calcarenites at the base (shallow marine).

Source: adapted from CPRM, 2017.

Overall, despite the presence of calcareous materials in the local lithology, mineral carbonate supply requires rocky outcrop, so the rocks can be able to be weathered and provide its chemical compounds.

5.3.3. Sand mineralogy – optical microscopy

The mineralogic composition of the sand were similar in all mangrove forests (Table 8). The minerals at the sand fraction were mainly quartz and muscovite. Furthermore, feldspar, fragments of quartz/muscovite, and opaque minerals were identified in smaller proportion.

Table 8 - Mineralogy and morphology of sand fraction of soils from Botafogo River mangrove.

Location	Sand (2 – 0.05 mm)			
	Minerals	Proportion (%)	Roundness + Sphericity	Pattern + Alteration class
Upper section				
1	Hyaline Quartz	28	Well-rounded - Rounded / Spherical - Subspherical	Irregular linear: B/0 (13%) and B/1 (15%)
	Milky Quartz	65	Well-rounded - Rounded / Spherical - Subspherical	Irregular linear: B/0 (50%) e B/1 (15%)
	Muscovite	2	--- / ---	Parallel Linear: C1/0
	Opaque	2	Well-rounded / Spherical	Dotted: D/0
	Fragments	1	Rounded - Subrounded/ Subspherical – Subelongated	Irregular linear: B/0
	Feldspar - Kaolinite	2	Subangular / Subelongated	Film: A/1
2	Hyaline Quartz	28	Well-rounded - Rounded / Spherical - Subspherical	Irregular linear: B/0 (13%) e B/1 (15%)
	Milky Quartz	30	Well-rounded - Rounded / Spherical - Subspherical	Irregular linear: B/0 (15%) e B/1 (15%)
	Muscovite	2	--- / ---	Parallel Linear: C1/0
	Opaque	2	Well-rounded / Spherical	Dotted: D/0
	Fragments	1	Rounded - Subrounded/ Subspherical – Subelongated	Irregular linear: B/0
	Feldspar - Kaolinite	2	Subangular / Subelongated	Film: A/1
3	Hyaline Quartz	40	Well-rounded - Rounded / Spherical - Subspherical	Irregular linear: B/0 (20%) e B/1 (20%)
	Milky Quartz	36	Well-rounded - Rounded / Spherical - Subspherical	Irregular linear: B/0 (26%) e B/1 (10%)
	Muscovite	2	--- / ---	Parallel Linear: C1/0
	Opaque	2	Well-rounded / Spherical	Dotted: D/0
	Fragments	1	Rounded - Subrounded/ Subspherical – Subelongated	Irregular linear: B/0
	Feldspar - Kaolinite	3	Subangular / Subelongated	Film: A/1
Middle section				
4	Hyaline Quartz	44	Rouded – Subrounded Spherical - Subspherical	Irregular linear: B/0 (24%) e B/1 (20%)
	Milky Quartz	50	Rounded – Subrounded Spherical - Subspherical	Irregular linear: B/0 (25%) e B/1 (20%)

	Muscovite	3	--- / ---	Parallel Linear: C1/0
	Opaque	1	Well-rounded / Spherical	Dotted: D/0
	Fragments	1	Rounded – Subrounded Subspherical - Subelongated	Irregular linear: B/1
	Feldspar - Kaolinite	1	Subangular - Subelongated	Film: A/1
5	Hyaline Quartz	50	Rounded – Subrounded Spherical - Subspherical	Irregular linear: B/0 (25%) e B/1 (25%)
	Milky Quartz	43	Rounded – Subrounded Spherical - Subspherical	Irregular linear: B/0 (23%) e B/1 (20%)
	Muscovite	4	--- / ---	Parallel Linear: C1/0
	Opaque	1	Well-rounded / Spherical	Dotted: D/0
	Fragments	1	Rounded – Subrounded Subspherical - Subelongated	Irregular linear: B/1
	Feldspar - Kaolinite	1	Subangular - Subelongated	Film: A/1
6	Hyaline Quartz	24	Rounded – Subrounded Spherical - Subspherical	Irregular linear: B/0 (14%) e B/1 (10%)
	Milky Quartz	20	Rounded – Subrounded Spherical - Subspherical	Irregular linear: B/0 (10%) e B/1 (10%)
	Muscovite	2	--- / ---	Parallel Linear: C1/0
	Opaque	2	Well-rounded / Spherical	Dotted: D/0
	Fragments	1	Rounded – Subrounded Subspherical - Subelongated	Irregular linear: B/1
	Feldspar - Kaolinite	1	Subangular - Subelongated	Film: A/1
			Lower section	
7	Hyaline Quartz	30	Rounded – Subrounded Spherical - Subspherical	Irregular linear: B/0 (15%) e B/1 (15%)
	Milky Quartz	62	Rounded – Subrounded Spherical - Subspherical	Irregular linear: B/0 (32%) e B/1 (30%)
	Muscovite	1	--- / ---	Parallel Linear: C1/0
	Opaque	2	Rounded / Spherical	Dotted: D/1
	Fragments	1	Rounded – Subrounded Subspherical - Subelongated	Irregular linear: B/0
	Feldspar – Kaolinite	4	Subangular - Subelongated	Film: A/1
8	Hyaline Quartz	25	Rounded – Subrounded Spherical - Subspherical	Irregular linear: B/0 (15%) e B/1 (15%)
	Milky Quartz	67	Rounded – Subrounded Spherical - Subspherical	Irregular linear: B/0 (32%) e B/1 (30%)

	Muscovite	1	--- / ---	Parallel Linear: C1/0
	Opaque	2	Rounded / Spherical	Dotted: D/1
	Fragments	2	Rounded – Subrounded Subspherical - Subelongated	Irregular linear: B/0
	Feldspar - Kaolinite	3	Subangular - Subelongated	Film: A/1
9	Hyaline Quartz	35	Rounded – Subrounded Spherical - Subspherical	Irregular linear: B/0 (25%) e B/1 (10%)
	Milky Quartz	57	Rounded – Subrounded Spherical - Subspherical	Irregular linear: B/0 (37%) e B/1 (20%)
	Muscovite	1	--- / ---	Parallel Linear: C1/0
	Opaque	1	Rounded / Spherical	Dotted: D/1
	Fragments	3	Rounded – Subrounded Subspherical - Subelongated	Irregular linear: B/0
	Feldspar - Kaolinite	3	Subangular - Subelongated	Film: A/1

Fragments – Quartz/muscovite

Quartz proportion achieved the following mean values: 92% (upper section); 93% (middle section), and 92% (lower section). It reveals the quartz domain in the soils. A significant part of the quartz from middle section (50% - site 6) and upper section (35% - site 2; 15% - site 3) is covered by brownish material, probably humified organic matter (OM). All samples had coalesced aggregates of fibrous OM with minerals. In addition, at the lower section, the quartz was identified mainly as milky particles, in some sites (7 and 8) achieving 2 times more the hyaline type.

Muscovite, on the other hand, presented less than 5% of the sand composition. The decrease proportion of this mineral in the sections were: 3% (middle section) > 2% (upper section) > 1% (lower section). However, the opposite occurred at the feldspar proportion: 3% (lower section) > 2% (upper section) > 1% (middle section).

As discussed early, quartz has allochthonous origin, provided by sandy coastal sediments derived from quartz sandstones (VALENÇA; SOUZA, 2017). Hyaline quartz are mineral particles that have the highest content of SiO_2, while milky one is represented by those that has higher concentration of other elements on its composition, such as: Cl, Fe, S, Ca, and K (SILVA et al., 2023). The prevalence of milky quartz at the lower section is probably associated with higher concentration of salts in this zone, such carbonates and halite, that provides Ca, Mg, and Cl to SiO_2 association. This location also represents the border between the end of the Botafogo River and the Santa Cruz Channel, being considered the meeting point for chemical compounds coming from the river and sea water.

The optical microscopy confirms the muscovite identification by SEM/EDS. In contrast with mangrove soils from southeastern, muscovite was found in the sand fraction (SOUZA-JÚNIOR et al., 2008). Gneissic-migmatitic complexes of the local lithology is probable the main source of it (VALENÇA; SOUZA, 2017).

5.3.4. Sulfur speciation – XPS

The S 2p XPS spectrum of mangrove samples has two primary peaks, representing two distinct sulfur groups (Figure 19). First one, at 170 to 166 eV, represents the relative proportion of oxidized S components. The second peak, at 166 to 162 eV, corresponds to the low oxidation state groups. All sections showed prevalence of oxidized S groups compared to reduced ones, confirmed by the higher peaks situated at a higher energy. Furthermore, considering the spectrum represents the relative proportion of the components low oxidation S are more present at the upper section and lower section.

Figure 19 - S 2p spectra of soil of Botafogo river mangrove.

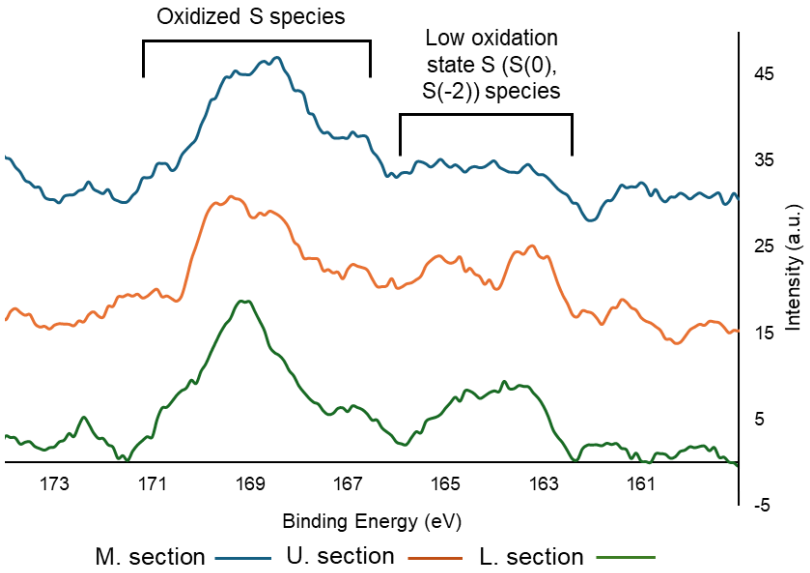

M. section (medium section); U. section (upper section), and L. section (lower section).

XPS data corroborates our observation about pyrite identification (Figure 11). Features at 166 to 162 eV correspond to important reduced inorganic and organic components, such as pyrite (162.9 eV) (SHCHUKAREV et al., 2008); and C-S functionalities (e.g., thiol: C-S-C – 163.5 eV), respectively (BHATTACHARYYA et al., 2018).

The pyrite occurrence and its association with Hg were confirmed by the SEM evaluation. Thiol is also a relevant Hg retainer in aquatic systems (DING et al., 2017). These are products of the O_2 depletion promoted by the decomposition of OM, mediated by sulfate-reducing-bacteria (SRB) (LEI et al., 2019). As the anaerobic conditions increases, it favors the accumulation of inorganic and organic S forms. Summed with oxygen-containing functional groups (e.g., carboxylic acid), these groups represent the major complexation of Hg in estuarine sediments (CHAKRABORTY et al., 2015). In this study we did not evaluate the thiol contribution on Hg retention, but it must be performed in order to better elucidate the contribution of organic matter in the retention of this metal.

XPS data contributes for the Hg contamination discussion. Studying the dynamic of Hg in 6 soil profiles distributed along the same mangrove, Araújo et al. (2019) identified a significant effect of OM on Hg retention, which up to 47% of this heavy metal was complexed with organic compounds. According to them, the greater OM-Hg phase was identified at the lower and middle section, where the Hg concentration was lower. However, considering their sequential extraction and our XPS data, at the upper section, where we both identified Hg concentration up to 14.3 mg kg^{-1} (Figure 4 - chapter 2), the retention of this heavy metal might be controlled by S reduction reactions. According to recent studies, high Hg loading soils are

dominated by reduction reactions, while complexation with oxidized C has been reported mainly at lower Hg concentration (CHENNURI et al., 2020).

Overall, in this discussion two points must be highlighted, 1) despite the fact upper and middle section are considered a pool for reactive oxidized C (Figure 8 – chapter 3), it seems Hg are incorporated in the structure of low oxidation state S, especially pyrite. Araújo et al. (2019) in their sequential extraction identified a low phase of Hg-S, however this phase access predominantly Hg bound sulfides, cinnabar and metacinnabar (BLOOM et al., 2003). 2) their sequential extraction also revealed a greater OM contribution at the lower section, which indicates the following reflection: lower section dominated by *R. mangle* has a lower OM oxidation/decomposition occasioned by releasement of refractory C (e.g., tannin) and its higher anoxic condition. At this case, Hg can be associated with the part of OM that is founded reduced, such thiol and inorganic S, pyrite (Figure 18).

Moreover, the higher intensity of oxidized S in all sections is related to the fact we are studying the surface layer (0-10 cm) of the soil profile. The basin of the forests shows a convex form, and the samples were collected among a high-density roots area. Therefore, during the low tide, the surface zone of the soil becomes rapidly oxidized, and the chemical components are exposed to the air for long periods of the time (FERREIRA et al., 2007).

5.4. Conclusions

The mangrove soils on the estuary of the Botafogo River present an assemblage consisting predominantly of kaolinite as allochthonous mineral, but also other autochthones ones were identified, such smectite. Essentially, kaolinite is originated from the Barreiras formation. Smectite is probably a result of neogenesis formation, as absence of this mineral at local lithology, in addition to neutral pH, and abundance of Fe. The anaerobic conditions favor the pyrite formation, especially at mangroves distant from the river mouth. SEM/EDS also revealed pyrite-Hg association, and carbonate occurrence at the lower section. Soil S speciation had predominance of oxidized forms, but the spectrum showed relevant reduced components for Hg adsorption, such pyrite and thiol.

Considering the historic Hg contamination context, silicates present in the sand and clay fraction are known to play a minor role in Hg retention. Nevertheless, the S reduced components can control Hg fate on soil. Therefore, the Hg maintenance on the soil is related to maintenance of these reducing conditions. The present study reaffirms the careful in avoid change at the soil biogeochemical condition, especially by the anthropic activities, otherwise these mangrove soils will no longer be a contaminant filter, but a source of it for all environments.

References

ANDRADE, G. R. P.; CUADROS, J.; PARTITI, C. S.; COHEN, R.; VIDAL-TORRADO, P. Sequential mineral transformation from kaolinite to Fe-illite in two Brazilian mangrove soils. **Geoderma**, v. 309, p. 84–99, 2018. https://doi.org/10.1016/j.geoderma.2017.08.042

ANDRADE, G. R. P.; DE AZEVEDO, A. C.; CUADROS, J.; SOUZA JR, V. S.; CORREIA FURQUIM, S. A.; KIYOHARA, P. K.; VIDAL-TORRADO, P. Transformation of Kaolinite into Smectite and Iron-Illite in Brazilian Mangrove Soils. **Soil Science Society of America Journal**, v. 78, p. 655-672, 2014. https://doi.org/10.2136/sssaj2013.09.0381

ARAÚJO, P. R. M.; BIONDI, C. M.; DO NASCIMENTO, C. W. A.; DA SILVA, F. B. V.; ALVAREZ, A. Bioavailability and sequential extraction of mercury in soils and organisms of a mangrove contaminated by a chlor-alkali plant. **Ecotoxicology and Environmental Safety**, v. 183, p. 109469, 2019. https://doi.org/10.1016/j.ecoenv.2019.109469

ARAÚJO, P. R. M.; BIONDI, C. M.; DO NASCIMENTO, C. W. A.; DA SILVA, F. B. V.; FERREIRA, T. O.; DE ALCÂNTARA, S. F. Geospatial modeling and ecological and human health risk assessments of heavy metals in contaminated mangrove soils. **Marine Pollution Bulletin**, v. 177, p. 113489, 2022. https://doi.org/10.1016/j.marpolbul.2022.113489

BEHLING, H.; DA COSTA, M. L. Mineralogy, geochemistry, and palynology of modern and late Tertiary mangrove deposits in the Barreiras Formation of Mosqueiro Island, northeastern Pará state, eastern Amazonia. **Journal of South American Earth Sciences**, v. 17, p. 285–295, 2004. https://doi.org/10.1016/j.jsames.2004.08.002

BHATTACHARYYA, A.; SCHMIDT, M. P.; STAVITSKI, E.; MARTÍNEZ, C. Iron speciation in peats: chemical and spectroscopic evidence for the co-occurrence of ferric and ferrous iron in organic complexes and mineral precipitates. **Organic Geochemistry**, v. 115, p. 124–137, 2018. https://doi.org/10.1016/j.orggeochem.2017.10.012

BROWN, G.; BRINDLEY, G. W. **X-ray Diffraction Procedures for clay mineral Identification**. In: BRINDLEY, G.W; BROWN, G. London: Mineralogical Society, chapter 5, p.305-360, 1980.

BLOOM, N. S.; PREUS, E.; KATON, J.; HILTNER, M. Selective extractions to assess the biogeochemically relevant fractionation of inorganic mercury in sediments and soils. **Analytica Chemical Acta**, v. 479, p. 233–248, 2003. https://doi.org/10.1016/S0003-2670(02)01550-

CHAKRABORTY, P.; SARKAR, A.; VUDAMALA, K.; NAIK, R.; NATH, B. N. Organic matter — A key factor in controlling mercury distribution in estuarine sediment. **Marine Chemistry**, v. 173, p. 302–309, 2015. https://doi.org/10.1016/j.marchem.2014.10.005

CHENNURI, K.; CHAKRABORTY, P.; JAYACHANDRAN, S.; MOHAKUD, S. K.; ISHITA, I.; RAMTEKE, D.; BABU, K. R. Operationally defined mercury (Hg) species can delineate Hg bioaccumulation in mangrove sediment systems: A case study. **Science of The Total Environment**, v. 701, p. 134842, 2020. https://doi.org/10.1016/j.scitotenv.2019.134842

COMPAINHA DE RECURSOS MINERAIS (CPRM). **Mapa hidrogeológico da região metropolitana do Recife**. 2017.

DING, X.; WANG, R.; LI, Y.; GAN, Y.; LIU, S.; DAI, J. Insights into the mercury (II) adsorption and binding mechanism onto several typical soils in China. **Environmental Science and Pollution Research**, v. 24, p. 23607–23619, 2017. https://doi.org/10.1007/s11356-017-9835-2

EHRHARDT, J. J.; BEHRA, P.; BONNISSEL-GISSINGER, P.; ALNOT. XPS study of the sorption of Hg (II) onto pyrite FeS_2. **Surface and Interface Analysis**, v. 30, p. 269–272, 2000. https://doi.org/10.1002/1096-9918(200008)30:1<269::AID-SIA758>3.0.CO;2-N

FERREIRA, T. O.; OTERO, X. L.; VIDAL-TORRADO, P.; MACÍAS, F. Redox processes in mangrove soils under *Rhizophora mangle* in relation to different environmental conditions. **Soil Science Society of America Journal**, v. 71, p. 484–491, 2007. https://doi.org/10.2136/sssaj2006.0078

FERREIRA, T. O.; NÓBREGA, G. N.; ALBUQUERQUE, A. G.; SARTOR, L. R.; GOMES, I. S.; ARTUR, A. G.; OTERO, X. L. Pyrite as a proxy for the identification of former coastal lagoons in semiarid NE Brazil. **Geo-Marine Letters**, v. 35, p. 355–366, 2015. https://doi.org/10.1007/s00367-015-0412-8

HUERTA-DIAZ, M. A.; MORSE, J. W. Pyritization of trace metals in anoxic marine sediments. **Geochimica et Cosmochimica Acta**, v. 56, p. 2681–2702, 1992. https://doi.org/10.1016/0016-7037(92)90353-K

INSTITUTO NACIONAL DE PESQUISAS ESPACIAIS (INPE). **Centro de previsão de tempo e estudos climáticos**. Disponível em <http:// http://www.cptec.inpe.br/>. Acesso em 8 de dezembro de 2023.

JACKSON, M. L. **Soil chemical analysis: advance course**. 29. ed. Madison, p. 895, 1975.
LEI, P.; ZHONG, H.; DUAN, D.; PAN, K. LEI, P. A review on mercury biogeochemistry in mangrove sediments: hotspots of methylmercury production? **Science of The Total Environment**, v. 680, p. 140–150, 2019. https://doi.org/10.1016/j.scitotenv.2019.04.451

LUGO, A. E.; SNEDAKER, S. C. The ecology of mangroves. **Annual review of ecology and systematics**, v. 5, p. 39-64, 1974. https://doi.org/10.1146/annurev.es.05.110174

MACHADO, W.; BORRELLI, N. L.; FERREIRA, T. O.; MARQUES, A. G. B.; OSTERRIETH, M.; GUIZAN, C. Trace metal pyritization variability in response to mangrove soil aerobic and anaerobic oxidation processes. **Marine pollution bulletin**, v. 79, p. 365–370, 2014. https://doi.org/10.1016/j.marpolbul.2013.11.016

MOORE, D. M.; REYNOLDS, R. C. **X-ray diffraction and identification and analysis of clay minerals**. Oxford: Oxford University Press, p. 332, 1989.

OTERO, X. L.; FERREIRA, T. O.; HUERTA-DÍAZ, M. A.; PARTITI, C. S. DE M., SOUZA JR, V.; VIDAL-TORRADO, P.; MACÍAS, F. Geochemistry of iron and manganese in soils and sediments of a mangrove system, Island of Pai Matos (Cananeia—SP, Brazil). **Geoderma**, v. 148, p. 318–335, 2009. https://doi.org/10.1016/j.geoderma.2008.10.016

OTERO, X. L.; GUEVARA, P.; SÁNCHEZ, M.; LÓPEZ, I.; QUEIROZ, H. M.; FERREIRA, A.; CARBALLO, R. Pyrites in a salt marsh-ria system: Quantification, morphology, and mobilization. **Marine Geology**, v. 455, p. 106954, 2023. https://doi.org/10.1016/j.margeo.2022.106954

PELAGE, L.; GONZALEZ, J. G.; LE LOC'H, F.; FERREIRA, V.; MUNARON, J. M.; LUCENA-FREDOU, F.; FREDOU, T. Importance of estuary morphology for ecological connectivity with their adjacent coast: A case study in Brazilian tropical estuaries. **Estuarine, Coastal and Shelf Science**, v. 251, p. 107184, 2021. https://doi.org/10.1016/j.ecss.2021.107184

SHCHUKAREV, A.; GÄLMAN, V.; RYDBERG, J.; SJÖBERG, S.; RENBERG, I. Speciation of iron and sulphur in seasonal layers of varved lake sediment: an XPS study. **Surface and Interface Analysis**, v. 40, p. 354–357, 2008. https://doi.org/10.1002/sia.2704

SILVA, S. H. G.; RIBEIRO, D.; DIJAIR, T. S. B.; SILVA, F. M.; TEIXEIRA, A. F. D. S.; ANDRADE, R.; CURI, N. Different Quartz Varieties Characterized by Proximal Sensing and Their Relation to Soil Attributes. **Minerals**, v. 13, p. 529, 2023. https://doi.org/10.3390/min13040529

SOUKUP, D. A.; BUCK, B. J.; HARRIS, W. **Preparing soils for mineralogical analyses**. Methods of Soil Analysis Part 5—Mineralogical Methods, v. 5, p. 13–31, 2008.

SOUZA-JÚNIOR, V. S. D.; VIDAL-TORRADO, P.; GARCIA-GONZALÉZ, M. T.; OTERO, X. L.; MACÍAS, F. Soil mineralogy of mangrove forests from the state of São Paulo, southeastern Brazil. **Soil Science Society of America Journal**, v. 72, p. 848–857, 2008. https://doi.org/10.2136/sssaj2007.0197

SUN, Y.; LV, D.; ZHOU, J.; ZHOU, X.; LOU, Z.; BAIG, S. A.; XU, X. Adsorption of mercury (II) from aqueous solutions using FeS and pyrite: a comparative study. **Chemosphere**, v. 185, p. 452–461, 2017. https://doi.org/10.1016/j.chemosphere.2017.07.047

STOKES, G. G. **Transactions of the Cambridge Philosophical Society**, v. 9, n. 2, p. 8–106, 1851.

VALENÇA, L. M. M.; SOUZA, N. G. A. **Unidades estratigráficas. Geologia e recursos minerais da folha Itamaracá SB. 25-YC-VI: estados de Pernambuco e Paraíba**. In: VALENÇA, L. M. M.; SOUZA, N. G. A. Recife: CPRM, 2017. p. 23-41.

VILHENA, M. D. P. S. P.; COSTA, M. L. DA; BERRÊDO, J. F. Continental and marine contributions to formation of mangrove sediments in an Eastern Amazonian mudplain: The case of the Marapanim Estuary. **Journal of South American Earth Sciences**, v. 29, p. 427–438, 2010. https://doi.org/10.1016/j.jsames.2009.07.005

WOODROFFE, C. D.; ROGERS, K.; MCKEE, K. L.; LOVELOCK, C. E.; MENDELSSOHN, I. A.; SAINTILAN, N. Mangrove sedimentation and response to relative sea-level rise. **Annual review of marine science**, v. 8, p. 243–266, 2016. https://doi.org/10.1146/annurev-marine-122414-034025

6. FINAL CONSIDERATIONS

Our data contributed to the assessment of contamination of the area by heavy metals, especially for Hg, observing the concentration variation across different mangrove forests.

Evaluations on soil organic matter and mineralogy quality along different contaminated mangrove forest are essential to contribute on the Hg dynamic explanation.

The isotope signal of $\delta^{13}C$ and $\delta^{15}N$, FTIR and DSC-TG are fundamental tools to characterize soil organic matter variation along estuaries.

SEM/EDS can be better used as an identification technique of minerals and contaminants association in mangrove soils.

XPS S speciation is an interesting technique to identify the predominance of oxidized and reduced groups in mangrove soils.

This study contributes on the identification of mangrove soil heterogeneity, promoted by the species variation, soil attributes and estuary position. This variation is relevant for heavy metals dynamic, especially Hg, which has a high affinity with organic compounds. In the pursuit of environmental evaluation, this study provides an overview of the geochemical filter characteristics in this contaminated mangrove. It also highlights the substantial relevance of organic and mineral phase of mangrove soils and need for constant preservation.